universität wien

MASTERARBEIT/MASTER'S THESIS

Titel der Masterarbeit/Title of the Master's Thesis

"Functional Elucidation of Pathogen Triggered Immunity (PTI) Inhibiting Effectors of *Ustilago maydis*"

verfasst von / submitted by

Indira Saado

angestrebter akademischer Grad/ in partial fulfillment of the requirements for the degree of

Master of Science (MSc)

Wien, 2018 / Vienna 2018

Studienkennzahl lt. Studienblatt / degree programme code as it appears on the student record sheet:	A 066 877
Studienrichtung lt. Studienblatt / degree programme as it appears on the student record sheet:	Masterstudium Genetik und Entwicklungsbiologie
Betreut von / Supervisor:	Dipl.-Biol. Dr. Armin Djamei, Privatdoz.

Confidentiality Clause

This master thesis contains confidential data of the Gregor Mendel Institute.

This work may only be made available to the first and second reviewers and authorized members of the board of examiners. Any publication and duplication of this master thesis - even in part - is prohibited.

An inspection of this work by third parties requires the expressed permission of the author and the Gregor Mendel Institute.

ACKNOWLEDGMENTS

This project would not have been possible without the support of many people. Many thanks to Dr. Armin Djamei who gave me the opportunity to conduct my master thesis in his lab, for his constant support, guidance and encouragement.

I would also like to express my gratitude to my supervisor André Alcântara for the useful comments, remarks and engagement through the learning process of this master thesis.

Additionally, I would like to acknowledge Joana Marques and Julia Freund, for always making my days in the lab fun and being wonderful friends.

Completing this work would have been more difficult without an outstanding help from the other members of the lab. Thank you, Janos, Angelika, Martin, Ruben, Fernando, Simon, Jason, Denise, Emiliya, Sam, Lukas, Gesa, Nenad, Benjamin, Julia and Daniel.

Furthermore, big thanks go to all members of the GMI and the support facilities at the whole Vienna Biocenter Campus.

Finally, the biggest thank goes to my family, my parents, Delal, Nadja and Haris and all my friends, for always offering support and help throughout the entire process. I will be grateful forever for your love.

ABSTRACT

Exploring the molecular mechanism how pathogens successfully colonize on their host plant is crucial for developing sustainable strategies to decrease crop yield losses. Fungal colonization on plants depends upon the ability to manipulate the immune defense response of the plant. Pattern recognition receptors (PRR) recognize molecules associated with the invading pathogen, so called pathogen associated molecule pattern (PAMP), which leads to activation of immune responses (PAMP-triggered immunity; PTI). One of the earliest observable aspects of plant defense, is the production of reactive oxygen species in the apoplast (ROS burst), generated by the NADPH oxidase. For pathogens to overcome this response, they secrete molecules, called effectors, which suppress local and systemic defense responses. ROS burst screening of *Ustilago maydis* effectors by heterologous expression in *Nicotiana benthamiana* revealed a group of putative effectors that show ROS burst inhibition. For this purpose, out of 288 *Ustilago maydis* effectors that were expressed without signalpeptide in *Nicotiana benthamiana* plants, 34 were identified to interfere with the plant defense by inhibiting ROS accumulation upon PAMP perception.

The main purpose of this study was to elucidate the mode of action of four identified *Ustilago maydis* effectors ROSIE1-4 (Ros-burst Inhibiting Effectors 1-4). To illuminate potential ways effectors mediate ROS burst inhibition, ROSIE 1-4 were transiently expressed in *Nicotiana benthamiana* plants without signalpeptide and with epitope tags. Potential interacting proteins were identified by mass spectrometry after co-immunoprecipitation. Comparative analysis of the MS data revealed 21 plant proteins that showed to be potentially specifically in the complex with one or more of the tested effector candidates. To gain more insight into their involvement in PTI, virus induced gene silencing of putative host targeted proteins were tested in *Nicotiana benthamiana* and the efficiency of silencing was verified by performing qPCR to monitor the decrease of gene expression. Interestingly, 8 potentially interacting proteins were showing a significantly increase or decrease of ROS activity upon PAMP treatment when silenced in plants, which suggest that they genetically behave as negative or positive regulators in PAMP-triggered immunity.

Furthermore, subcellular localization assays linked to ROS-burst assays provided important information about the place of action of observed ROSIE´s within the cell. Ectopic expression of the effectors fused to various mislocalisation tags, showed that ROSIE 1 is highly active in the nucleus and the cytosol, while ROSIE 4 acts likely at the cytosolic side of the plasma membrane upon PAMP perception in plants. In contrary, ROSIE 2 and ROSIE 3 demonstrate a strong suppression of ROS in all tested cellular compartments.

The *U. maydis* deletion strains of ROSIE 2 and ROSIE 3 genes did not show any visible virulence defect. A slight but not significant loss of gall formation was however observed for the deletion strain of ROSIE 1.

In summary, this master thesis demonstrates that several plant proteins that are potentially in a complex with ROS-burst inhibiting effectors, either having a positive or negative influence on PTI-signaling in plants adding novel players of the plant Immune network to the puzzle. Additionally, the results shed new light on how the biotrophic fungus *U. maydis* dampens PTI.

ZUSAMMENFASSUNG

Das Erforschen von molekularen Mechanismen die es dem phytopathogenen Pilzen ermöglichen erfolgreich Wirtspflanzen zu kolonisieren, ist ein entscheidender Faktor für die Entwicklung von effektiven Strategien zur Verringerung von Nutzpflanzenbefall. Eine pilzliche Kolonisation bedingt dabei das pflanzlich Immunsystem zu manipulieren und zu überwinden. Die basalen induzierten Abwehrmechanismen einer Pflanze werden durch das Erkennen pathogen assoziierter Molekülen (PAMP-pathogen associated molecule pattern) über spezifische pflanzliche Rezeptoren (PRR-pattern recognition receptor) aktiviert, was letztendlich eine Immunantwort (PTI-PAMP triggered immunity) auslöst. Eine der frühesten Abwehrmaßnahmen stellt die Bildung von reaktiven Sauerstoffspezies im Apoplast (ROS burst) dar, die mit Hilfe der NADPH-Oxidase erzeugt werden. Um diese Erkennungskaskade zu unterbrechen, sekretieren Pathogene kleine Proteinmoleküle in das Wirtsgewebe, die sogenannten Effektoren, die in der Lage sind pflanzenseitig die Immunität zu unterdrücken und den Metabolismus zu manipulieren. Mit Hilfe eines ROS – Burst Screens in dem *Ustilago maydis* Effektoren ohne Signalpeptid in *Nicotiana benthamiana* Pflanzen, produziert wurden, konnte eine Gruppe potenzieller Effektoren identifiziert werden, welche die Bildung von ROS unterdrücken. Dafür wurden 288 *Ustilago maydis* Effektoren getestet, wobei 34 verschiedene Effektoren eine ROS Akkumulation verhindern konnten.

Ziel dieser Studie war es vier dieser Effektorenkandidaten von *Ustilago maydis*, ROSIE1-4 (ROS-burst Inhibiting Effector 1-4) im Zusammenhang mit der Unterdrückung von ROS Bildung näher zu charakterisieren. Im ersten Schritt wurden zur Identifizierung möglicher interagierender Proteine, diese in *Nicotiana benthamiana* exprimiert. Potenziell interagierende Proteine wurden durch Massenspektrometrie nach einer Ko-immunpräzipitation identifiziert und davon wurden 21 für weitere Analysen ausgewählt. Um mehr über die Rolle dieser pflanzlichen Proteine in Bezug auf die PTI zu erfahren, wurden ihre Gene durch Virus-induziertes Gen-Silencing in *Nicotiana benthamiana* gesilenced und ihre transkriptionelle Stilllegung mit qPCR auch überprüft. Die jeweils in einem möglichen Zielgen stillgelegten Pflanzen wurden für ROS-burst assays mit PAMPs behandelt. Interessanterweise führte die transkriptionelle Reduktion bei 8 Genen

zu einer signifikanten Zunahme bzw. Abnahme der ROS Aktivität nach PAMP Behandlung in der Pflanze. Dieses deutet darauf hin, dass sich die mit den ROS-burst interferierenden Effektoren im Komplex befindlichen Wirtsgene mögliche positive oder negative Regulatoren in der ROS-burst vermittelten pflanzlichen Abwehr sind.

Darüber hinaus lieferte ein subzellulärer Lokalisierungstest in Kombination mit ROS burst assays wichtige Informationen über den Ort ihrer Wirksamkeit innerhalb einer Zelle. Nach Flagellinbehandlung konnte beobachtet werden, dass ROSIE 1 bei der ektopischer Expression in verschiedene Zellkompartimente hochaktiv im Kern und im Zytosol ist, während ROSIE 4 seine stärkste Aktivität in der Plasmamembrane zeigte. Hierbei konnte auch gezeigt werden, dass ROSIE 2 und ROSIE 3 eine starke Unterdrückung von ROS in allen getesteten Zellkompartimenten aufweisen.

Ustilago maydis Deletions-Mutanten der entsprechenden Effektor Gene, zeigten keinen sichtbaren Virulenzdefekt. Allerdings konnte für ROSIE 1 eine leichte Abnahme der Gallenbildungsrate in der Pflanze festgestellt werden.

In dieser Masterarbeit konnten mehrere Pflanzenproteine identifizieren werden, die mit ROS-burst inhibierenden Effektoren interagieren und einen direkten positiven oder negativen Einfluss auf das Pflanzenabwehrsystem haben. Diese Ergebnisse werfen ein neues Licht auf mehrere verschiedene Pflanzenproteine und deren Involvierung in die ROS-burst vermittelte pflanzliche Abwehr.

ABBREVIATIONS

%	percent	**dNTP**	deoxynucleoside triphosphate
°C	degree celsius	**dpi**	days post infection
∞	infinty	**DRP1E**	dynamin related protein 1e like
4CL	4-coumarate-coa ligase	**DRP5A**	dynamine-related protein 5a
Aa	amino acids	**ET**	ethylene
ABA	abscisic acid	**HR**	hypersensitive cell death response
AIM1	fatty acid beta-oxidation multifunctional protein aim1-like	**HRP**	horse radish peroxidase
ANOVA	analysis of variance	**JA**	jasmonic acid
ARC5	dynamin-like protein arc5 isoform x1	**kb**	kilobase pair(s)
ARM	agrobacterium resuspension medium	**kDa**	kilodalton(s)
BAK1	brassinosteroid intensive 1-associated receptor kinase	**L**	liter
bp	base pair(s)	**LOX**	lipoxygenase
BR	brassinosteroids	**M**	molar
C4H	trans-cinnamate 4-monooxygenase	**M17L**	myosin 17-like
cDNA	complementary dna	**min**	minute(s)
Ch	chromosome	**MYR**	myristoylation
CK	cytokinin	**NaCl**	natrium chloride
cm	centimeter	**Nb**	nicotiana benthamiana
COPA	coatomer subunit alpha	**NB-LRR**	nucleotide binding/leucin rich repeat
COPB	coatomer subunit beta	**NES**	nuclear export signal
C-terminal	carboxy-terminal	**NFXL1**	nfxl1 type zinc finger protein nfxl1
CXE	nbputative carboxylesterase 120	**ng**	nanogram
ddH20	double distilled water	**NLS**	nuclear localization signal
DMSO	dimethyl sulphoxide	**NPR1**	non expressor of pr genes 1
DNA	deoxyribonucleic acid	**N-terminal**	amino terminal

O_2^-	superoxide	**ROS**	reactive oxygen species
OD_{600}	optical density at 600 nm	**ROSIE**	ros inhibiting effector
OPDA	12-oxophytodienoic acid	**rpm**	rounds per minute
PAGE	polyacrylamide gelelectrophoresis	**RT**	room temperature
PAMP	pathogen-associated molecular pattern	**SA**	salicylic acid
PCD	programmed cell death	**SD**	standard deviation
PCR	polymerase chain reaction	**SDS**	sodium dodecyl sulphate
PDS	phytoene desaturase	**SE**	standard error
PED1	3-ketoacyl-coa thiolase 2	**sec**	second(s)
PIRP	potential interacting rosie proteins	**STPP2A**	serine/threonine protein phosphatase pp2acatalytic subunit
PR	pathogenesis related	**Tris**	trishydroxymethylaminomethane
PRR	pattern recognition receptor	**TRV**	tobacco rattle virus
PS	ponceau staining	**VIGS**	virus induced gene silencing
PTI	pamp-triggered immunity	**Y2H**	yeast two-hybrid
qPCR	quantitative real time pcr	**Zm**	zea mays
RBOHD	respiratory burst oxidases homolog d	**α**	alpha
Rel.	relative	**ß**	beta
RH3	dead-box atp dependent rna helicase 3	**Δ**	deletion
RNA	ribonucleic acid	**µ**	micro

TABLE OF CONTENTS

1. INTRODUCTION

According to the Food and Agricultural Organization of the United Nations (FAO), the global population is predicted to reach almost 10 billion by 2050 placing a high pressure for food production to rise (FAO 2010). To meet rising food demands, increasing plant yields is imperative. One way to achieve it, is to increase crop protection since plants such as rice (*Oryza sativa*), maize (*Zea mays*), wheat (*Triticum ssp*.), and potato (*Solanum tuberosum*) are threatened by a huge number of pathogens causing huge seed losses worldwide (Lanver et al. 2017). From an economical perspective, the most detrimental pathogens are biotrophs (Koeck et al. 2011).

Protecting the crops relies heavily on understanding the fundamentals of plant-defense-responses and the mechanisms of plant-pathogen interactions.

1.1. Fungal pathogens

Fungi are responsible for most plant diseases and cause enormous damage to plant tissue. Most of them belong to the phylum Ascomycota and Basidiomycota. Classifying fungi into the two groups depends on how their sexual spores are formed. Ascomycetes are mainly characterized by forming asci and ascospores, where basidiomycetes produce basidia and basidiospores (Gladieux et al. 2010).

Fungi can also be classified into three categories according to the type of lifestyle they have on their hosts. While necrotrophic fungi, kill the plant to feed of the remains, biotrophic fungi establish an intimate interaction with its host to exploit living plant tissue. Additionally, a functional intermediate group, the hemibiotrophs are sharing characteristics of the other groups (Doehlemann et al. 2017).

1.1.1. Plant - pathogen interaction

A successful interaction between a plant and its pathogen relies on mutual communication. The importance to sense and recognize a potential pathogen and defend itself is on one hand a crucial factor for the plant survival, whereas on the other hand the pathogen needs to create a successful zone that suits for its growth and reproduction through manipulating the host environment (Li and Zhang 2016). To enable the

communication between both, plant and pathogen, molecular signals and gene regulation are involved in plant infection mechanism and host responses. In the plant apoplast, the first interaction is mediated, by which the plant recognizes fungal elicitors also known as pathogen-associated molecular patterns (PAMPs) with their membrane-localized pattern recognition receptors (PRRs) located on the plasma membrane (Gupta et al. 2015). Successful recognition of fungal derived PAMPs by PRRs leads to activation of PAMP-triggered immunity (PTI) which is the first line of plant defense responses. One way to overcome and dampen plant defenses is by delivering small protein molecules so called “effectors” into the plant tissue, which suppresses the components of the PTI. Contradictory, plants evolved resistance genes (R) that recognize effectors, secreted from the pathogen and activate the effector triggered immunity (ETI). The R genes encode nucleotide binding/leucine rich repeat (NB-LRR) proteins that sense the effector, or the changes mediated by it. In case of an attempted effector attack on the plant targets, NB-LRRs directly bind to the effector and trigger the ETI. This effect often leads to a hypersensitive response which as consequence causes apoptosis in the plant (Boyd et al. 2013) (Figure 1).

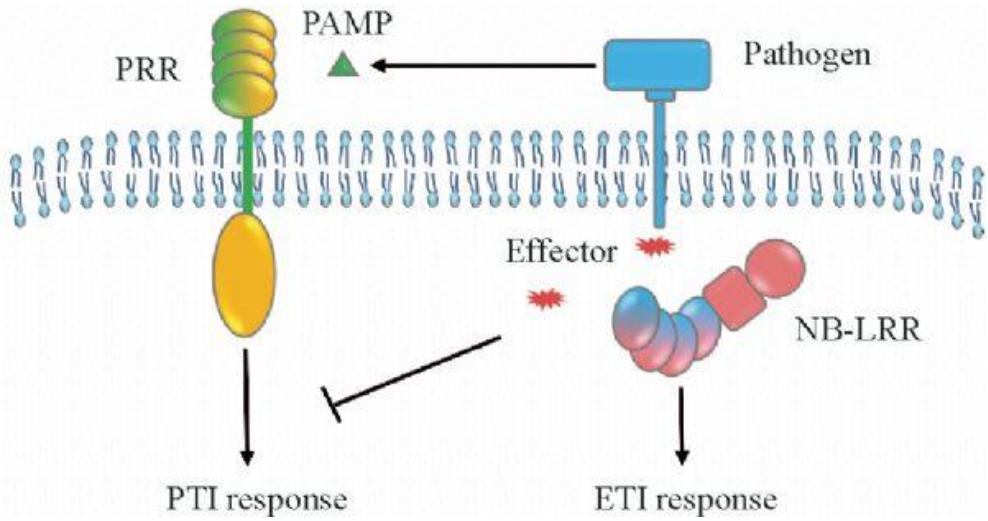

Figure 1: Plant defense responses. Plants recognize pathogen associated molecular patterns (PAMPs) released from pathogens with on the surface of the plasma membrane lying pattern recognition receptors (PRR) which activate the PAMP triggered immunity (PTI). To dampen PTI, pathogen also secrete effectors into the plant. They are then recognized by nucleotide binding/leucine-rich-repeat NB-LRR proteins and initiate effector-triggered immunity (ETI). Image adapted from: Li and Zhang 2016.

1.1.2. Fungal effectors

A successful infection of plants is achieved by the secretion of small protein molecules so called fungal effectors. These effectors can be secreted either outside the plant cell and are termed as apoplastic effectors (Mueller et al. 2013), or they can be translocated inside the plant cell and are referred to as cytoplasmic effectors (Tanaka et al. 2014). The implementation of an effective infection and effector secretion can be first established after the pathogen is in a direct contact with the plant (Lo Presti et al. 2015). Fungal effectors mainly play a key factor in suppressing the plant innate immunity system. However, they have also been identified to have other functions. Some of the effectors act like self-modifiers and alter the cell wall of the pathogen to minimize the recognition upon invasion. While, some of them were identified to be activators, where they are degrading interacting plant proteins to modify plant biological processes (Uhse and Djamei 2018).

1.2. *Ustilago maydis* – model system for fungal pathogenicity

Model organisms in molecular biology have contributed enormously to our knowledge about the insights into fundamental processes in life. A well-established model organism to study plant-pathogen interaction is the biotrophic fungus *Ustilago maydis* (Basse and Steinberg 2004). This basidiomycete fungus, also known as corn smut, infects *Zea mays* and its predecessor Teosinte and proliferates and develops in these hosts (Kämper et al. 2006). The prominent macroscopic infection symptoms are galls which are induced all over the aerial parts of the plant. (Bölker 2001). The availability of public genome data, as well as the ability to grow under controlled laboratory conditions, makes it accessible for genetic manipulation and therefore it is used extensively in biological research (Steinberg and Perez-Martin 2008).

1.2.1. The life cycle of *Ustilago maydis*

The pathogenic development of the smut fungus *Ustilago maydis* begins with teliospore germination (Brefort et al. 2009), and through the process of meiosis haploid basidiospores are formed. The actual invasion of the plant starts first by fusing two nonpathogenic haploids of compatible mating type (conjugated tubes) together which leads to the formation of a dikaryotic filament (J. et al. 2012). Now, during this stage the fungus is able to generate an appressorium that induces a successful penetration inside

the plant (Castanheira and Pérez-Martín 2015), either by secreting lytic enzymes or mechanical force which leads to cell wall modification (Lanver et al. 2014). After successful penetration, the fungus starts proliferating within the host cell eliciting the formation of galls. To accomplish its life cycle, *Ustilago maydis* hyphae starts to fragment and differentiate resulting in karyogamy creating diploid teliospores. In this state, which is also known as the resting state, teliospores germinate and undergo meiosis to form again haploid sporidia (Banuett and Herskowitz 1996) (Figure 2).

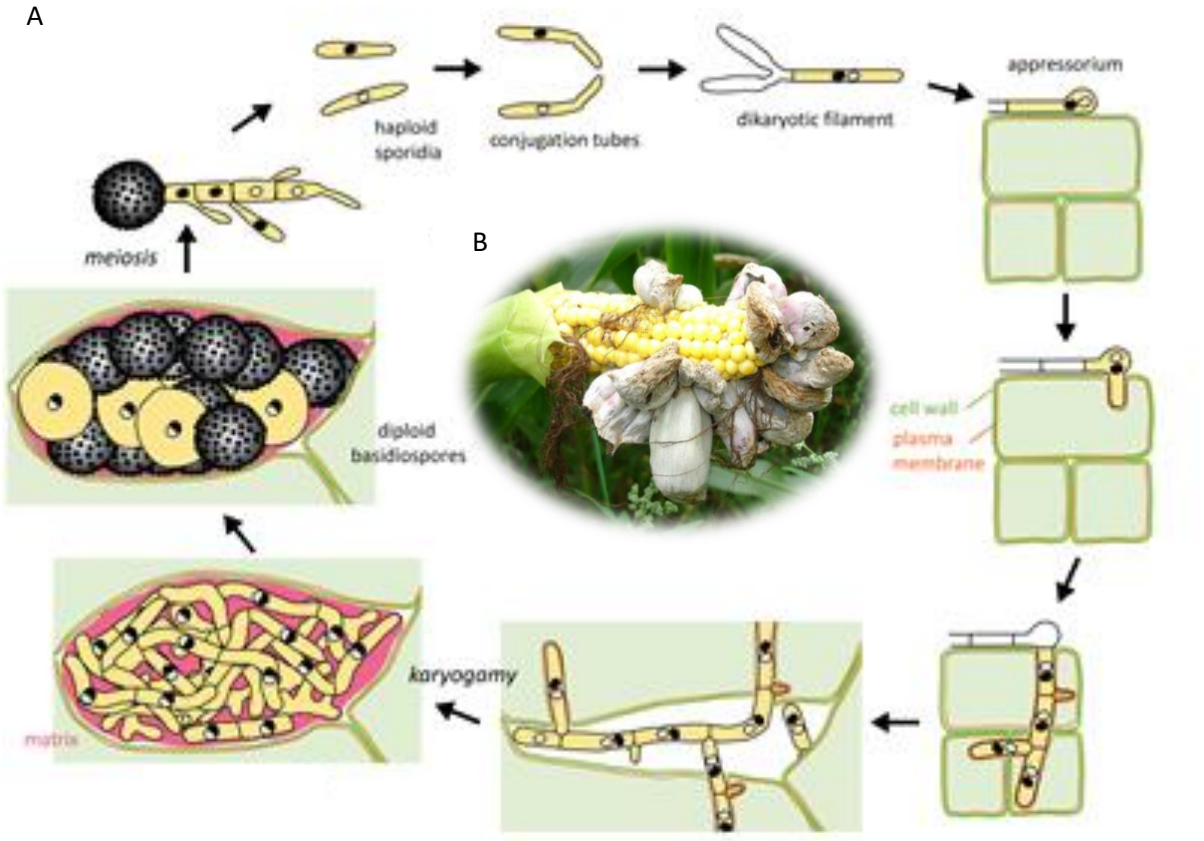

Figure 2: The life cycle of *Ustilago maydis*. (A) Two sporidia with different matting types (shown by black and white colored nuclei) form conjugated tubes resulting in a dikaryotic filament. Plant invasion is supported by an infection structure called appressorium. In this way the fungus can penetrate and colonize the plant successfully forming galls. Nuclear fusion occurs and leads to spore formation. Diploid spores germinate and undergo meiosis producing haploid sporidia. A new cycle is entered. Image adapted from: Lay Sun Ma, original from: Lanver et. al. 2017 (B) Gall formation on *Zea mays*. Image adapted from: Kai Hirdes, 2006

1.2.2. *Ustilago maydis* effectors

The "*Ustilago maydis* genome project" was undertaken at the Broad Institute and the genome was sequenced using the haploid *Ustilago maydis* strain 521 at 10x coverage with the use of whole genome shotgun (Kämper et al. 2006). By its genome size of approximately 20.5 mega base pairs corresponding to 23 identified chromosomes, 6,784 proteins were identified to be expressed by the fungus. Out of them, 467 are potentially secreted proteins of which 203 cannot be ascribed any functional or structural domain (Lanver et al. 2017). In addition, sequencing the *Ustilago maydis* genome also revealed that some of the secreted proteins are contained in 12 clusters on the chromosome. Expression analysis of these clustered genes showed transcriptional upregulation in infected plant tissue. However, deleting complete individual cluster genes did only show in four of the twelve clusters reductions of virulence (Kämper et al. 2006).

Effectors remain key players in altering host functions during pathogenicity. They either have a functional role in the intercellular space to hold the first layer of plant defense or act inside the cell to execute transcriptional and metabolic changes of the host. For most effectors, despite their pathogenic impact, single deletions of *Ustilago maydis* effectors did not necessarily lead to reduced virulence, which is probably due to functional redundancy. So far in the functional effector research only a few *Ustilago maydis* effectors have been functionally characterized (Lanver et al. 2017).

The effectors Pep1 (Protein essential for penetration 1) and Pit2 (Protein involved in tumors 2) were identified to be apoplastic effectors. As seen in figure 3A, Pit2 is involved in plant defense suppression and inhibition of host cysteine proteases (Doehlemann et al. 2011; Mueller et al. 2013). Pep1 is known to be involved in penetration and also inhibits ROS activity in the apoplast of the host (Doehlemann et al. 2009; Hemetsberger et al. 2012). Deletion strains of both Pit2 and Pep1 result in virulence defect in infected *Zea mays* (Figure 3A and B).

Translocated cytoplasmic *Ustilago maydis* effector that has been so far described, is the chorismate mutase Cmu1 which contributes to virulence by preventing salicylic acid synthesis by rechanneling chorismate into the phenylpropanoid pathway (Djamei et al. 2011). The effector Tin2 (Tumor inducing 2) targets secondary plant metabolites by

interacting with the maize kinase ZmTTK1 that regulates the anthocyanin biosynthetic pathway by decreasing lignin biosynthesis (Tanaka et al. 2014) (Figure 3C and D).

In addition to the above-mentioned effectors, See1 (Seedling efficient effector1) is an effector which is considered to disrupt the cell cycle, resulting in DNA synthesis reactivation and cell division in infected *Zea mays* leaves (Redkar et al. 2015) (Figure 3E).

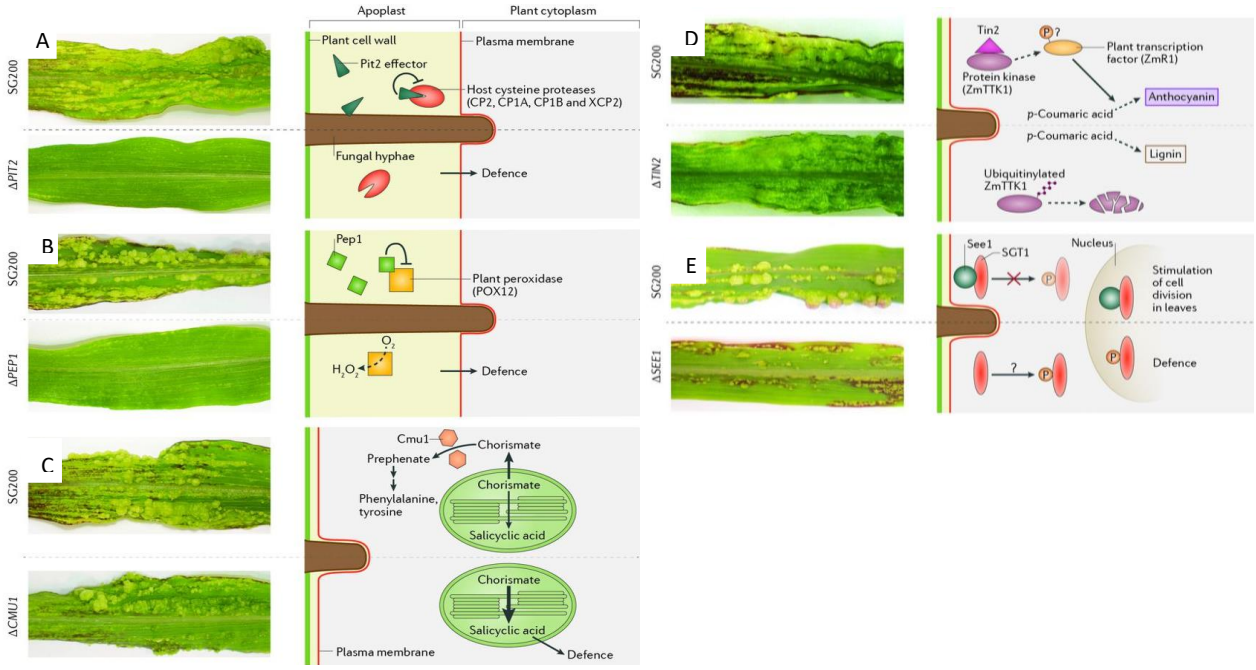

Figure 3: Some of functionally characterized *Ustilago maydis* effectors. Apoplastic effectors (A) Pit2 and (B) Pep1, and translocated cytoplasmic effectors (C) Cmu1, (D) Tin2 and (E) See1. Left panel: Maize leaves 12 dpi with the solopathogenic strain SG200 and the respective effector deletion mutant. Right Panel: Molecular function of the respective effectors. Image adapted from: (Lanver et al. 2017).

1.3. Plant defense responses

To improve their survival and reproduction, plants evolved various strategies to defend themselves against fungi and other herbivores. Besides the constitutive defense responses, plants contain an induced immune response which develops only after attack (Fürstenberg-Hägg et al. 2013). Induced plant responses rely on pathogen recognition and is regulated by a network of signaling molecules that activates signaling pathways (Thatcher et al. 2005). A significant role in plant protection plays primary signaling molecules such as salicylic acid (SA), jasmonic acid (JA) and ethylene (ET) (Koornneef and Pieterse 2008). Other hormones have also been implicated in plant defense signaling pathway, like abscisic acid (ABA), auxin, gibberellic acid (GA), cytokinin (CK) and

brassinosteroids (BR) (Bari and Jones 2009). However, their role is better known to be involved in plant stress as well as in plant growth and development. In plant defense they usually function in conjunction with primary defense molecules (Kazan and Lyons 2014).

1.3.1. Pathogen recognition and induction of resistance

Upon pathogen attack, plants activate different mechanisms of defense such as stomatal closure to prevent penetration (Underwood et al. 2007), reduction of nutrient efflux in the apoplast to arrest pathogenic growth (Wang et al. 2012), generating reactive oxygen species (ROS) which harm the pathogen (O'Brien et al. 2012) and plays a role as signaling molecules (Torres et al. 2006), as well as programmed cell death (PCD) inducing hypersensitive response (HR) to limit pathogen progression (Camagna and Takemoto 2018).

As mentioned before, plant hormones such as SA, JA and ET play a crucial role during pathogenic outbreaks and coordinate a complex network of signaling pathways (Bigeard et al. 2015).

In the year 1979 White already demonstrated the important role of SA in defense responses, which get activated in a complex system of defense signaling pathways upon pathogen perception. One important player in SA signaltransduction is NPR1 (Nonexpressor of PR genes 1) which is translocated to the nucleus to activate SA-responsive genes which occurs as part of the SA-triggered defense response (Mou et al. 2003).

Jasmonic acid is another important defense hormone. It is known to be activated in defenses against necrotrophs (Glazebrook 2005). One of the biosynthetic intermediates of JA is 12-oxophytodienoic acid (OPDA) during plant defense (Staswick and Tiryaki 2004). As JA and SA act antagonistically, biotrophic pathogen make this to their advantage to promote infection by JA signaling activation (Takahashi et al. 2004).

Together with SA and JA, another significant defense related hormone, ethylene has been shown to be involved in the pathogen-induced response by expressing numerous defense-related genes (Thomma et al. 1999). A master regulator of the ET signaling pathway is EIN3 (Ethylene-insensitive 3), a transcriptional factor that initiates downstream transcription cascades upon ethylene responses (Boutrot et al. 2010).

1.3.2. ROS burst – early plant defense response

The production of ROS in the apoplast is the first indication of a pathogen recognition from the plants site. The recognition of an intruder is regulated through plant receptors on the plant plasmamembrane which trigger upon activation an oxidative burst mediated by plant NADPH oxidases respiratory burst oxidases homolog D (RBOHD) (Kadota et al. 2015). The best studied PRR is the Arabidopsis receptor FLS2 which directly recognizes the bacterial flagellin flg22 (immunogenetic peptides of flagellin) (Kadota et al. 2014). Interestingly, FLS2 is able to activate the downstream responses first by interacting with its coreceptor BAK1 (Brassinosteroid intensive 1-associated receptor kinase (Sun et al. 2013). Interaction of these two receptors leads to cross-phosphorylation and also BIK1 (Botrytis-induced kinase 1) becomes phosphorylated (Lu et al. 2010; Macho and Zipfel 2014) and triggers RBOHD activation which catalyze the production of superoxide (O_2^-) that can then be converted into hydrogen peroxide (H_2O_2) by peroxidases (Torres and Dangl 2005) (Figure 4). This oxidative burst is linked to plant responses by acting as signal molecules to control cellular activities.

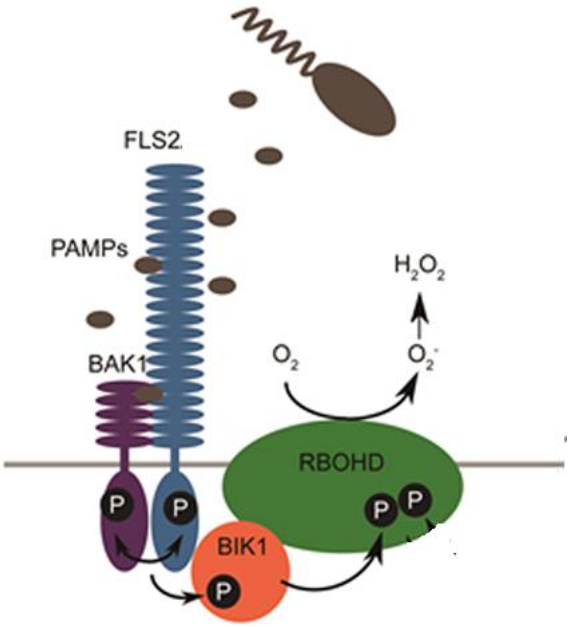

Figure 4: Regulation of ROS burst upon pathogen perception. Flagellin recognition (flg22) by plant receptors FLS2 and BAK1 which activates BIK1 phosphorylation and so triggers ROS accumulation mediated by RBOHD. Image adapted from: (Kadota et al. 2014).

Since the pathogen secretes also effector proteins besides PAMPs to invade and colonize plants, as described before, these effectors are capable of suppressing plant defense responses and alter its physiology. Some of the effectors can suppress ROS accumulation and therefore prevent the plant to sense pathogen invasions as shown in figure 5. How the direct linking of effectors and ROS signaling network in plants works are not fully understood.

Improved understanding of effector functions by which they suppress plant defense responses will be the key in decreasing vulnerability of crop plants towards pathogens.

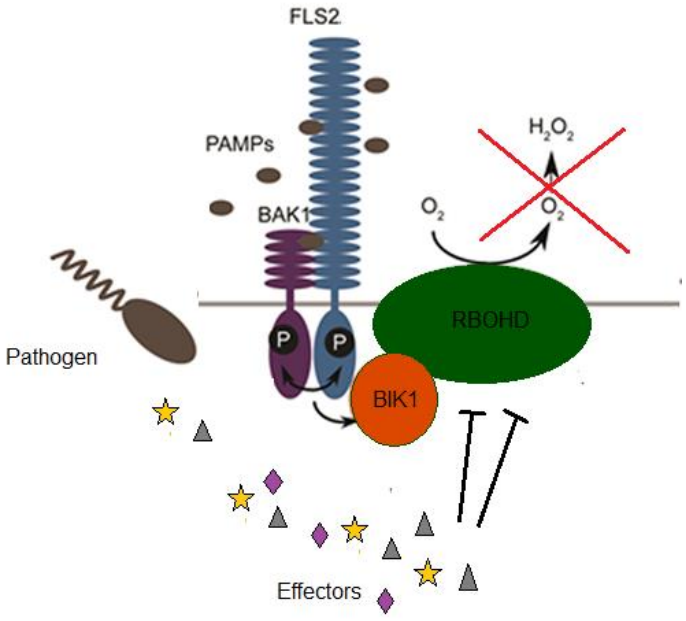

Figure 5: ROS burst suppression by pathogen released effectors. Effectors target plants signaling molecules to dampen plant defenses and successful colonize its host plant. Image adapted and modified from: (Kadota et al. 2014).

1.4. Aims of the study

In an attempt to investigate effectors which may account for ROS burst suppression in plants, ROS burst suppression screening of 288 *Ustilago maydis* effectors has been performed by Fernando Navarrete. This was done by heterologous expression of the candidate effectors lacking a signal peptide in *Nicotiana benthamiana*. In his study, he was able to identify 34 effectors, showing ROS inhibition upon flagellin treatment.

The primary aim of this research is to get an understanding of the functions and mode of action of four selected *Ustilago maydis* effectors, named ROS Inhibiting Effectors, ROSIE 1 (UMAG_04039), ROSIE 2 (UMAG_05927), ROSIE 3 (UMAG_02826) and ROSIE 4 (UMAG_06119). All ROSIEs show either a completely or partially ROS-suppression activity when expressed in plants. This master thesis therefore intends to provide first insights in their biological function and how they ultimately dampen PTI. To achieve this, mentioned effectors will be transiently expressed in *Nicotiana benthamiana* plants to identify potential interacting proteins, identified by mass spectrometry after co-immunoprecipitation. To further explore their involvement in the PTI of plants, virus induced gene silencing will be performed and ROS activity will be monitored via a luminol based assay.

This study seeks also to perform a subcellular localization assay to get important information about the activity of the tested *Ustilago maydis* effectors within the cell. Here we will assign the protein into particular cellular compartments such as to the plasma membrane, the cytosol or the nucleus to monitor ROS activity.

Finally, this study will also include a virulence assay where we will determine whether knocking out each of the four *Ustilago maydis* effectors one by one causes a virulence defect upon maize seedling infection.

2. RESULTS

To illuminate potential ways by which *U. maydis* effectors ROSIE 1-4 suppress ROS production after pathogenic invasion, different assays were performed in *N. benthamiana* and *Z. mays* plants. This part of the master thesis will include a virulence assay performed on *Z. mays* by knocking out some of the ROS inhibiting effectors of *U. maydis*. Further, a subcellular localization assay will provide important information about the effector activity within the cell. Potential interacting ROSIE proteins previously identified by mass spectrometry will be silenced through VIGS and its ROS activity will be monitored, to shed new light on the function of these effectors.

2.1. Characterization of ROSIEs

Among the 34 identified *U. maydis* effectors in the ROS burst screen done by Fernando Navarrete, ROSIE 1-4 did show ROS-burst-inhibiting effects upon flagellin treatment. As demonstrated in table 1, these effectors are located on different chromosomes and their protein sequence have a length ranging from 166 to 521 amino acids with a molecular weight from 19117 to 56224.5 Da. Their isoelectric point ranges from 6.6 to 9.4 and they all are predicted to contain signal peptides.

ROS burst screen of studied *U. maydis* effectors, as shown in Figure S1, indicate that ROSIE 1 and ROSIE 3 inhibit ROS accumulation completely when transiently expressed in *N. benthamiana*. Whereas, the other two ROS inhibitors, ROSIE 2 and ROSIE 4, partially suppressed the production of ROS induced by flagellin.

Table 1. Characteristics of the four ROS Inhibiting Effectors

	Genetic Locus	Protein Length (aa)	Molecular Weight (DA)	Isoelectric point	Signal Peptide	Cluster	ROS Burst Inhibition
ROSIE 1	*Ch. 11*	*166*	*19117.0*	*9.1*	√	*X*	*Completely*
ROSIE 2	*Ch. 20*	*370*	*42270.9*	*9.4*	√	*X*	*Partially*
ROSIE 3	*Ch. 07*	*399*	*44754.7*	*6.6*	√	*X*	*Completely*
ROSIE 4	*Ch. 21*	*521*	*56224.5*	*8.8*	√	*X*	*Partially*

2.2. Deletion strains of ROSIE 1 show a tendency of a virulence defect during seedling infection

To determine if ROSIE 1-3 cause an alteration of virulence in *Z. mays*, deletion strains previously generated in the solopathogenic haploid strain SG200 were tested. Plant infections were performed with the variety EGB (Early Golden Bantam) by injecting seedlings after seven days. The experiment was performed in triplicates and symptoms were scored as described by Kamper et al. (2006) twelve days post infection (Figure 6).

The results of the virulence assay illustrate that none of the tested deletion strains contribute significantly to virulence during seedling infection under the tested conditions. This fact might be due to redundancy and could account for the lack of a detectable virulence phenotype. However, deletion strains of ROSIE 1, indicate a slight but not statistically significant tendency to be impaired in virulence compared to the reference strain SG200. Another observation to be noted is that one deletion strain of ROSIE 3 showed a significant reduction of virulence but was not taken into consideration since the other two tested deletion strains did not indicate an impaired virulence implicating additional mutations in this specific deletion strain.

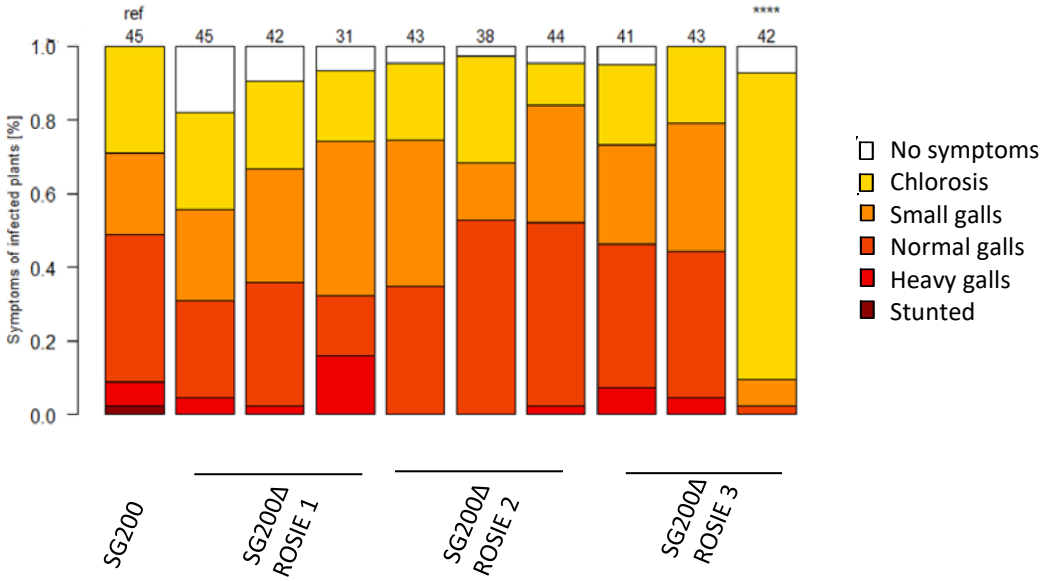

Figure 6: Deletion of *ROSIE 1-3* does not significantly alter the virulence of *U. maydis* in seedling infections. Disease symptoms of maize seedlings were determined twelve days post infection. Disease symptom categories are color-coded and depicted on the right; the darker the color the more severe the symptoms. Experiments were performed in triplicates. Mean values from three independent infections are shown with the total number of infected plants above each column. No significant differences in disease

symptoms were scored. Significance was tested by employing Fisher's exact test with Benjamini-Hochberg multiple testing correction.

This master thesis is not showing the virulence impact of ROSIE 4 on *Z. mays* seedling since deletion strains were not generated successfully.

2.3. ROS burst activity of ROSIE 1-4 in different cellular compartments

To test for the effectors activity within the plant cell, the effectors were tagged with different localization tags either at its C- or N-terminus and expressed under the constitutive strong promoter 35S or Ubiquitin 10 promoter (Ubq10) *in N. benthamiana*. By doing this, the effectors were forced to be active in only one cell compartment such as the plasma membrane (tagged with the myristoylation tag - MYR), the nucleus (tagged with the nuclear localization signal - NLS) or the cytosol (tagged with the nuclear export signal - NES). Microscopic analysis confirmed the correctness of the subcellular localization constructs as seen in Figure S2. The control plant was infiltrated with mCherry. Leaf discs were punched after 1 or 2 days post infiltration and measured one day after for ROS burst activities, respectively. Three biological replicates were performed using *N. benthamiana* plants grown in a controlled chamber.

2.3.1. ROSIE 1 suppresses ROS production in the nucleus and the cytosol

To elucidate the importance of ROSIE 1 and its impact on suppressing the accumulation of ROS during a pathogenic attack, ROS burst activity was measured upon flagellin induction. For this purpose, ROSIE 1 was fused to different localization tags and expressed under the constitutive strong promoter 35S. (see Material and Methods section 4.5.1 Strains and Plasmids, for ROSIE 1 constructs used for subcellular localization assay). The agroinfiltration was carried out in 2 leaves of 4 weeks old *N. benthamiana* plants. Previous agroinfiltration of ROSIE 1 with an OD_{600} of 0.2, showed a complete suppression of ROS burst in all cellular compartments as seen in figure S3A. Also, expressing ROSIE 1 subcellular localization constructs under a less strong promoter, the Ubq10 promoter by agroinfiltration with an OD_{600} at 0.2, did not seem to lower the activity of ROS suppression in any of the cell compartments (see figure S3B). Therefore, plants were agroinfiltrated with an OD_{600} at 0.05, and 3 days post infiltration leaf samples were used for ROS activity measurements.

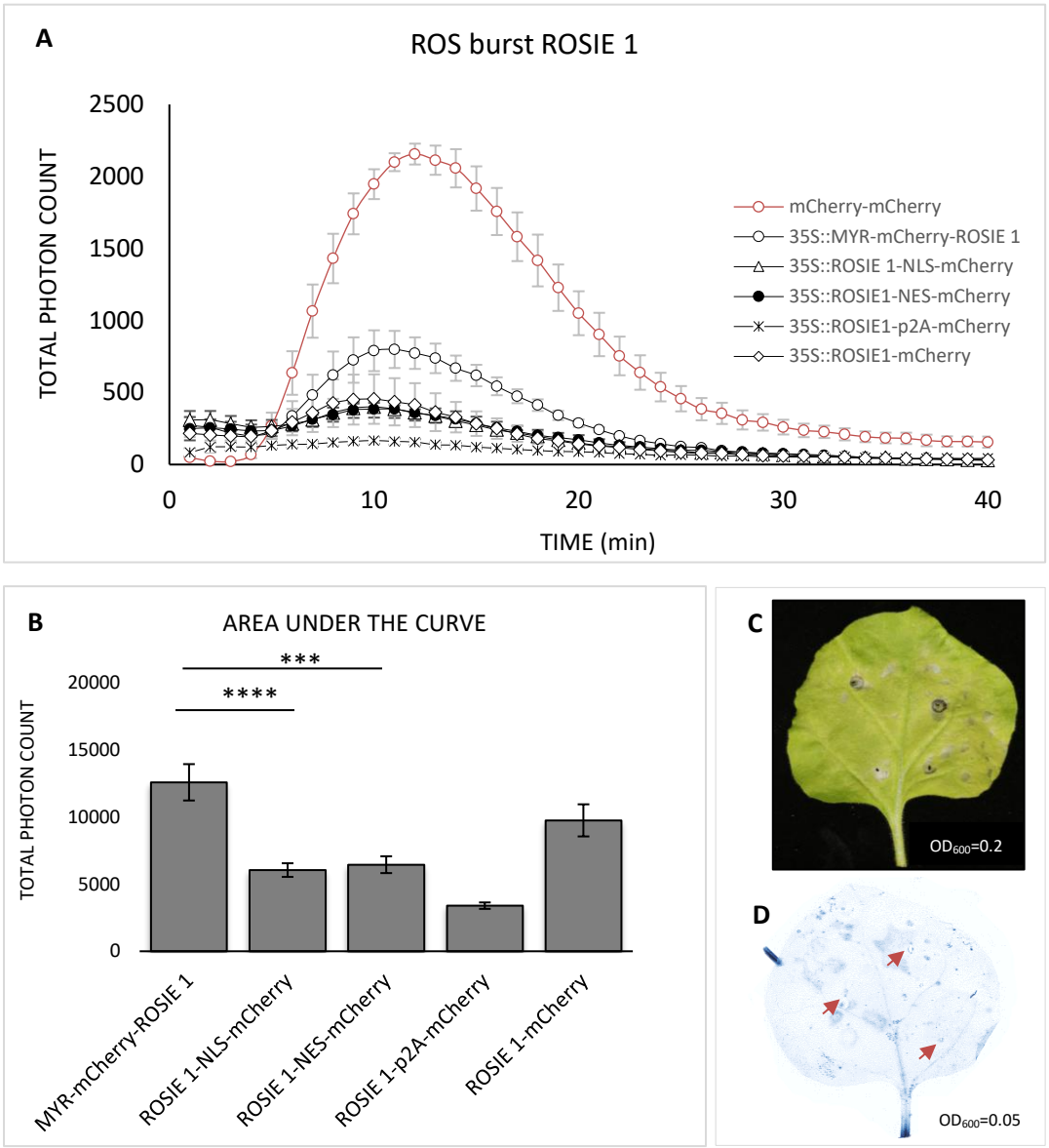

Figure 7: ROSIE 1 shows suppression of ROS burst in the nucleus and the cytosol. (A) Flg22-induced ROS burst activity in different cellular compartments of *N. benthamiana*. Leaf discs from 4-weeks old plants were treated with flagellin and ROS was recorded as emitted light over time. **(B)** Flg22-induced ROS production in the indicated genotypes is represented as the integrated area under the curve measured during 40 min and referred to as total photon count. Results are presented as mean ± SE (N=15) for three independent experiments. Asterix indicate a significant difference (P < 0332-*; .0021-**; .0002-***; <.0001-****, ANOVA, Multiple Mean Comparison; Tuckey test). **(C)** *N. benthamiana* leaf infiltration with ROSIE 1-mCherry and **(D)** Trypan blue staining for cell death observation (Arrows indicate infiltration areas).

Comparing the activity of the effector subcellularly, no obvious difference was observed between the nucleus and cytosol relative to ROS burst suppression, respectively (Figure 7A and 7B). On the other hand, when looking at the effectors activity in the plasma membrane it shows an increase of ROS burst, indicating lower activity of

the effector in this cellular compartment. Furthermore, to assess if cell death might have an impact on the measurements, ROSIE 1-mCherry was infiltrated in *N. benthamiana* leaves with an OD_{600} of 0.2 and were observed 10 days post infection on the phenotype for cell death. An additional test has been performed with trypan blue staining after 3 days post infection with an OD_{600} of 0.05. As seen in figure 7C and 7D, cell death did not have an influence on the measurements, respectively.

2.3.2. ROSIE 2 suppresses ROS production most probably in the cytosol

To clarify the cellular function of ROSIE 2, subcellular localization was done as described before and ROS suppressive was measured upon flg22 induction, respectively. Therefore, ROSIE 2 subcellular localization constructs were expressed under the constitutive strong promoter 35S. (see Material and Methods, section 4.5.1, Strains and Plasmids, for ROSIE 2 constructs used for subcellular localization assay). The agroinfiltration was carried out in 2 leaves of 4 weeks old *N. benthamiana* plants with an OD_{600} of 0.2, and ROS activity was monitored 3 days post infiltration.

A slight decreasing tendency of ROS activity was observed in the cytosol in comparison to the nucleus and the plasma membrane. However, this fact was not shown to be statistically significant (Figure 8A and 8B).

Furthermore, to assess if cell death might have an impact on the measurements, ROSIE 2-mCherry was infiltrated in *N. benthamiana* leaves with an OD_{600} of 0.2 and were observed 10 days post infection on the phenotype for cell death. An additional test has been performed with trypan blue staining after 3 days post infection with an OD_{600} of 0.2. As seen in figure 8C and 8D, cell death did not have an influence on the measurements, as anticipated.

Therefore, it can be speculated that ROSIE 2 is most likely suppressing ROS burst mainly in the cytosol.

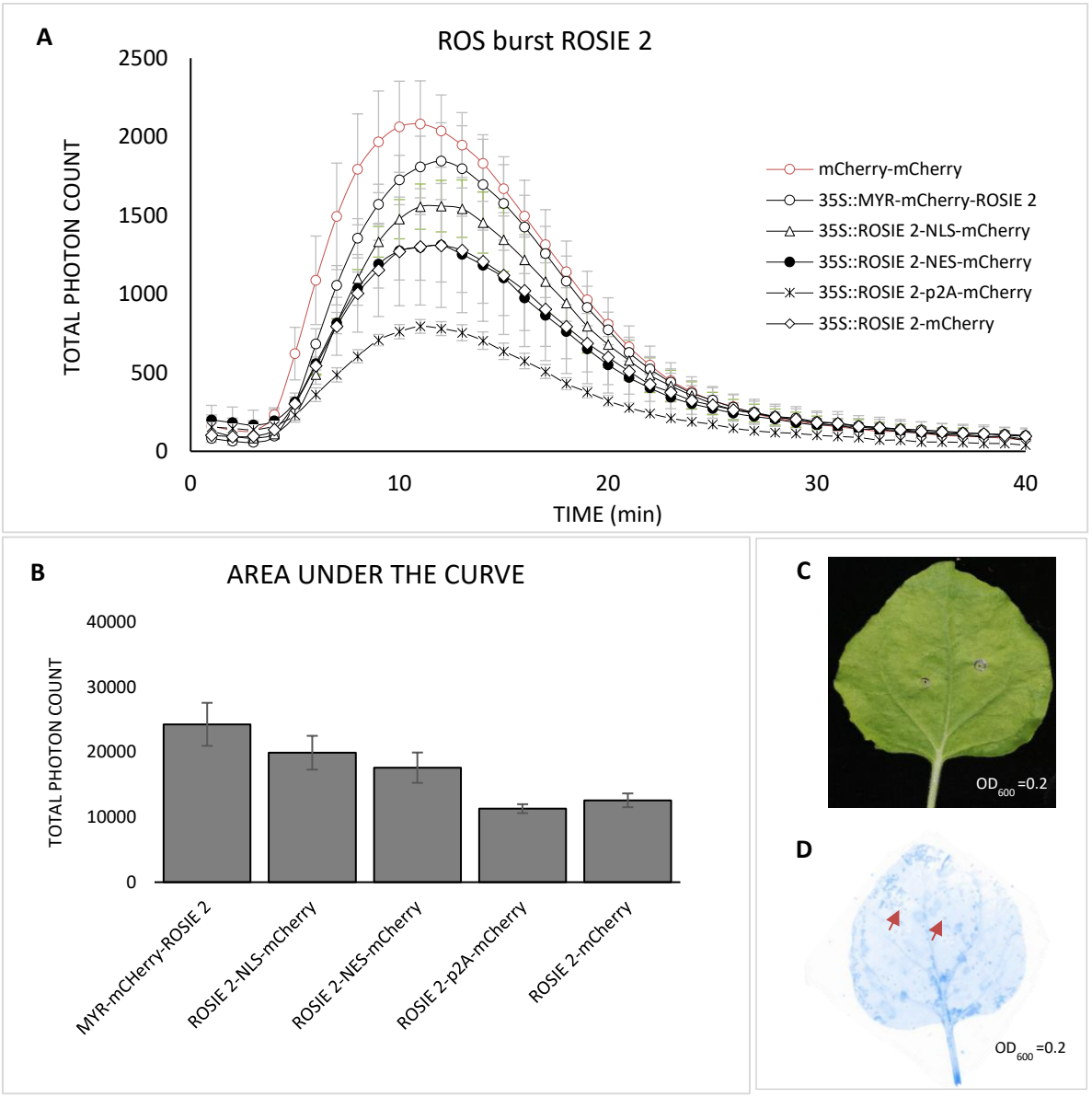

Figure 8: ROSIE 2 shows suppression of ROS burst in the cytosol. (A) Flg22-induced ROS burst activity in different cellular compartments of *N. benthamiana*. Leaf discs from 4-weeks old plants were treated with flagellin and ROS was recorded as emitted light over time. **(B)** Flg22-induced ROS production in the indicated genotypes is represented as the integrated area under the curve measured during 40 min and referred to as total photon count. Results are presented as mean ± SE (N=15) for three independent experiments. **(C)** *N. benthamiana* leaf infiltration with ROSIE 2-mCherry and **(D)** Trypan blue staining for cell death observation (Arrows indicate infiltration areas).

2.3.3. ROSIE 3 suppresses ROS production at the plasma membrane, in the cytosol and the nucleus

To get an insight into the ROS suppressing activity of ROSIE 3 within the cell, ROS burst was monitored upon flg22 induction.For this purpose, subcellular localization tags as mentioned before were fused to the effector protein and expressed under the strong constitutive promoter 35S (see Material and Methods, section 4.5.1. Strains and Plasmids, for ROSIE 3 constructs used for subcellular localization assay). The agroinfiltration was carried out in 2 leaves of 4 weeks old *N. benthamiana* plants with an OD_{600} of 0.2. ROS burst activity was observed 3 days post infiltration and similarly to ROSIE 1, a suppression of ROS burst could be seen in all subcellular compartments (Figure S4A).

Assuming that the expression under the 35S promoter facilitates higher expressions of the construct within the plant cell, subcellular localization constructs were designed with a less strong promoter activity, the Ubq10 promoter (see Material and Methods, section 4.5.1. Strains and Plasmids, for ROSIE 3 constructs used for subcellular localization assay). Therefore, agroinfiltration was done into *N. benthamiana* plants with an OD_{600} at 0.2 and ROS activity was measured 3 days post infiltration. Identical to 35S promoter, expressing the subcellular localization constructs under the Ubq10 promoter did not seem to lower the effector activity in relation to ROS performance (Figure S4B). To further lower the expression levels, same constructs under the Ubq10 promoter were agroinfiltrated into *N. benthamiana* with the same optical density, however, measurements of ROS activity were performed after 2 days post infiltration (Figure 9A and 9B). Despite the fact of enhancing the ROS activity, it did not give a clear indication where in the cell it is most likely to be active.

Furthermore, to assess if cell death might have an impact on the measurements, ROSIE 3-mCherry was infiltrated in *N. benthamiana* leaves with an OD_{600} of 0.2 and were observed 10 days post infection on the phenotype for cell death. An additional test has been performed with trypan blue staining after 3 days post infection with an OD_{600} of 0.05. As seen in figure 9C and 9D, cell death did not have an influence on the measurements, respectively. Even though, plants did not indicate cell death, infiltrated leaves showed a yellowish phenotype, which might be related to some stress response of the plant.

Thus, it appears that ROSIE 3 suppresses ROS activity in all exploratory subcellular compartments within the plant upon flg22 perception.

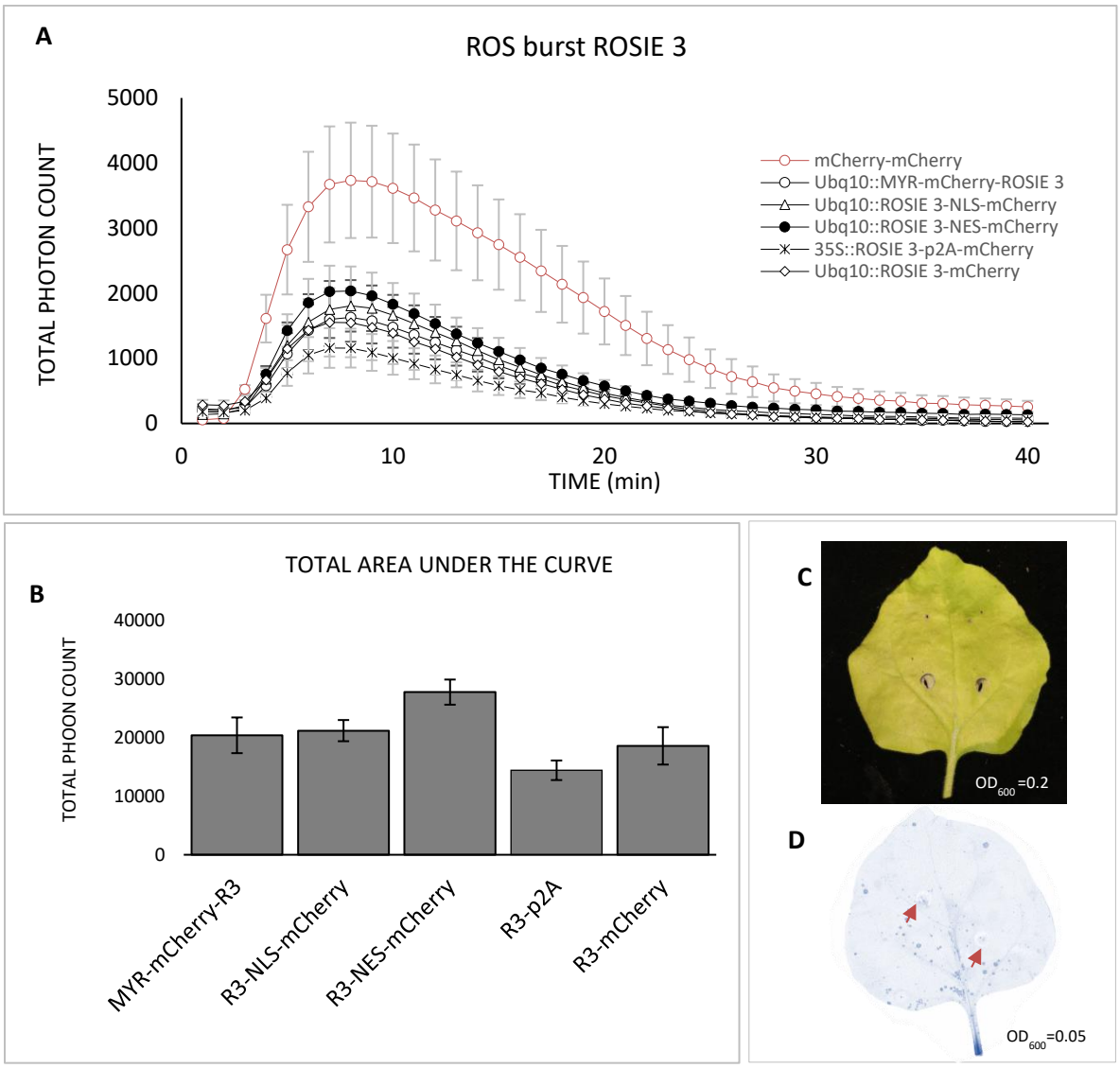

Figure 9: ROSIE 3 shows suppression of ROS burst in all subcellular compartments. (A) Flg22-induced ROS burst activity in different cellular compartments of *N. benthamiana*. Leaf discs from 4-weeks old plants were treated with flagellin and ROS was recorded as emitted light over time. **(B)** Flg22-induced ROS production in the indicated genotypes is represented as the integrated area under the curve measured during 40 min and referred to as total photon count. Results are presented as mean ± SE (N=15) for three independent experiments. **(C)** *N. benthamiana* leaf infiltration with ROSIE 3-mCherry and **(D)** Trypan blue staining for cell death observation (Arrows indicate infiltration areas).

2.3.4. ROSIE 4 suppresses ROS production at the plasma membrane

To determine and understand the cellular function of ROSIE 4, subcellular localization was done as described before and ROS activity was measured upon flg22 induction, respectively.

Therefore, ROSIE 4 subcellular localization constructs were expressed under the constitutive strong promoter 35S. (see Material and Methods, section 4.5.1. Strains and

Plasmids, for ROSIE 4 constructs used for subcellular localization assay). The agroinfiltration was carried out in 2 leaves of 4 weeks old *N. benthamiana* plants with an OD_{600} of 0.2, and ROS activity was monitored 3 days post infiltration. In contrast to ROSIE 1 which showed to be most active in the nucleus and cytosol, ROSIE 4 showed the highest suppression of ROS production at the plasma membrane as seen in figure 10A and 10B. Furthermore, to assess if cell death might have an impact on the measurements, ROSIE 4-mCherry was infiltrated in *N. benthamiana* leaves with an OD_{600} of 0.2 and were observed 10 days post infection on the phenotype for cell death. An additional test has been performed with trypan blue staining after 3 days post infection with an OD_{600} of 0.2. As seen in figure 10C and 10D, cell death did not have an influence on the measurements, respectively.

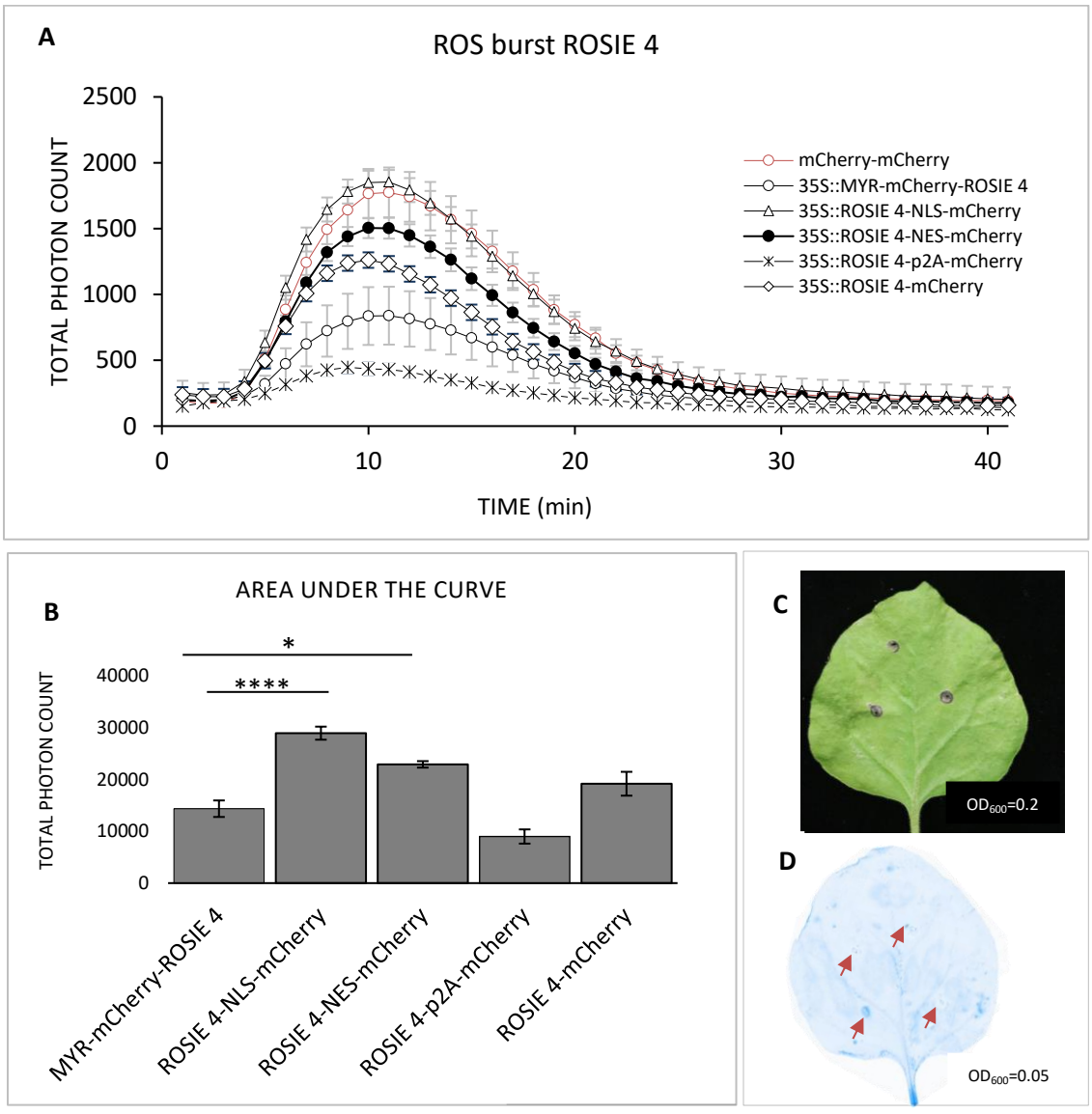

Figure 10: ROSIE 4 shows significant suppression of ROS burst in the plasma membrane. (A) Flg22-induced ROS burst activity in different cellular compartments of *N. benthamiana*. Leaf discs from 4-weeks old plants were treated with flagellin and ROS was recorded as emitted light over time. **(B)** Flg22-induced ROS production in the indicated genotypes is represented as the integrated area under the curve measured during 41 min and referred to as total photon count. Results are presented as mean ± SE (N=15) for three independent experiments. Asterix indicates a significant difference (P < 0332-*; .0021-**; .0002-***; <. 0001-****, ANOVA, Multiple Mean Comparison; Tuckey test). **(C)** *N.benthamiana* leaf infiltration with ROSIE 4-mCherry and **(D)** Trypan blue staining for cell death observation (Arrows indicate infiltration areas).

2.4. Protein Detection and Mass Spectrometry analysis of ROSIEs

To further investigate the role of ROS inhibiting effectors, samples were sent for mass spectrometry to identify interacting proteins after verifying the expression levels of proteins using western blot.

2.4.1. Protein expression levels of *ROSIE 1-3*

Four weeks old *N. benthamiana* plants were infiltrated with *A. tumefaciensis* strains expressing ROSIE 1-3 fused to mCherry (Figure 11A). Three days post infiltration plants were harvested and used for protein analysis.

Subsequently, the expression of the effectors was examined using western blot analysis. As seen in figure 11B, all of them were successfully expressed indicated by a band corresponding to their protein size.

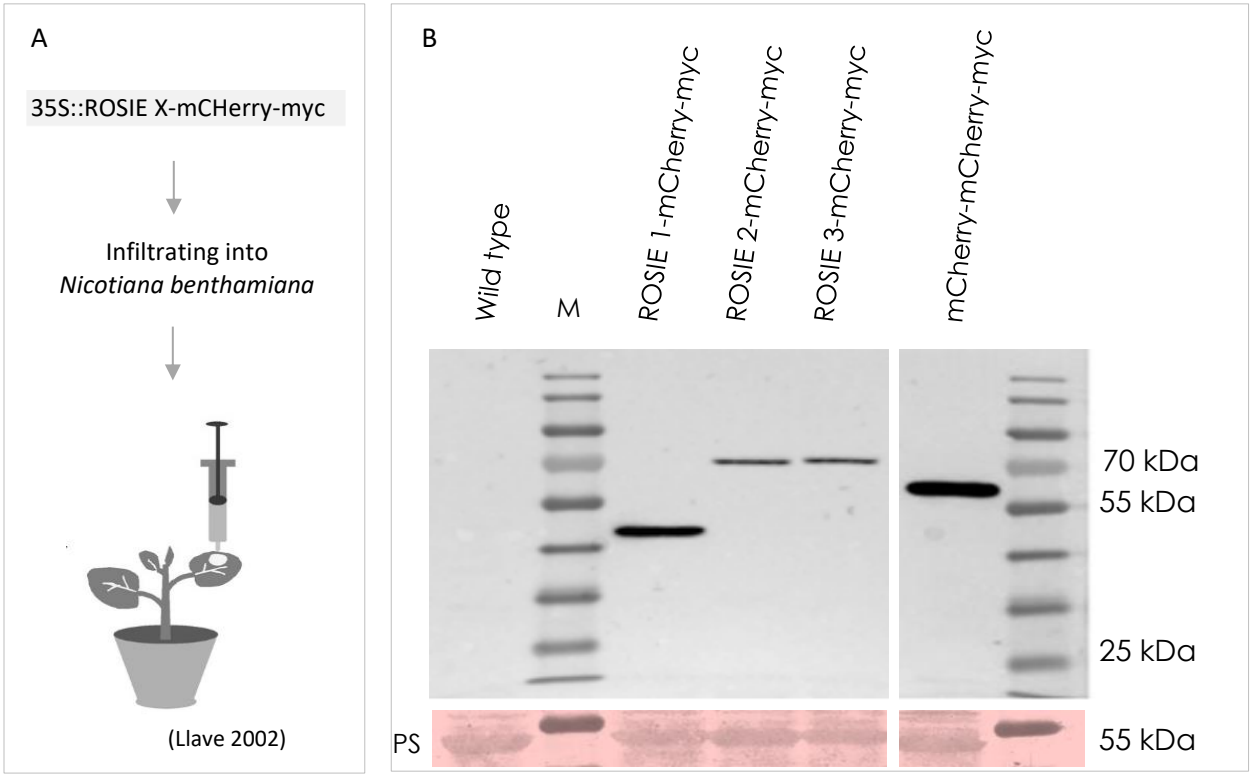

Figure 11: Transient overexpression of *ROSIE 1*-mCherry, *ROSIE 2*-mCherry and *ROSIE 3*-mCherry in *N. benthamiana.* (A) *A. tumefaciens* strain expressing *ROSIE 1*-mCherry, *ROSIE 2*-mCherry and *ROSIE 3*-mCherry under the strong 35S promoter was infiltrated into *N. benthamiana* and harvested 3 days post infection. (B) Western blot analysis of infected *N. benthamiana* leaf extracts were performed using anti-myc antibodies for detection. mCherry-mCherry-myc was used as positive control. Wild type of *N. benthamiana* as negative control. Numbers on the right indicate protein size in kDA. M-protein marker, PS-Ponceau Staining.

2.4.2. Identification of Potential Interacting ROSIE Proteins (PIRPs)

To reveal potential interacting proteins of ROSIE 1-3, same samples used for western blot were sent out for mass spectrometry. All identified proteins showing to be specifically co-immunoprecipitated with studied ROS inhibiting effectors and were not found in the mCherry control sample and were further studied in this master thesis are listed in table 2.

2.5. VIGS of PIRPs in *Nicotiana benthamiana*

2.5.1. Cloning of PIR genes and VIGS vector construction

N. benthamiana PIRP gene-specific primers amplified around 300 bp fragment, and the amplified genes were cloned from cDNA according to the *N. benthamiana* sequence data base https://solgenomics.net; http://vigs.solgenomics.net, and sequenced. Silencing vectors TRV1:*NbPIRP* were constructed using a Gateway cloning method as explained before. Gene-specific amplification of the around 300 bp fragment confirmed the cloning of *NbPIRP* into the TRV1 vector. Subsequently, the binary vector was used to transform *Agrobacterium tumefaciens* GV3101.

2.5.2. Agroinfiltration and VIGS

Gene silencing in *N. benthamiana* was carried out by agroinfiltration of TRV2 and *NbPIRP* in 2 leaves of 2-3 weeks old *N. benthamiana* plants. The control plants were agroinfiltrated with an empty vector (hereafter, TRV:GFP) and phytoene desaturase which is causing photobleaching in plants (hereafter, TRV:*NbPDS*) as seen in figure 12, 13 and 14. Three biological replicates of potted plants were infiltrated for each experiment independently and maintained in a controlled chamber for 25 days before being sampled. To confirm the efficiency and specificity of gene silencing, *NbPIRP* transcript levels were quantified in eGFP (GFP empty vector) and *NbPIRP* plants using qPCR.

Table 2. Potential Interacting Proteins of ROS inhibiting effectors identified by Mass Spectrometry and their functions

	Accession #	Protein Name	Protein Length (aa)	Molecular Weight (Da)	Unique Peptide Count	Function
ROSIE 1	R4S2V6	9 - Lipoxygenase	862	97.446	3	*Fungal infection induces levels of 9-lipoxygenases; probable role as defense signaling molecule to induce defense responses in parts of the plant that are not yet under attack (Woldemariam et al. 2018)*
	A0A1J6IEQ0	Putative carboxylesterase 120	325	36,858	4	*Plays a role in the modification of esters of signaling molecules in jasmonic acid, salicylic acid and auxin; protection from pathogen infection (Schilmiller et al. 2016)*
	O24145	4-coumarate--CoA ligase 1	547	59,842	3	*Synthesizes 3,4',5-trihydroxystilbene from trans-4-coumarate; involved in channeling carbon flow into branch pathways of the phenylpropanoid metabolism (Soltani et al. 2006)*

ROSIE 1	Q9XGH7	Serine/threonine-protein phosphatase PP2A catalytic subunit	312	35,639	2	*Involved in establishing auxin gradients (Ballesteros et al. 2013). Studies show that it acts as a negative regulator during pathogenic attack (País et al. 2009)*
	A0A1J6I9C1	Trans-cinnamate 4-monooxygenase	506	58,436	2	*Synthesis of salicylic acid signaling molecules during biotic stress; part of the phenylpropanoid pathway (Sadeghi et al. 2013)*
	A0A1S4BHF0	5'-nucleotidase domain-containing protein 4-like isoform X1	626	71,476	1	
	A0A1S4CLK2	uncharacterized protein LOC107820356	126	14,499	1	
	A0A1S3Y190	Eukaryotic translation initiation factor 3 subunit J	224	25,156	1	*Involved in protein synthesis; inhibited in response to stress due to high consumption of cellular energy (Muñoz and Castellano 2012)*
ROSIE 2	A0A1S3XJA5	myosin-17-like	1529	172,668	10	*Functioning in mobility of Golgi and other organelles (Avisar et al. 2009)*
	A0A1S4CW91	carbamoyl-phosphate synthase largechain,chloroplastic-like	1198	131,522	8	*Plays a role in arginine biosynthesis (Mollá-Morales et al. 2011)*

ROSIE 2	A0A1S4BTR8	dynamin-related protein 1E-like	614	68,825	8	*Plays a role in plasma membrane maintenance and cell wall integrity (Kang 2003)*
	A0A1S3Y6L1	dynamin-2A-like	916	98,974	6	*Involved in the division of plant mitochondria (Arimura et al. 2004)*
	A0A1U7XFG7	Coatomer subunit beta	948	105,920	5	*Cytosolic protein complex; essential for protein transport (Ahn et al. 2015)*
	A0A1S3YFI6	Coatomer subunit alpha	1219	137,109	11	*Cytosolic protein complex; essential for protein transport (Ahn et al. 2015)*
	A0A1S3YK08	uncharacterized protein LOC107777101 isoform X2	405	45,675	9	
	A0A1J6IJ82	Nf-x1-type zinc finger protein nfxl1	1122	121,193	2	*Promotes H_2O_2 production; negative regulator of some defense related genes via salicylic signaling pathway (Asano et al. 2008)*
	A0A1J6JKH5	Dynamin-related protein 5a	609	68,229	4	*Microtubule-associated force producing protein during cytokinesis; may play a role in cell division (Miyagishima et al. 2008)*

ROSIE 3	A0A1S3YU74	dynamin-like protein ARC5 isoform X1	773	86,851	3	*Mediated chloroplast (Gao et al. 2003) and peroxisome (Zhang and Hu 2010) division*
	A0A1J6J3H5	Dead-box atp-dependent rna helicase 3, chloroplastic	741	80,843	4	*Essential for chloroplast function and abiotic stress responses (Gu et al. 2014)*
	A0A1S3XJA5	myosin-17-like	1529	172,668	10	*Functioning in mobility of Golgi and other organelles (Avisar et al. 2009)*
	A0A1S4A6H4	peroxisomal fatty acid beta-oxidation multifunctional protein AIM1-like	724	78,042	5	*Plays a role in plant hormone synthesis and seed germination (Arent et al. 2010); involved in fatty acid beta – oxidation (Richmond 1999)*
	A0A1J6K4R7	3-ketoacyl-coa thiolase 2, peroxisomal	465	49,112	3	*Breakdown of fatty acid (Pye et al. 2010); contributes to ROS and illuminate a ROS signaling role in plants (Kao et al. 2018)*
	A0A1S3Y190	Eukaryotic translation initiation factor 3 subunit J	224	25,156	1	*Involved in protein synthesis; inhibited in response to stress due to high consumption of cellular energy (Muñoz and Castellano 2012)*

2.5.3. VIGS of ROSIE 1 Interacting Proteins

To determine potential ways ROSIE 1 is involved in suppressing ROS production upon pathogen invasion, 8 potential interacting proteins were taken into deeper analysis previously identified by mass spectrometry. Plants were co-infiltrated with Agrobacterium carrying the constructs TRV2-*NbPutative Carboxylesterase 120* silenced (hereafter, TRV:*NbCXE*), TRV2-*NbLipoxygenase* silenced (hereafter, TRV:*NbLOX*), TRV2-*Nb4-Coumarate-CoA ligase 1* silenced (hereafter, TRV:Nb4CL), TRV2-*NbTrans-cinnamate 4-monooxygenase* silenced (hereafter, TRV:NbC4H), TRV2-*NbSerine/threonine protein phosphatase PP2Acatalytic subunit* silenced (hereafter, TRV:*NbSTPP2A*), TRV2-*Nb5'nucleotidase domain-containing protein 4-like isoform X1* silenced (hereafter, TRV:NbNT5DC4), TRV2-*NbUncharacterized protein LOC107820356* silenced (hereafter, TRV:*NbLOC107820356*) and TRV2:*NbEucaryotic translation initiation factor 3 subunit J* silenced (hereafter, TRV:*NbEIF3J*). After 25 days post infiltration, leaf samples were collected and used for ROS burst measurements. TRV-PDS (phytoene desaturase), causing photobleached phenotype was used as a positive control of silencing and TRV-GFP (empty vector) which appears similar as uninfiltrated plants (Figure 12 A and 12B) (see Material and Method, section 4.5.1 Starins and Plasmids for ROSIE 1 PIRP silenced constructs).

2.5.3.1. The NbEIF3J silenced plants show a dwarfed phenotype and function as a positive regulator in a ROS depending defense response

The *NbEIF3J* silenced *N. benthamiana* plants exhibit apparent dwarfed growth compared to controlled plants. This protein is known to be involved in protein synthesis and is also inhibited in response to different plant stresses due to high consumption of cellular energy (Muñoz and Castellano 2012) (Table 2). Knocking down the expression of TRV:*NbEIF3J* through VIGS shows a highly significant decrease of ROS accumulation upon flagellin induction compared to TRV:GFP control plants. Silencing levels tested by qPCR in each of the three independent biological replicates showed that transcript levels were reduced by 80% in plants expressing TRV:*NbEIF3J* compared with plants expressing the TRV:GFP control. Since TRV:*NbEIF3J* was observed to suppress ROS production when transiently expressed in *N. benthamiana*, cell death staining was performed to examine if this might be the cause. However, there were no visible differences in TRV:*NbEIF3J* cell death compared to TRV:GFP plants after 25 dpi (Figure 12J). These results confirmed that EIF3J is a positive regulator of plant immunity.

2.5.3.2. *The NbLOX, NbCL4 and NbC4H function as negative regulators in a ROS dependent defense response*

The LOX, CL4 and C4H proteins have been identified so far to be involved in plant immunity serving as signaling molecules. The CL4 and C4H proteins share the same branching part of the phenylpropanoid pathway. Research papers suggest that 4CL is involved in channeling carbon flow (Soltani et al. 2006), whereas C4H plays a role in the synthesis of salicylic acid signaling molecules during biotic stress (Sadeghi et al. 2013). The LOX protein, however was shown to act as a signaling molecule which induces a defense response in parts of the plants that are not yet under pathogen attack (Sadeghi et al. 2013) (Table 2).

Transient expression of TRV:*NbLOX*, TRV:*NbCL4* and TRV:*NbC4H* in *N. benthamiana* plants revealed a significantly higher ROS production compared to TRV:GFP controlled plants. Silencing levels were tested by qPCR in each of the three independent biological replicates (for Nb*LOX* two biological replicates were tested for qPCR, since one sample did not show any decrease in transcriptional levels) showing a 70-80% reduction of transcription levels in plants expressing TRV:*NbLOX,* TRV:*NbCL4* and TRV:*NbC4H* compared with TRV:GFP control. Furthermore, cell death staining was done in silenced plants, even though they were displaying higher ROS levels, for technical purposes. As anticipated, no cell death was influencing the high accumulation of ROS upon flagellin perception in plants (Figure 12D, 12E and 12F). These results indicate that CL4, C4H and LOX are negative regulators of plant immunity.

2.5.3.3. *ROS independent silenced genes in Nicotiana benthamiana*

Other silenced PIRPs (*NbCXE, NbSTPP2A, NbNT5DC4* and *NbLOC107820356*) by transiently expressing in *N. benthamiana* did not show any significant impact related to ROS burst induced by flagellin (Figure 12C, 12G, 12H and 12I). However, some of them were previously shown to be involved in plant defense responses, such as STPP2A which was discovered to act as negative regulators during pathogen attack (País et al. 2009). Also, the protein CXE, was identified to play a role in the modification of esters of signaling molecules in jasmonic acid, salicylic acid and auxin and is involved in the protection of pathogen infection (Schilmiller et al. 2016). Therefore, we can conclude that these proteins are not interfering in the ROS signaling pathway, but might be involved in an independent pathway in plant defense response.

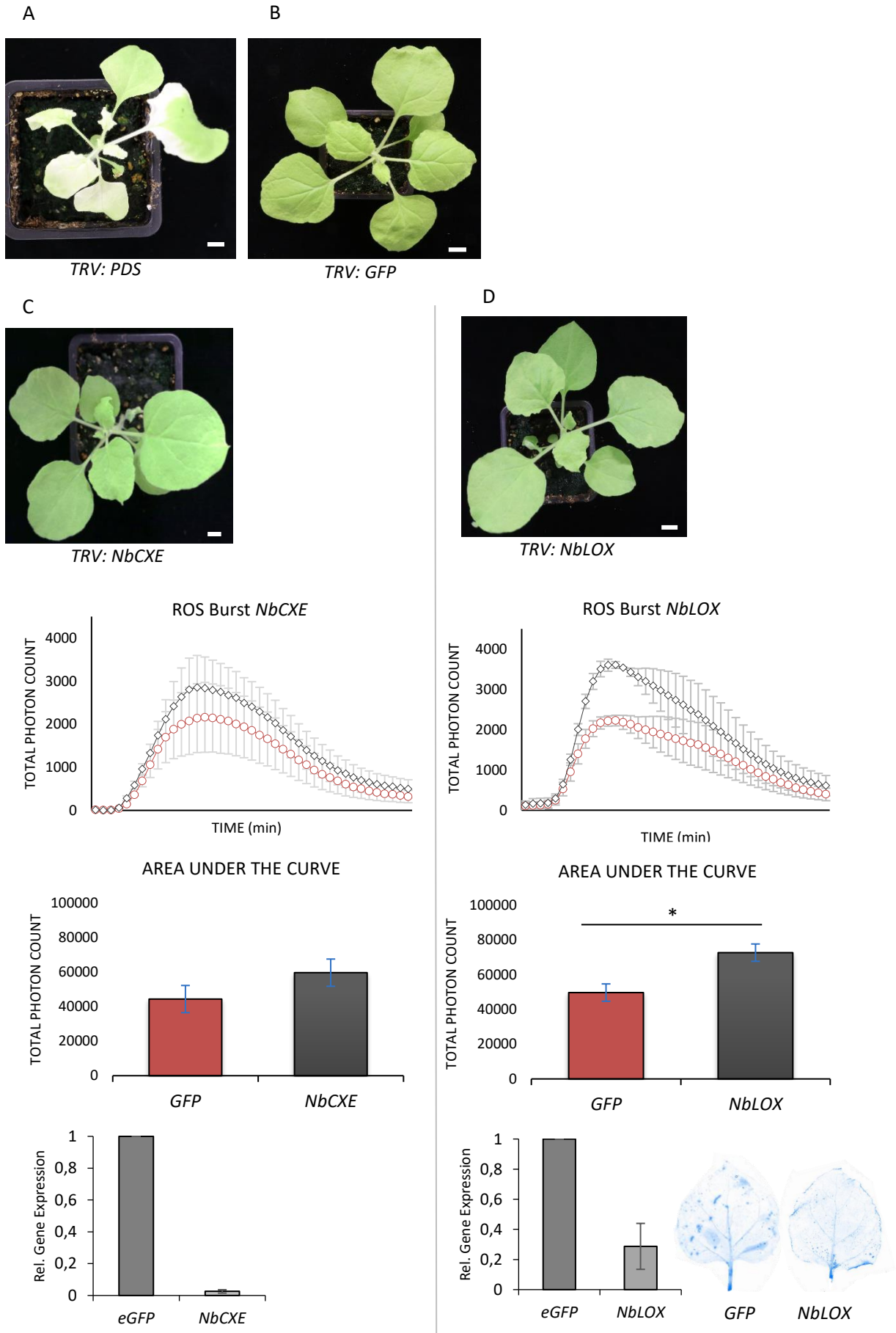
A
B
TRV: PDS
TRV: GFP
C
D
TRV: NbCXE
TRV: NbLOX
ROS Burst NbCXE
TOTAL PHOTON COUNT
4000
3000
2000
1000
0
TIME (min)
ROS Burst NbLOX
TOTAL PHOTON COUNT
4000
3000
2000
1000
0
TIME (min)
AREA UNDER THE CURVE
TOTAL PHOTON COUNT
100000
80000
60000
40000
20000
0
GFP
NbCXE
AREA UNDER THE CURVE
*
TOTAL PHOTON COUNT
100000
80000
60000
40000
20000
0
GFP
NbLOX
Rel. Gene Expression
1
0,8
0,6
0,4
0,2
0
eGFP
NbCXE
Rel. Gene Expression
1
0,8
0,6
0,4
0,2
0
eGFP
NbLOX
GFP
NbLOX

E

TRV: Nb4CL

ROS Burst *Nb4CL*

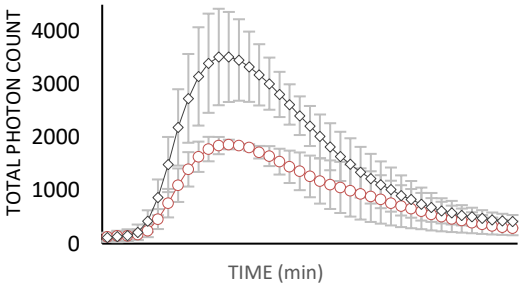

AREA UNDER THE CURVE

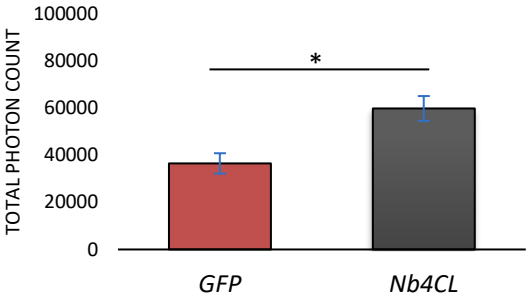

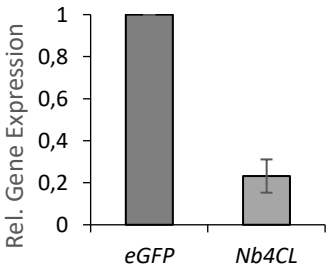

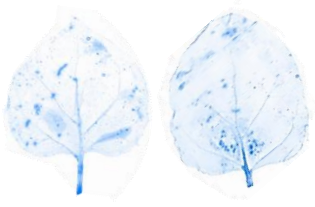

GFP *Nb4CL*

F

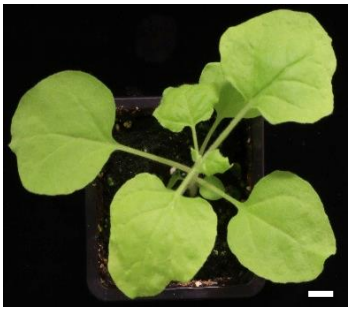

TRV: NbC4H

ROS Burst *NbC4H*

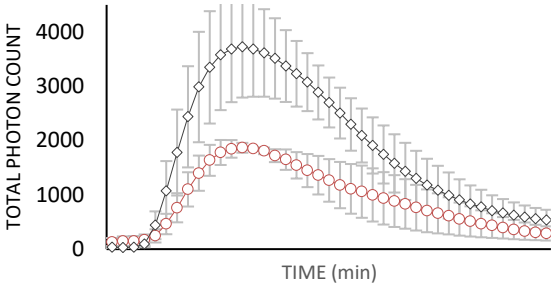

AREA UNDER THE CURVE

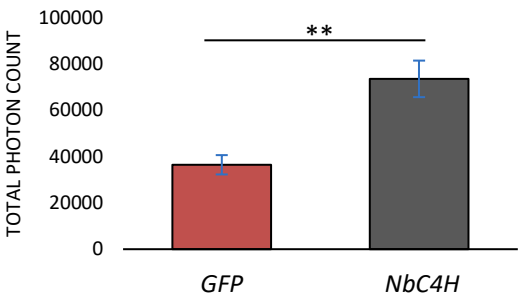

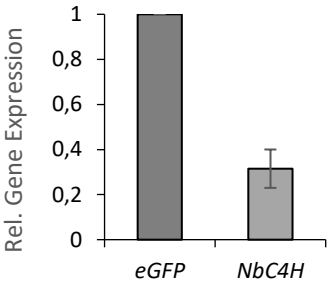

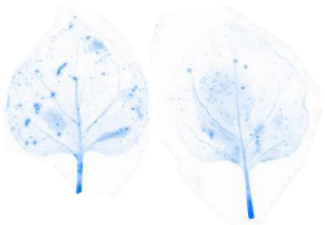

GFP *NbC4H*

G

TRV: NbSTPP2A

ROS Burst *NbSTPP2A*

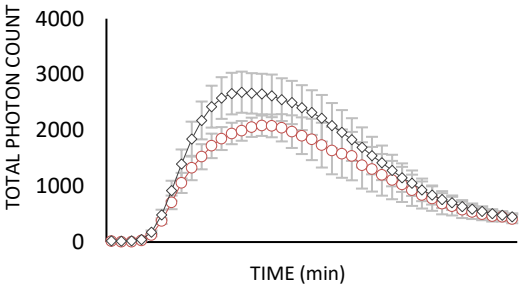

AREA UNDER THE CURVE

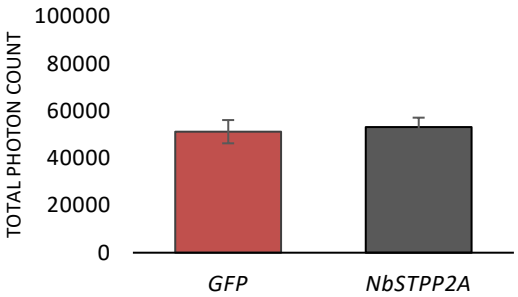

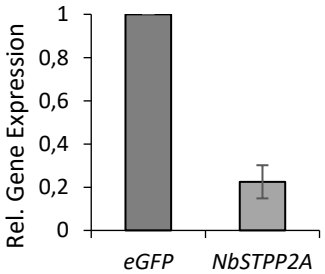

H

TRV: NbNT5DC4

ROS Burst *NbNT5DC4*

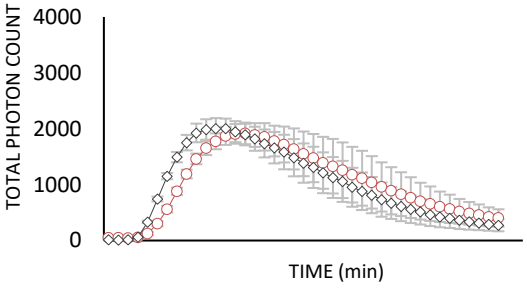

AREA UNDER THE CURVE

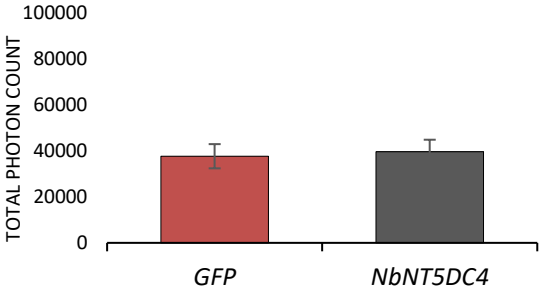

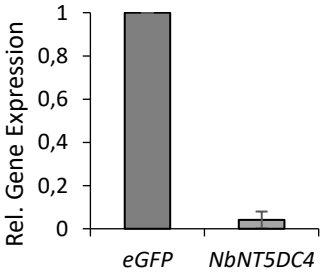

I

TRV: NbLOC107820356

ROS Burst *NbLOC107820356*

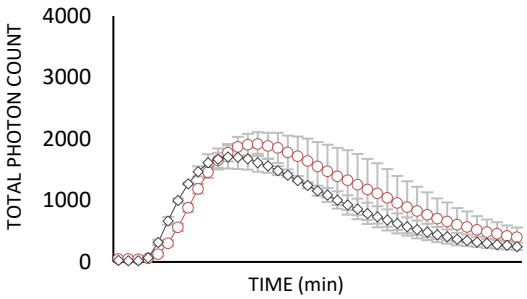

AREA UNDER THE CURVE

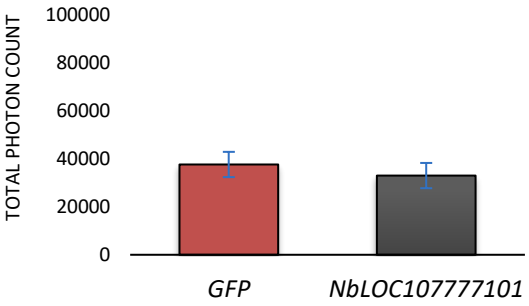

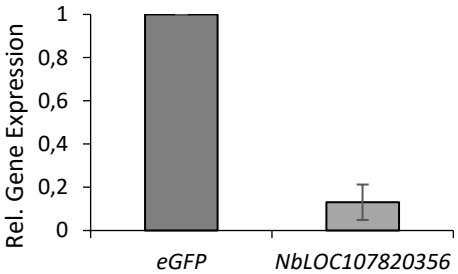

J

TRV: NbEIF3J

ROS Burst *NbEIF3J*

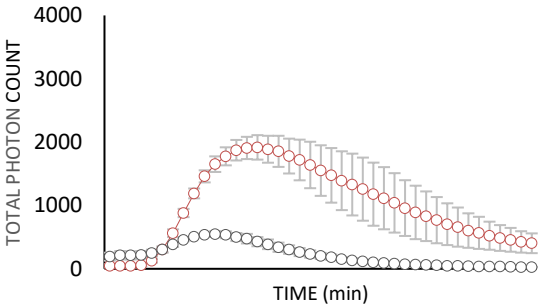

AREA UNDER THE CURVE

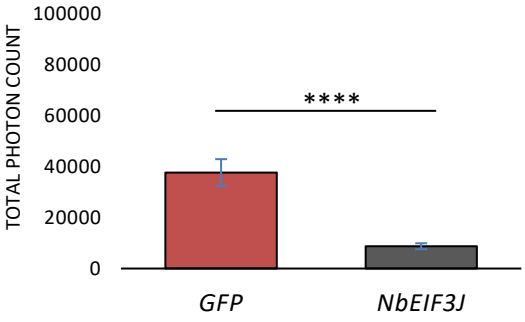

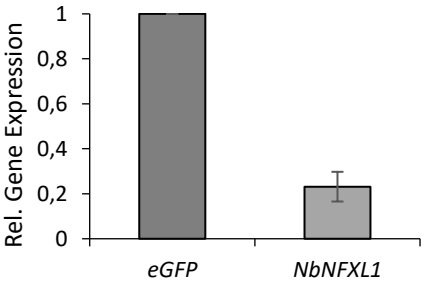

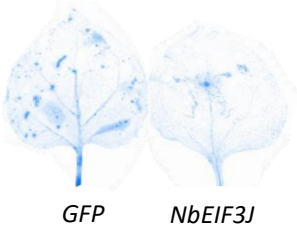

Figure 12: Effects of ROSIE 1 Interacting Proteins. Silencing of IRPs (Interacting Rosie Proteins) using VIGS*. N. benthamiana* plants were co-infiltrated with Agrobacterium containing (**A)** TRV-PDS (phytoene desaturase), causing a photobleached phenotype as a positive control of silencing; (**B)** TRV-GFP (empty vector), appearing similar as uninfiltrated plants; TRV-IRPs [(**C)** *NbCXE, (**D**) NbLOX, (**E**) Nb4CL, (**F**) NbC4H, (**G**) NbSTPP2A, (**H**) NbNT5DC4, (**I**) NbLOC107820356, (**J**) NbEIF3J*). Plants were photographed 25 days post-infiltration. Bars equals 1 cm. Flg22-triggered ROS burst was monitored using a luminol based assay and 25 days post-infiltration pretreatment with H_2O (control) or flagellin solution (horseradish peroxidase, luminol and flagellin22). Signals were recorded for 40 min after treatment. Data shows total integrated photon counts presented as ROS burst curves as well as the area under the curves for all ROSIE 1 interacting proteins. Values represents avarages ± SE (N=15) from three independent experiments. Asterix indicate significat differences from the controled GFP plant (t-test, P value .0332-*; .0021-**; .0002-***; .0001-****). Gene expression was quantified by qPCR. RNA was extracted from same plants used for ROS burst assay (25 days post-infiltration). Actin was used as reference gene. The data are shown as mean ±SD from three independent experiments. Trypan blue staining was used as control for cell death.

2.5.4. VIGS of ROSIE 2 Interacting Proteins

To illuminate potential ways ROSIE 2 is involved in suppressing ROS accumulation upon pathogen invasion, 10 potential interacting proteins identified by mass spectrometry were further analyzed. Plants were co-infiltrated with Agrobacterium carrying the constructs TRV2-NbUncharacterized protein *LOC107777101* silenced (hereafter, TRV:*NbLoc107777101*), TRV2-*NbDynamin-like Protein Arc5 Isoform X1* silenced (hereafter, TRV:*NbARC5*), TRV2-*NbCarbamoyl-Phosphate Synthase large chain* silenced (hereafter, TRV:*NbCARB*), TRV2-*NbDead-box ATP Dependent RNA helicase 3* silenced (hereafter, TRV:*NbRH3*), TRV2- *NbNFXL1 type zinc finger protein nfxl1* silenced (hereafter, TRV:*NbNFXL1*), TRV2-*NbDynamine-Related Protein 5a* silenced (hereafter, TRV:*NbDRP5A*), TRV2-*NbDynamin 2A like* silenced (hereafter, TRV:*NbD2A*), TRV-*NbDynamin related protein 1E like* silenced (hereafter, TRV:*DRP1E*), TRV-*NbCoatomer subunit alpha* silenced (hereafter, TRV:*NbCOPA*) and and TRV2:*NbCoatomer subunit beta* silenced (hereafter, TRV:*NbCOPB*). After 25 days post infiltration, leaf samples were collected and used for ROS burst measurements. TRV-PDS (phytoene desaturase), causing photobleached phenotype was used as a positive control of silencing and TRV-GFP (empty vector) which appears similar as uninfiltrated plants (Figure 13A and 13B). (see Material and Method, section 4.5.1 Strains and Plasmids for ROSIE 2 PIRP silenced constructs).

2.5.4.1. *The NbNFXL1 and NbDRP5A function as negative regulators in a ROS dependent defense response*

In the paper published by Asano et al. 2008, NFXL1 was already identified to play a role in plant defense signaling as a negative regulator of some defense related genes via the salicylic signaling pathway. This is consistent with the results shown in this master thesis. Transient expression of TRV:*NbNFXL1* in *N.benthamiana* plants induced a significantly higher ROS production compared to TRV:GFP controlled plants (Figure 13G).

Silencing of *NbDRP5A* in *N. benthamiana* plants showed a bigger morphological phenotype compared to control plants. So far, DRP5A was not found to be involved in plant defense responses. The functional role of DRP2A is related to microtubule-associated force producing protein during cytokinesis and this protein may play a role in cell division (Miyagishima et al. 2008). Silencing in TRV:*NbDRP5A* plants showed a significant increase of ROS accumulation upon flagellin induction (Figure 15H).

Silencing levels were tested by qPCR in each of the three independent biological replicates showing a 80-90% reduction of transcription levels in plants expressing TRV:*NbNFXL1* and TRV:*DRP5A* compared with TRV:GFP controlled plants. Furthermore, cell death staining was done in TRV:*NbNFXL1* and TRV:*DRP5A* plants, even displaying higher ROS levels for technical purposes. There was no cell death that influenced the high accumulation of ROS upon flagellin perception in plants, as expected (Figure 13G and 13H). These results indicate that NFXL1 and DRP5A act as negative regulators in a ROS dependent signaling response in plant immunity.

2.5.4.2. *ROS independent silenced genes in Nicotiana benthamiana*

Other silenced ROSIE 2 potential interacting proteins, the *NbLOC107777101, NbARC5, NbCARB* and *NbRH3*, which were transiently expressed in *N.benthamiana* did not indicate any significant influence in relation to ROS production induced by flagellin (Figure 13C, 13D, 13E and 13F). Interestingly, the *NbRH3* silenced plants showed a photobleached phenotype similar to the TRV:PDS silenced control.

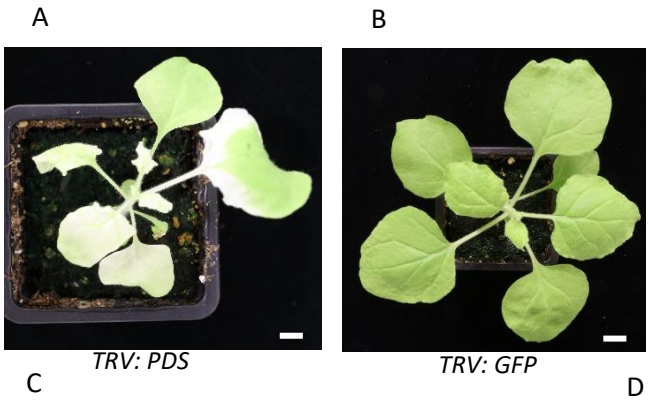
A
B
TRV: PDS
TRV: GFP

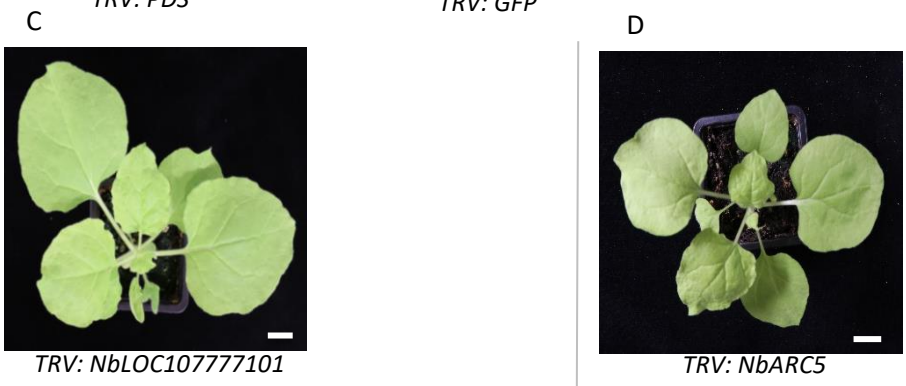
C
D
TRV: NbLOC107777101
TRV: NbARC5

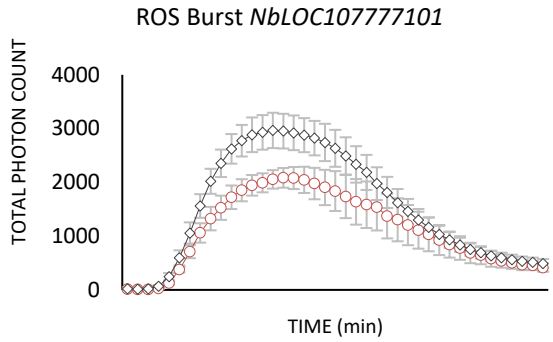
ROS Burst NbLOC107777101
TOTAL PHOTON COUNT
4000
3000
2000
1000
0
TIME (min)

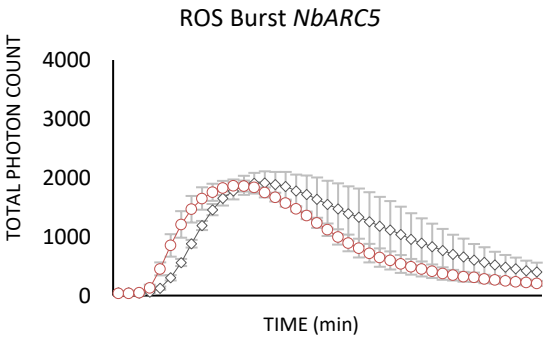
ROS Burst NbARC5
TOTAL PHOTON COUNT
4000
3000
2000
1000
0
TIME (min)

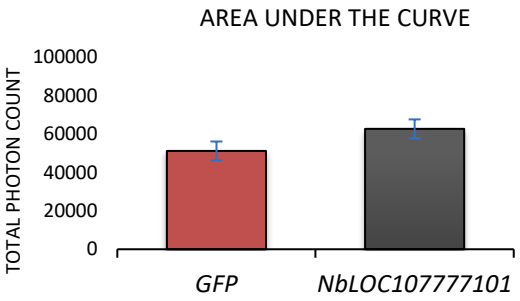
AREA UNDER THE CURVE
TOTAL PHOTON COUNT
100000
80000
60000
40000
20000
0
GFP
NbLOC107777101

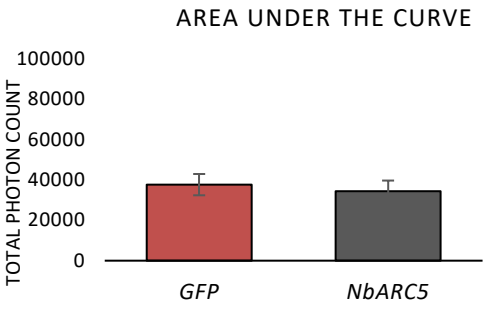
AREA UNDER THE CURVE
TOTAL PHOTON COUNT
100000
80000
60000
40000
20000
0
GFP
NbARC5

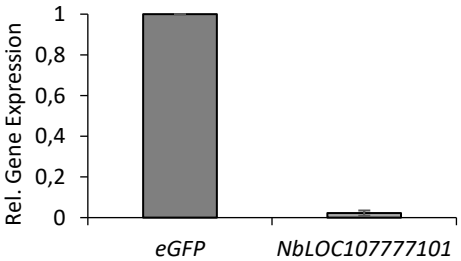
Rel. Gene Expression
1
0,8
0,6
0,4
0,2
0
eGFP
NbLOC107777101

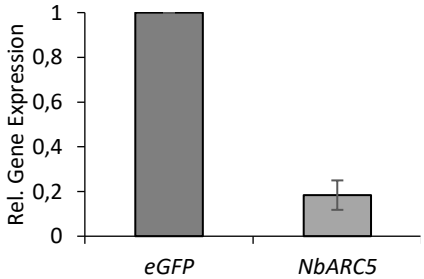
Rel. Gene Expression
1
0,8
0,6
0,4
0,2
0
eGFP
NbARC5

E

TRV: NbCARB

F

TRV: NbRH3

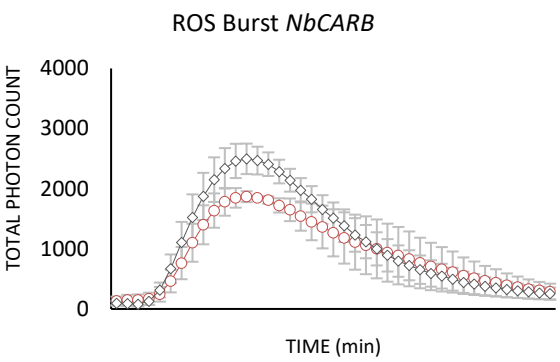

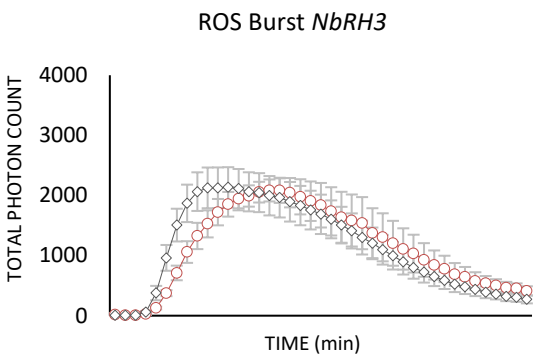

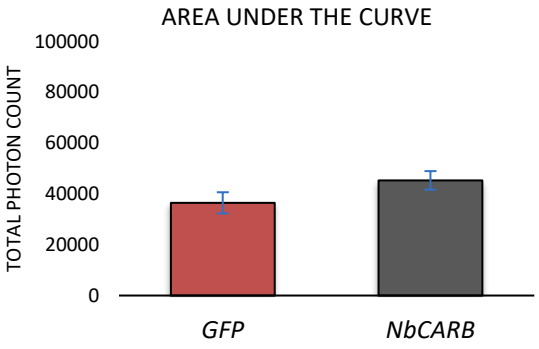

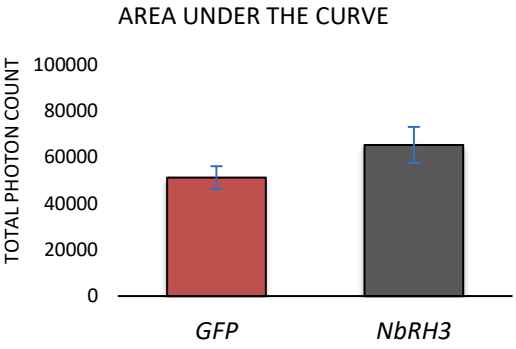

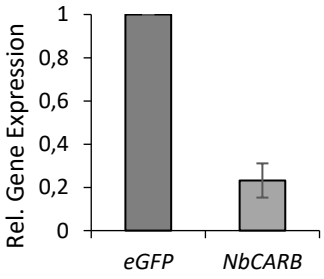

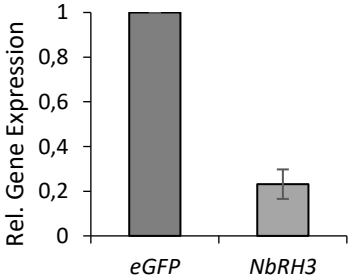

G

TRV: NbNFXL1

H

TRV: NbDRP5A

ROS Burst *NbNFXL1*

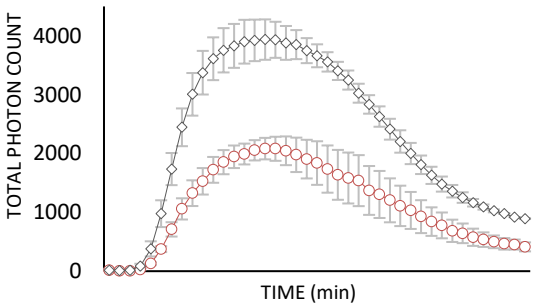

ROS Burst *NbDRP5A*

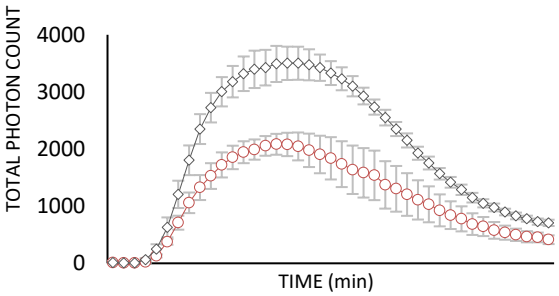

AREA UNDER THE CURVE

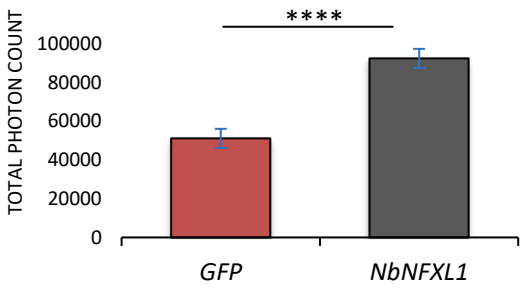

AREA UNDER THE CURVE

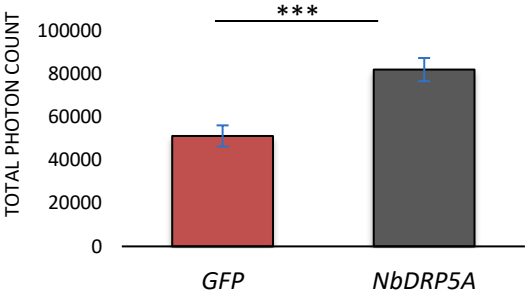

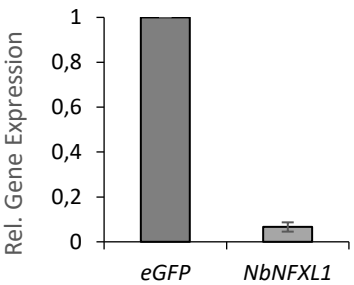

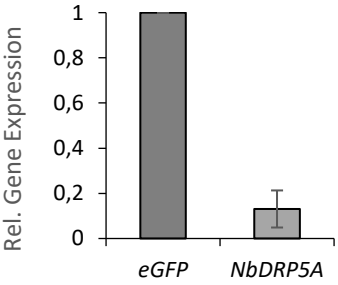

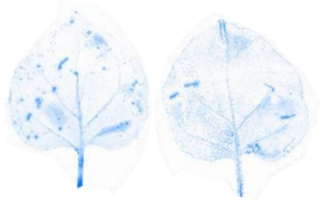

GFP *NbNFXL1*

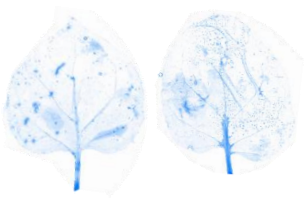

GFP *NbDRP5A*

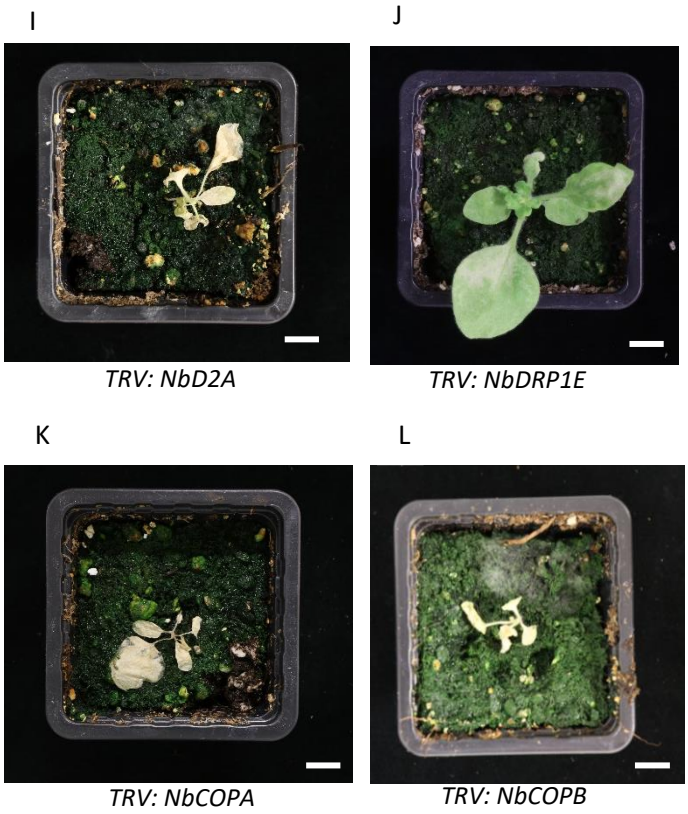

Figure 13: Effects of ROSIE 2 Interacting Proteins. Silencing of IRPs (Interacting Rosie Proteins) using VIGS. N. benthamiana plants were co-infiltrated with Agrobacterium containing (**A)** TRV-PDS (phytoene desaturase), causing photobleached phenotype as a positive control of silencing; (**B**) TRV-GFP (empty vector), appearing similar as uninfiltrated plants; TRV-IRPs [(**C**) *NbLOC107777101, (**D**) NbARC5, (**E**) NbCARB, (**F**) NbRH3, (**G**) NbNFXL1, (**H**) NbDRP5A, (**I**) NbD2A, (**J**) NbDRP5A, (**K**) NbCOPA and (**L**) NbCOPB*]. Plants were photographed 25 days post-infiltration. Bars equals 1 cm. Flg22-triggered ROS burst was monitored using a luminol based assay and 25 days post-infiltration pretreatment with H_2O (control) or flagellin solution (horseradish peroxidase, luminol and flagellin22). Signals were recorded for 40 min after treatment. Data shows total integrated photon counts presented as ROS burst curves as well as the area under the curves for all ROSIE 2 interacting proteins. Values represent averages ± SE (N=15) from three independent experiments. Asterix indicates significant differences from the control GFP plants (t-test, P value.0332-*; .0021-**; .0002-***; .0001-****). Gene expression was quantified by qPCR. RNA was extracted from same plants used for ROS burst assay (25 days post-infiltration). Actin was used as reference gene. The data are shown as mean ±SD from three independent experiments. Trypan blue staining was used as a control for cell death.

2.5.4.3. Essential proteins for Nicotiana benthamiana

VIGS using four ROSIE 2 PIRPs, namely, TRV:*NbD2A*, TRV:*NbDRP5A*, TRV:*NbCOPA* and TRV:*NbCOPB*, exhibit morphological changes. TRV:*NbD2A*, TRV:*NbCOPA* and TRV*:NbCOPB* silenced plants resulted in plant death, whereas TRV:*DRP5A* showed a stunted phenotypical appearance 25 d after agroinfiltration

in *N. benthamiana* plants. This result indicates that these four proteins are essential for the plant survival (Figure 13I, 13J, 13K and 13L).

2.5.5. VIGS of ROSIE 3 Interacting Proteins

To determine potential ways ROSIE 3 is involved in suppressing ROS production upon pathogen invasion, 3 potential interacting proteins were taken into deeper analysis previously identified by mass spectrometry. Plants were co-infiltrated with Agrobacterium carrying the constructs TRV2- *NbFatty Acid Beta-oxidation Multifunctional Protein Aim1-like* silenced (hereafter, TRV:*NbAIM1*), TRV2-*NbMyosin 17-like* silenced (hereafter, TRV:*NbM17L*) and TRV2-*Nb3-ketoacyl-CoA thiolase 2* silenced (hereafter, TRV:*NbPED1*). After 25 days post infiltration, leaf samples were collected and used for ROS burst measurements. TRV-PDS (phytoene desaturase), causing photobleached phenotype was used as a positive control of silencing and TRV-GFP (empty vector) which appears similar as uninfiltrated plants (Figure 14 A and 14B). (see Material and Method, section 4.5.1 Starins and Plasmids for ROSIE 3 PIRP silenced constructs).

2.5.5.1. The NbM17L and NbPED1 function as negative regulators in a ROS dependent defense response

According to a paper from Kao et al., published 2018, the PED1 protein has shown to be involved in ROS production and plays a role in ROS signaling. Evidently, a lack of *NbPED1* within the plant cells resulted in a significant increase in ROS accumulation compared to TRV: GFP controlled plants upon flagellin induction.

Same accumulating levels of ROS were observed in silenced plants containing the construct TRV:*NbM17L*. Despite the fact, that M17L is functioning in the mobility of the Golgi apparatus and other organelles (Avisar et al. 2009) and has not been so far shown to be involved in ROS signaling plant response, a significant increase in ROS production upon flagellin perception (Figure 14D and 14E).

The expression levels of TRV:*NbM17L* and TRV:*NbPED1* were tested by qPCR in each of the three independent biological replicates showing a 80-90% reduction of transcription levels in plants expressing compared with TRV:GFP controlled plants. Furthermore, cell death staining was done in TRV:*NbM17L* and TRV:*NbPED1* plants, even displaying higher ROS levels, for technical purposes.

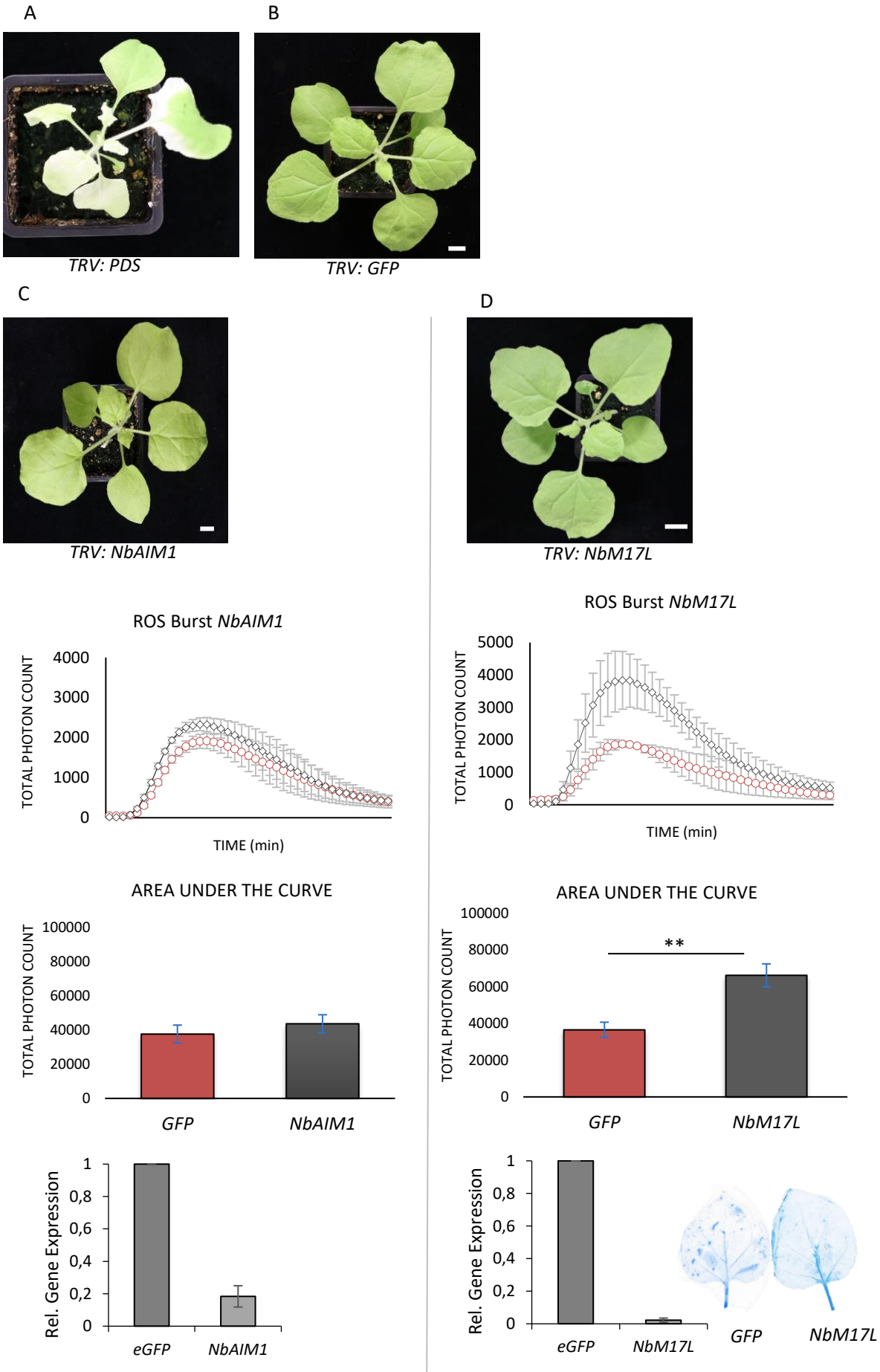
A
B
TRV: PDS
TRV: GFP
C
D
TRV: NbAIM1
TRV: NbM17L
ROS Burst NbAIM1
TOTAL PHOTON COUNT
4000
3000
2000
1000
0
TIME (min)
ROS Burst NbM17L
5000
4000
3000
2000
1000
0
TOTAL PHOTON COUNT
TIME (min)
AREA UNDER THE CURVE
100000
80000
60000
40000
20000
0
TOTAL PHOTON COUNT
GFP
NbAIM1
AREA UNDER THE CURVE
**
GFP
NbM17L
Rel. Gene Expression
1
0,8
0,6
0,4
0,2
0
eGFP
NbAIM1
eGFP
NbM17L
GFP
NbM17L

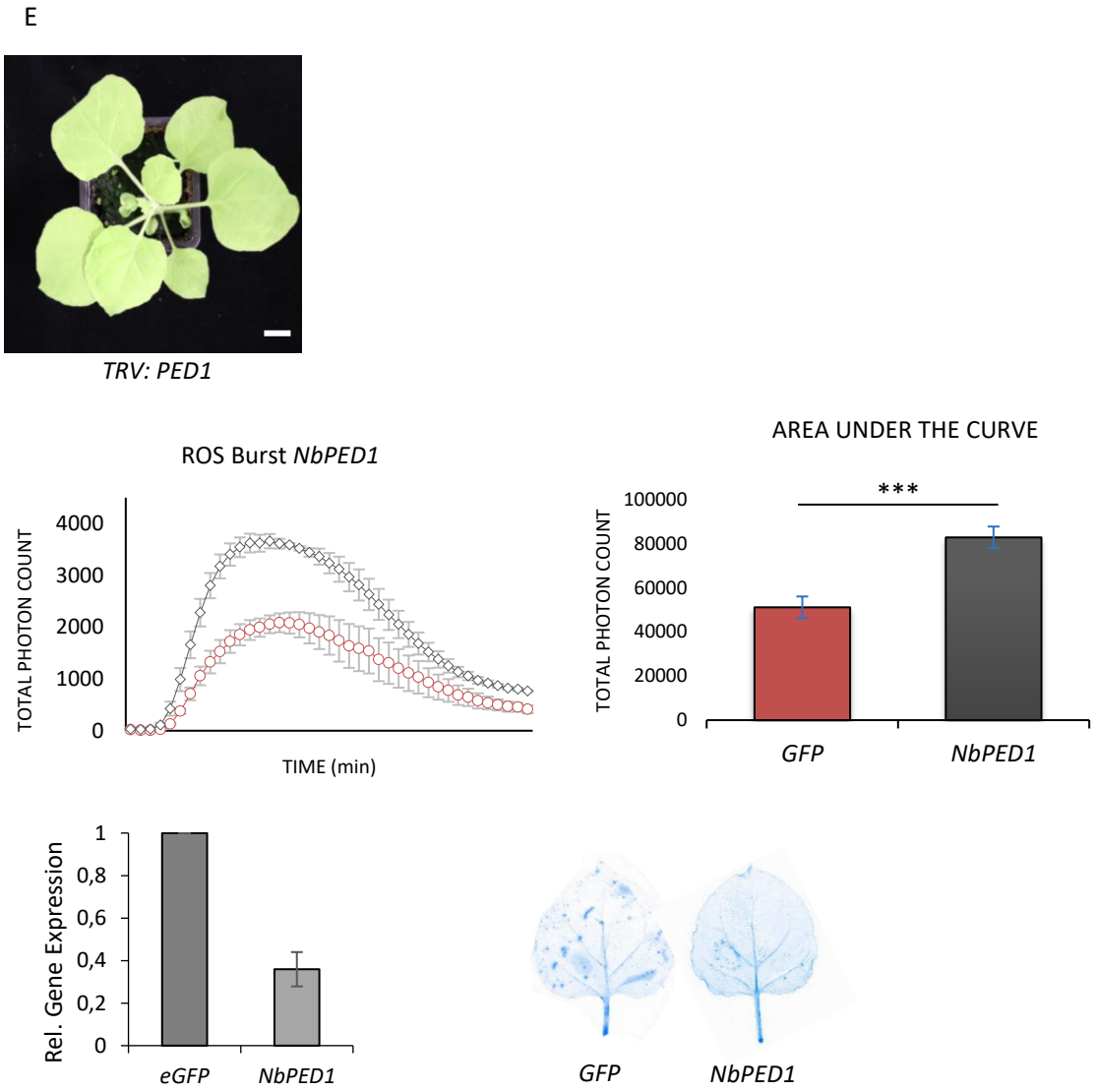

Figure 14: Effects of ROSIE 3 Interacting Proteins. Silencing of IRPs (Interacting Rosie Proteins) using VIGS. *N.benthamiana* plants were co-infiltrated with Agrobacterium containing A-TRV-PDS (phytoene desaturase), causing photobleached phenotype as a positive control of silencing; B-TRV-GFP (empty vector), appearing similar as uninfiltrated plants; TRV-IRPs (C-*NbAIM1, D-NbM17L and E-NbPED1)*. Plants were photographed 25 days post-infiltration. Bars equals 1 cm. Flg22-triggered ROS burst was monitored using a luminol based assay and 25 days post-infiltration pretreatment with H_2O (control) or flagellin solution (horseradish peroxidase, luminol and flagellin22). Signals were recorded for 40 min after treatment. Data shows total integrated photon counts presented as ROS burst curves as well as the area under the curves for all ROSIE 3 interacting proteins. Values represents avarages ± SE (N=15) from three independent experiments. Asterix indicate significat differences from the controled GFP plant (t-test, P value .0332-*; .0021-**; .0002-***; .0001-****). Gene expression was quantified by qPCR. RNA was extracted from same plants used for ROS burst assay (25 days post-infiltration). Actin was used as reference gene. The data are shown as mean ±SD from three independent experiments. Trypan blue staining was used as control for cell death.

There was no cell death that influenced the high accumulation of ROS upon flagellin perception in plants, as expected. These results indicate that M17L and

PED1 act as negative regulators in a ROS dependent signaling response in plant immunity.

2.5.5.2. ROS independent silenced genes in Nicotiana benthamiana

Another silenced ROSIE 3 potential interacting protein, the *NbAIM1*, which was transiently expressed in *N.benthamiana* did not indicate any significant fluctuation in relation to ROS burst induced by flagellin (Figure 14C).

2.5.6. VIGS of ROSIE 4 Interacting Proteins

This master thesis is not including any VIGS constructs for ROSIE 4 due to a non-functional construct of ROSIE 4-mCherry, that was sent out for mass spectrometry.

3. DISCUSSION

Due to the evidence gathered that ROS engages in plant signaling upon pathogen invasion, an increased interest in deciphering the role of ROS in the cell and their compartments has been shown. ROS are natural byproducts of the cellular metabolism and the balancing concentration is important to determine its function. In low concentrations they act as signaling molecules in a gene scavenging system to warn from intruders, whereas in high concentrations they become a serious threat leading to HR and PCD (Ali et al. 2018). In fact, ROS oxidative burst is characterized to be the first line of defense in plants produced by NADPH oxidase when the membrane receptors sense any invading pathogen (Torres et al. 2006).

In contrary, pathogen counteracts the defense system of the plant by penetrating protein molecules, so called effector, which modulate host's metabolism. Some of these effectors are capable of suppressing the generation and accumulation of ROS in the apoplastic space, ultimately leading to the inhibition of plant signaling pathways to promote successful colonization of its respective host plant (Jwa and Hwang 2017).

The presented work provides first insight into four *U. maydis* effectors, ROSIE1-4 previously identified to inhibit ROS burst in plants during pathogen perception. The next few subchapters will discuss the specific observations made in elucidating ROSIE 1-4, and how these results might help in further investigations to specify the role of this ROS inhibiting effectors.

3.1. Impact of ROSIE 1-3 on virulence in *Zea mays*

A few *U. maydis* effectors have been so far characterized to be key factors in promoting gall formations in maize. The secreted effector proteins ROSIE 1-3 were not given any indications to contribute to a virulence defect by testing deletion strains in the maize accession EGB, potentially due to functional redundancy. However, for ROSIE 1 it was observed that there is a slight but not statistically significant tendency in the reduction of gall formation on the maize leaf surface.

A recent study about a newly discovered effector ApB73, has proven that the outcome of an infection is not only depending of the pathogens strength but also on the susceptibility of its host (Stirnberg and Djamei 2016). Here, it was shown that virulence phenotypes caused by deletion strains that had a slight visible

virulence defect can be intensified by testing them in maize accession B73 instead of EGB. Considering the fact, that ROSIE 1 showed similar indications, it might be of use to infect deletion strains in maize accession B73 to further get some signs on its impact of virulence in maize.

3.2. Suppressing effects on ROS activity levels of ROSIE 1-4 in different subcellular compartments detected

Effectors can act after secretion either in the biotrophic interphase (space between the fungus and the plant) or further translocate inside the host cell. According to its place of action, diffused effectors inside the host cell can further target different sub-compartments in order to reduce pathogen recognition (Uhse and Djamei 2018).

The observation that all the ROSIEs were identified to suppress ROS burst within the plant cell, one of the major open questions was to determine in which cell compartment they mostly contribute to ROS suppression. Therefore, forcing the effectors to the plasma membrane, cytosol and nucleus were accomplished by different localization tags.

ROS burst activity measurements gave indications that ROSIE 1 was suppressing ROS burst highly in the nucleus. However, since there were no clear separations between the nucleus and the cytoplasm, it is also possible that ROSIE 1 execute its action in suppressing ROS in both cellular compartments or the target of ROSIE1 shuttles between both compartments allowing the interaction with the effector occurring independent of the mislocalisation of the effector. The results of a study leads to hypothesize that the ROS inhibiting effector might split up into two parts and in that way target the nucleus and the cytoplasm to ultimately block ROS accumulation upon pathogen infection. Still, since it is not yet completely clear how the signals are mediated and transmitted to the cytoplasm, a possible way might also be that there is a close interaction between the two subcellular compartments in activating defense related genes when sensing PAMPs (Shapiguzov et al. 2012). Consequently, ROSIE 1 in this case needs to react accordingly by targeting specific signaling molecules in order to promote a successful colonization of the respective host.

An already confirmed fact is that the first visible aspect of an invading intruder, is the high accumulation of ROS, generated by the plasma membrane NADPH oxidases known in plants as respiratory burst oxidase homolog D (RBOHD)

(Kadota et al. 2015). Indications that ROSIE 4 shows ROS inhibiting activities at the plasma membrane, leads to believe that the effector specifically targets components that would inhibit the ROS generation completely by modifying regulatory mechanisms controlling RBOHD activation. Since RBOHs have Ca2+-binding EF-hand motifs in their N-terminal regions which is experimentally shown to be required for ROS production (Ogasawara et al. 2008), one possible way to deactivate RBOHD through ROSIE 4 might be by inducing conformational changes that would lead to the closure of Ca^{2+} channels. Another possibility would be by targeting immune receptor related components (Li et al. 2014) and in that way make it capable to suppress ROS generation.

In comparison to ROSIE 1 and 4, no clear indications were detected for ROSIE 2 and 3, related to its probable place of action. Microscopy imaging of ROSIE 2-mCherry and ROSIE 3-mCherry showed that both effectors were expressed all over the cell. Considering this fact, an explanation might be that the effectors are multiplayers and target several components in different subcellular compartments to restrain molecules in a ROS dependent signaling network. Another possibility is that interaction partners of ROSIE 2 and 3 shuffles between different cellular compartments and therefore shows ROS suppression in all analysed parts of the cell. Furthermore, it can be speculated that the expression in the cytosol, even just small amounts, are sufficient to lead to ROS suppression, regardless if an NLS tag is added.

3.3. Interaction partners of ROSIE 1-3

One of the key questions regarding the ROSIEs is the specific mechanism of its function related to ROS suppression upon pathogen perception. To specify interacting proteins, co-immunoprecipitation followed by mass-spectrometry was performed. This identified 21 possible interacting partners. Interestingly, 8 out of them showed a significant shift in ROS activities when silencing them through VIGS.

3.3.1. ROSIE 1 targeting proteins

Plants respond to pathogens through an elaborate network of interactions. Therefore, it’s quite important for the pathogen to evolve attacking strategy by secreting effector proteins that target special cell proteins to modify the host metabolism and establish a successful infection.

Plants respond to pathogens through an elaborate network of interactions. Therefore, it’s quite important for the pathogen to evolve effector proteins that

target host proteins to modify the host metabolism and establish a successful infection.

According to the mass spectrometry data, ROSIE 1 showed to co-immunoprecipitate with lipoxygenases, two components of the phenylpropanoid pathway (4-coumarate CoA ligase 1 and trans-cinnamate 4-monooxygenase) and the eukaryotic initiation translation factor 3J. Silencing of lipoxygenase, 4-coumarate CoA ligase 1 and trans-cinnamate 4-monooxygenase in *N. benthamiana* revealed an increase of ROS production upon flagellin perception and therefore it can be assumed that it is negatively regulating the ROS burst. In contrast, the eukaryotic initiation translation factor 3J silenced plants showed a decreased level of ROS accumulation and probably stimulates the ROS burst in a positive way.

Induction of LOX genes during a pathogenic invasion in plants has been reported in several research papers so far. The function of LOX in plant defense response seems to be related in synthesizing different compounds with signaling functions (Creelman and Mullet 1997), activating HR responses (Rusterucci et al. 1999) and induce defense responses in parts of the plants that are not yet under the attack (Woldemariam et al. 2018) (Figure 15A). In this thesis, it was shown that lipoxygenases in relation to ROS accumulation act as negative regulators and decrease the levels of ROS upon pathogen attack. There is abundant evidence that the function of LOX pathway leads to formation of jasmonic acid which is involved as signaling molecule upon plant responses to pathogens (Creelman and Mullet 1997). In most cases JA and SA signaling pathways interact antagonistically in activating defense responses to pathogens. Once the JA signaling is activated, the SA levels will decrease and SA signaling will be suppressed (Koornneef and Pieterse 2008). To evaluate if this is the case here, jasmonic acid measurements should be performed as well as the effect of ROSIE 1 in *coi1* mutant, which has reduced sensitivity to jasmonate, should be tested.

Also, that the phenylpropanoid pathway is involved in defense signaling towards a pathogen attack by synthesizing different molecules such as phenylpropanoids or lignins has been shown (König et al. 2014). This branch of the pathway involves also 4CL and C4H (Figure 15A). Interestingly, a previously identified *U. maydis* effector Cmu1 was identified to alter the shikimate pathway (branch of phenylpropanoid pathway), and change the metabolic status through metabolic priming in neighboring cells (Djamei et al. 2011).

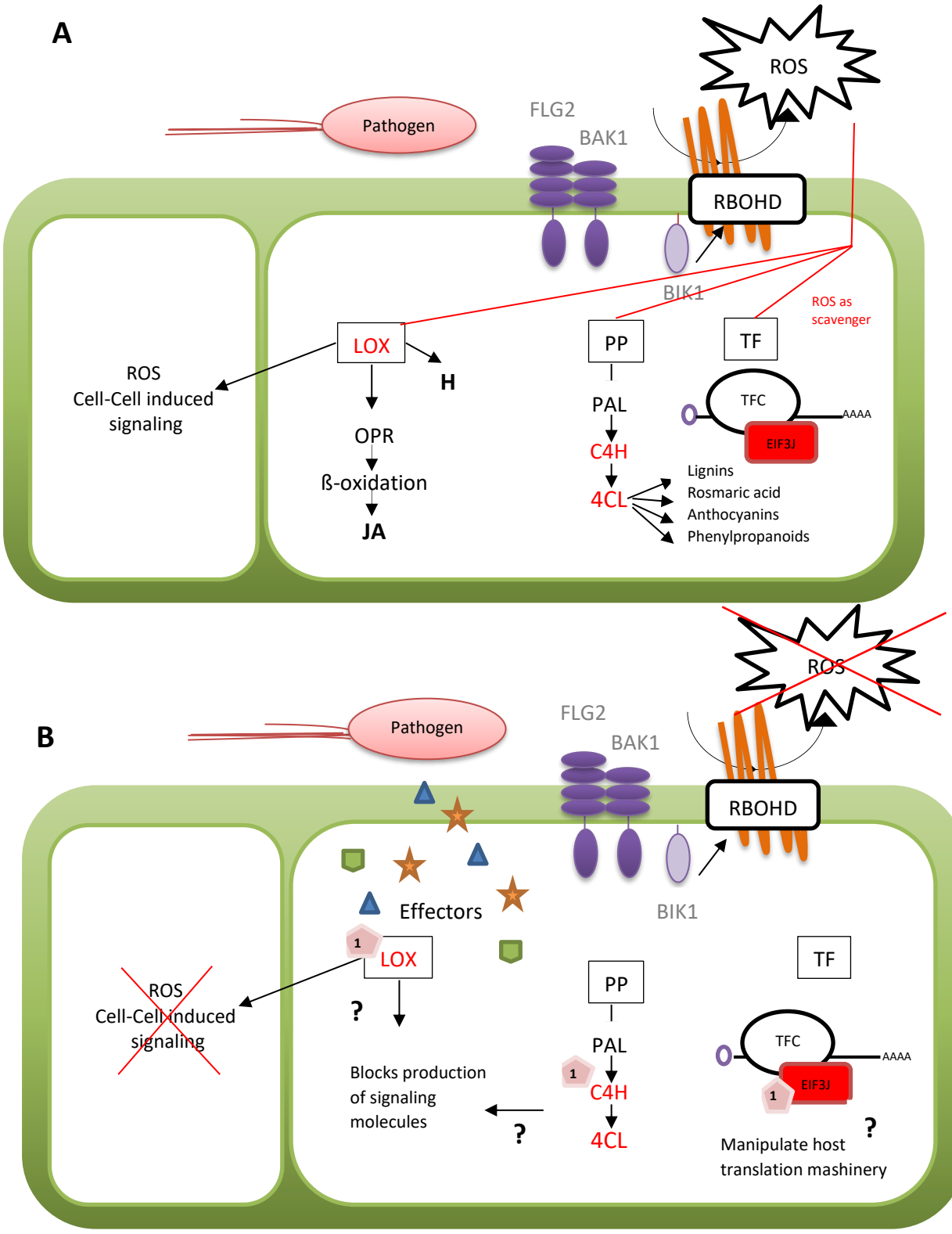

Figure 15: ROSIE 1 targets several plant components to help colonizing its host successfully. (A) Interacting proteins of ROSIE 1 and its function related to ROS burst. **(B)** Possible targeting strategies of ROSIE 1. JA-jasmonic acid; HR–hypersensitive response; PP-phenylpropanoid pathway; TF-translation factor; OPR-oligolipins; PAL-phenylalanine; C4H-cinnamate; 4CL-p-coumarate; TFC-translation factor complex; EIF3J-eukaryotic translation initiation factor 3; ROS-reactive oxygen species. ROSIE 1 effector marked pink.

Similarly, another *U. maydis* effector, the Tin2, was shown to interfere with the phenylpropanoid pathway changing metabolites into the anthocyanin pathway to lower their availability for other defense signaling responses. This result suggests that maybe 4CL and CH4 suppresses hyper activation of ROS in response to pathogens in order to keep the right concentrations of ROS levels not to cause huge damage to plant, but still to keep the levels ideal to signal other cells that the plant is under attack to respond accordingly.

The silencing of *NbEIF3J*, however, showed to positively regulate ROS levels upon pathogen invasion. Therefore, these results lead to assume that EIF3J which is involved in the translation machinery of proteins (Machado et al. 2017) activates the synthesis of proteins that sense the attack (Figure 15A).

How ROSIE 1 manipulates the signaling network within the plant, when being under attack, is not clear at the moment. But it can be speculated that it targets specifically the translation machinery to suppress host innate defenses which may act to impair the protein production capacity of attacked cells. The involvement of the effector might be also important in blocking signaling molecules of the LOX or phenylpropanoid pathway, and therefore disrupt the communication between the cells (Figure 15B). However, to completely identify the function of ROSIE 1 within the plant cell when being attacked, further investigations needs to be done.

3.3.2. ROSIE 2 targeting proteins

The involvement of ROS as a scavenger molecule in plants play a crucial role in activating several defense signaling pathways upon pathogen invasions. In this study, it is reported that NFXL1 and DRP5A, which were identified through mass spectrometry, are potential interacting partners of ROSIE 2.

A recent study showed that NFXL1 function as a negative regulator of some defense related genes via an SA-dependent signaling pathway (Asano et al. 2008). In a VIGS approach performed in this master thesis, silencing of *NbNFXL1* was identified to show an increased accumulation of ROS after flagellin treatment. This result suggests that NFXL1 acts as negative regulator of ROS in a defense signaling response and probably suppresses hyper activation of ROS in order to keep the right concentrations of ROS levels to activate downstream signaling events related to the SA-signaling pathway (Figure 16A).

Noteworthy, is the engagement of DRP5A in plant defense response. It is so far known that dynamin related proteins have an important role in microtubule associated events (Miyagishima et al. 2008). Recent evidence also suggest an important interplay between microtubules and ROS during a plant-pathogen interaction (Livanos et al. 2014; Hardham 2013). Taking all of this together and the fact that DRP5A showed an increased ROS burst upon flagellin induction in *NbDRP5A* silenced plants, it can be speculated that ROS serves as a scavenger molecule to lead the infected plant cell in a microtubule reorganization with the help of DRP5A as part of the plants defense responses.

Since ROSIE 2 showed a decreased level of ROS burst demonstrated in the ROS screen, the identified interacting proteins might shed some new information about its involvement in plant infection. On one hand, targeting NFXL1 from ROSIE 2 side might lead to a blockade of signaling components related to the SA depending signaling pathway. And on the other hand, ROSIE two might be involved in targeting and manipulating the cytoskeleton complex of the plant to promote the invasion of the plant (Figure 16B).

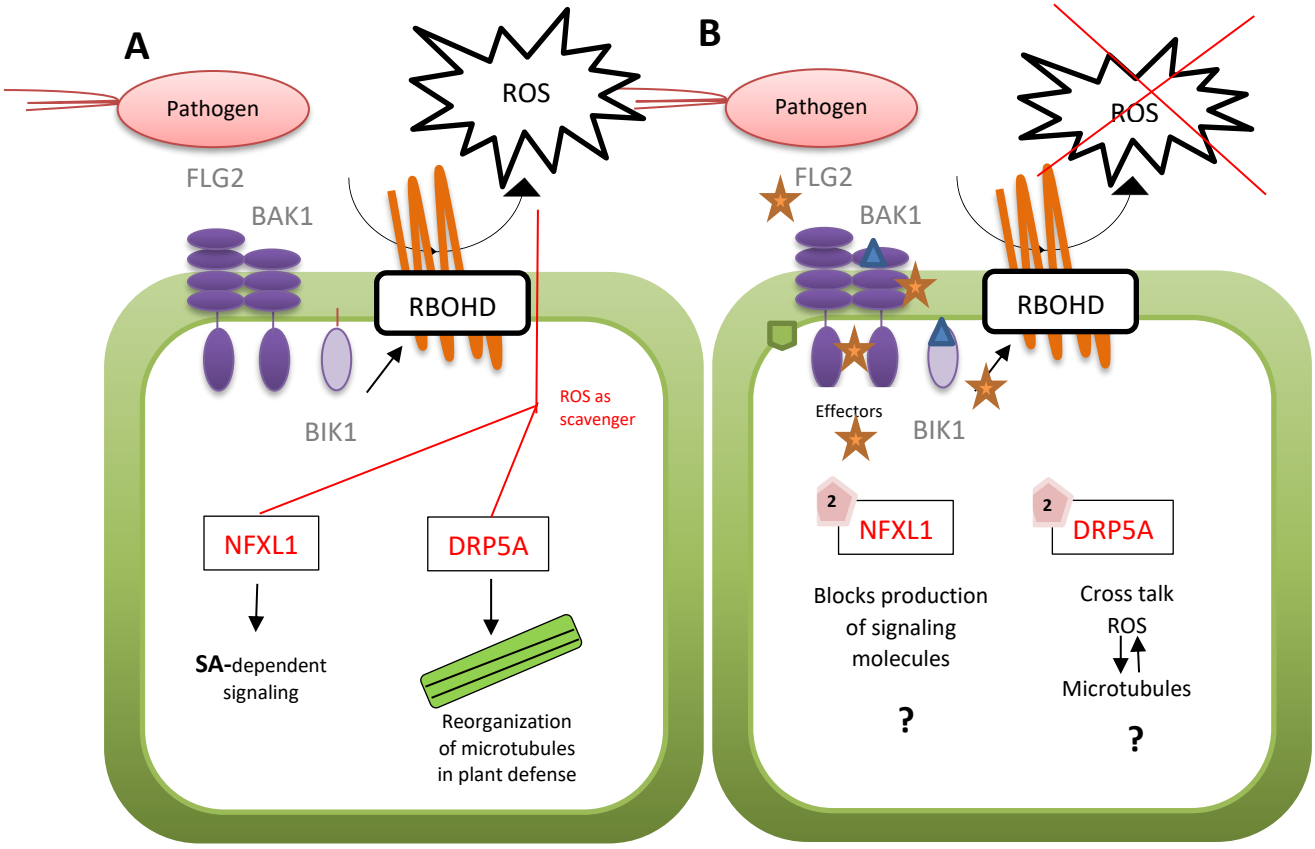

Figure 16: ROSIE 2 targets SA-signaling molecules and cytoskeleton elements of the plant to colonize it successfully. (A) Interacting proteins of ROSIE 2 and its function related to ROS burst. **(B)** Possible targeting strategies of ROSIE 2. SA-salicylic acid; NFXL1-nf-x1-type zink finger protein nfxl1; DRP5A-dynami related protein 5A; ROS-reactive oxygen species. ROSIE 2 effector marked pink.

Another important identified protein that showed a potential interaction with ROSIE 2 was myosin 17-like. This interaction partner will be in more details discussed in the part below, because mass spectrometry showed a higher coverage of it with ROSIE 3.

3.3.3. ROSIE 3 targeting proteins

PED 1 and M17L were identified through mass spectrometry to be potential interacting proteins of ROSIE 3. Silencing of these genes in *N. benthamiana* via VIGS, showed an increased ROS burst for both interacting partners. Therefore, these results suggest that PED 1 and M17L are negative regulators in ROS dependent response of the plants upon a pathogen attack.

Pathogen penetration through the plants cell wall, activates several components that remodel actin cytoskeleton to establish effective barrier against the pathogen ingress. There is less known about the regulation of molecular mechanisms that regulate this process but it is shown that myosin plays an important role as molecular motors for actin filament motility (Yang et al. 2014). Several organelles such as peroxisomes, Golgi etc., are moved during this time to the penetration site (Koh et al. 2005). In correlation to the findings of this thesis, it can be assumed that myosin motors remodel actin filaments during interactions with invading pathogens. But, there is still little information on how this process is regulated (Figure 17A).

Furthermore, PED1 is a peroxisomal thiolase and involved in the final step to produce acetyl CoA in the ß-oxidation cycle. PED1 is also implicated in the synthesis of JA (Koo et al. 2006) and NADPH oxidation in plants (Ying 2008). To overcome an intruder, it can be speculated that M17L and PED1 work as teamplayers. At the one side, myosin pulls the peroxisomes to the penetration side when the cell is sensing the pathogen whereas PED1 which is involved in NADPH oxidation, generates ROS in the apoplast of the plant to promote PTI (Figure 17A).

Therefore, it is important to regulate the concentration levels of ROS, to minimize its accumulation, upon pathogen attack not to cause serious damage to the cell but still to produce enough to activate ROS as signaling molecules.

So, targeting those proteins by ROSIE 3 leads to suspect, that it inhibits ROS generation by modifying regulatory and transport mechanism which control NADPH activation or the reprogramming of actin filaments.

Another important identified protein that showed a potential interaction with ROSIE 3 was the eukaryotic translation initiation factor 3J previously described as an interacting partner of ROSIE 1.

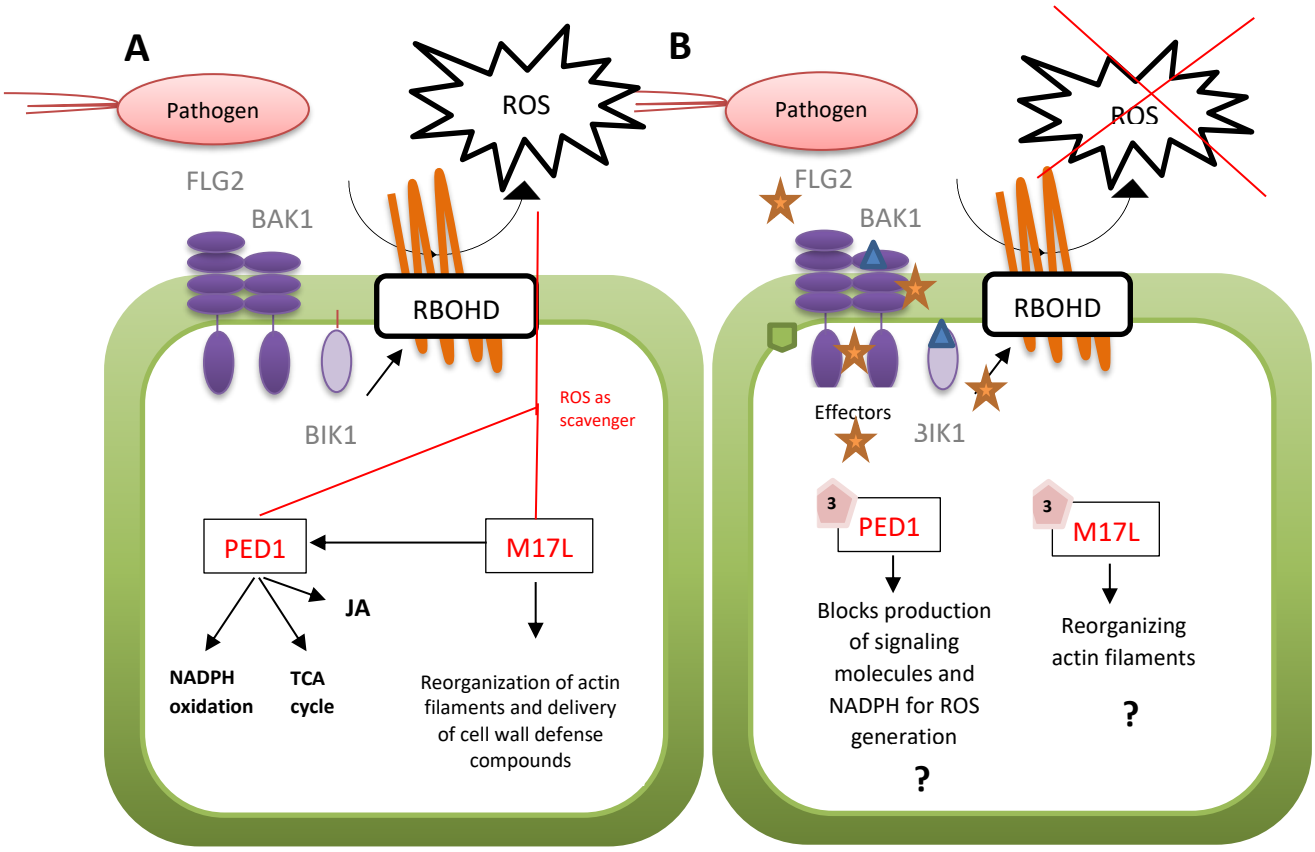

Figure 17: ROSIE 3 targets SA-signaling molecules and cytoskeleton elements of the plant to colonize it successfully. (A) Interacting proteins of ROSIE 3 and its function related to ROS burst. **(B)** Possible targeting strategies of ROSIE 3. PED1-3-ketoacyl CoA thiolase 2, peroxisomal; M17L-myosin 17-like; JA-jasmonate response; ROS-reactive oxygen species. ROSIE 3 effector marked pink.

4. CONCLUDING REMARKS

Functional elucidation of effectors is important to understanding plant-pathogen interactions. One aspect to get new insight into an effectors involvement within the plants cell is to monitor ROS burst. ROS homeostasis is of a particular importance during plants defense responses and emerges to be a significant regulator of many cell components.

Within this thesis, the so far uncharacterized ROSIEs were shown to be important effectors that suppress the ROS production upon pathogen attack. The shown experiments illustrate that ROSIEs interact with specific interacting partners to manipulate different regulatory mechanisms that support the fungus ingress and spread within its host. Additionally, it was shown that the ROSIEs target different signaling pathways to disrupt ROS accumulation.

Although this work provides first insight into the functional role of ROSIE 1-4, several questions still remains open. One question to address would be, how this whole signaling network functions in a ROS dependent manner and in which relation the ROSIEs contribute to its interruption.

Furthermore, since all of these experiments were conducted in *N. benthamiana* it would be interesting to see what impact this interacting partner of ROSIEs would have in *Z. mays.*

Overall, it is a quite surprising fact that almost all of the ROSIEs interacting partners are found to be negative regulators of ROS where one would expect that interfering with a positive regulator in the PTI response is much easier than activating a negative regulator of ROS.

5. OUTLOOK

To clearly define the function of ROSIE 1-4, further investigations need to be done. In a first step a Yeast 2 hybrid should be performed between the ROS inhibiting effectors and the identified interacting partners to confirm the direct interaction.

Also, the JA levels should be measured in the silenced *N. benthamiana* plants of interacting ROSIEs proteins. Furthermore, the effect of ROSIEs in JA signaling should be tested in *coi1* mutants which lacks the *coi1* gene required for response to jasmonate.

Additionally, the virulence impact of ROSIE 1 knock out strains needs to be performed in the maize accession B73, to get a more clear view on its virulence defect in maize.

Finally, Arabidopsis estradiol inducible and Arabidopsis overexpressed stable lines carrying ROSIEs needs to be grown to study the function further.

6. MATERIAL AND METHODS

6.1. Material

6.1.1. Chemicals

All chemicals that were used throughout this master thesis were purchased from Merck, Roche, PanReacAppliChem, Qiagen, CenticBiotec, Analytik Jena, Sigma-Aldrich, Thermo Fisher Scientific and Carl-Roth.

6.1.2. Enzymes and Antibodies

Restriction enzymes and polymerases were purchased from New England Biolabs and Thermo Fisher Scientific, lytic enzymes from Sigma-Aldrich. The α-MYC antibody (mouse) were purchased from Sigma-Aldrich (M4439-100UL) and the HRP-coupled anti-mouse antibody (sheep) from GE Healthcare (NA931VS).

6.1.3. Buffers and Solutions

Standard buffers and solutions were prepared according to Ausubel *et al.* (2003) and Sambrook *et al.* (1989). In case special buffers and solutions were required, they are mentioned within the corresponding method. If necessary, solutions were autoclaved at 121°C for 5 minutes. Heat sensitive solutions were filter sterilised using filters with a pore size of 0.2 µm.

6.1.4. Commerical kits and additional material

The following kits were used: InnuPrep Doublepure Kit (Jena Analytic) for the purification of PCR products and DNA fragments from agarose gels; Qiagen buffers and columns provided by Centic Biotec for plasmid preparation; Gateway LR ClonaseII Enzyme mix (Thermo Fisher Scientific) for gateway cloning; RNeasy (Qiagen) for RNA extraction, Super III First Strand Synthesis Super Mix Kit or RevertAid H Minus First Strand cDNA Synthesis Kit (Thermo Fisher Scientific) for cDNA synthesis from RNA; LightCycler FastStart Essential DNA Green Master (Roche) for quantitative real time PCR Amersham ECL Prime Western Blotting Detection Reagent (GE Healthcare) for chemiluminescence detection. Additional material is listed in individual method sections.

6.1.5. Strains and Plasmids

In this thesis following strain of E. coli was used:

Strain	Genotype	Application	Reference
One Shot® Mach1™-T1R Chemically Competent *E. coli*	F– Φ80lacZΔM15 ΔlacX74 *hsd*R(rK–, mK+) ΔrecA1398 *end*A1 *ton*A	Cloning	Invitrogen

The following plasmids were generated throughout this study:

Name	**Resistance**	**Note**
pJET_PDS	Amp^R	*DNA fragment of PDS in pJET for Virus Induced Gene Silencing*
pJET_Lipoxygenase	Amp^R	*DNA fragment of Lipoxygenase in pJET for Virus Induced Gene Silencing*
pJET_Putative Carboxylesterase 120	Amp^R	*DNA fragment of Putative Carboxylesterase 120 in pJET for Virus Induced Gene Silencing*
pJET_4-Coumarate –CoA ligase 1	Amp^R	*DNA fragment of 4-Coumarate –CoA ligase 1 in pJET for Virus Induced Gene Silencing*
pJET_Serine/Threonine Protein Phosphatase PP2A catalytic subunit	Amp^R	*DNA fragment of Serine/Threonine Protein Phosphatase PP2A catalytic subunit in pJET for Virus Induced Gene Silencing*
pJET_Trans-Cinnamate 4-Monooxygenase	Amp^R	*DNA fragment of Trans-Cinnamate 4-Monooxygenase in pJET for Virus Induced Gene Silencing*
pJET_Carbamoyl-Phosphate Synthase largechain, chloroplastic-like	Amp^R	*DNA fragment of Carbamoyl-Phosphate Synthase largechain, chloroplastic-like in pJET for Virus Induced Gene Silencing*
pJET_Dynamin-Related protein 1E-like	Amp^R	*DNA fragment of Dynamin-Related protein 1E-like in pJET*

		for Virus Induced Gene Silencing
pJET_Dynamin-2A-like	Amp^R	*DNA fragment of Dynamin-2A-like in pJET for Virus Induced Gene Silencing*
pJET_Coatomer subunit beta	Amp^R	*DNA fragment of Coatomer subunit beta in pJET for Virus Induced Gene Silencing*
pJET_Coatomer subunit alpha	Amp^R	*DNA fragment of Coatomer subunit alpha in pJET for Virus Induced Gene Silencing*
pJET_Myosin-17-like	Amp^R	*DNA fragment of Myosin-17-like in pJET for Virus Induced Gene Silencing*
pJET_Peroxisomal Fatty Acid Beta-Oxidation Multifunctional Protein AIM1-like	Amp^R	*DNA fragment of Peroxisomal Fatty Acid Beta-Oxidation Multifunctional Protein AIM1-like in pJET for Virus Induced Gene Silencing*
pJET_3-Ketoacyl-CoA thiolase 2, peroxisomal	Amp^R	*DNA fragment of 3-Ketoacyl-CoA thiolase 2, peroxisomal in pJET for Virus Induced Gene Silencing*
pJET_5´Nucleotidase domain-containing protein 4-like isoform X1	Amp^R	*DNA fragment of 5´Nucleotidase domain-containing protein 4-like isoform X1 in pJET for Virus Induced Gene Silencing*
pJET_Uncharacterized Protein LOC107820356	Amp^R	*DNA fragment of Uncharacterized Protein LOC107820356 in pJET for Virus Induced Gene Silencing*
pJET_Eukaryotic translation initiation factor 3 subunit J	Amp^R	*DNA fragment of Eukaryotic translation initiation factor 3 subunit J in pJET for Virus Induced Gene Silencing*
pJET_Uncharacterized Protein LOC107777101 isoform X2	Amp^R	*DNA fragment of Uncharacterized Protein LOC107777101 isoform X2 in pJET for Virus Induced Gene Silencing*
pJET_Nf-X1-type Zink Finger Protein nfxl1	Amp^R	*DNA fragment of Nf-X1-type Zink Finger Protein nfxl1 in*

		pJET for Virus Induced Gene Silencing
pJET_Dynamin-Related Protein 5a	Amp^R	*DNA fragment of Dynamin-Related Protein 5a in pJET for Virus Induced Gene Silencing*
pJET_Dynamin-like Protein ARC5 isoform X1	Amp^R	*DNA fragment of Dynamin-like Protein ARC5 isoform X1 in pJET for Virus Induced Gene Silencing*
pJET_ Dead´-Box ATP-dependent RNA helicase 3, chloroplastic	Amp^R	*DNA fragment of Dead´-Box ATP-dependent RNA helicase 3, chloroplastic in pJET for Virus Induced Gene Silencing*
pENTRY_PDS	$Spec^R$	*DNA fragment of PDS in pENTRY for Virus Induced Gene Silencing*
pENTRY_Lipoxygenase	$Spec^R$	*DNA fragment of Lipoxygenase in pENTRY for Virus Induced Gene Silencing*
pENTRY_Putative Carboxylesterase 120	$Spec^R$	*DNA fragment of Putative Carboxylesterase 120 in pENTRY for Virus Induced Gene Silencing*
pENTRY_4-Coumarate –CoA ligase 1	$Spec^R$	*DNA fragment of 4-Coumarate –CoA ligase 1 in pENTRY for Virus Induced Gene Silencing*
pENTRY_Serine/Threonine Protein Phosphatase PP2A catalytic subunit	$Spec^R$	*DNA fragment of Serine/Threonine Protein Phosphatase PP2A catalytic subunit in pENTRY for Virus Induced Gene Silencing*
pENTRY_Trans-Cinnamate 4-Monooxygenase	$Spec^R$	*DNA fragment of Trans-Cinnamate 4-Monooxygenase in pENTRY for Virus Induced Gene Silencing*
pENTRY_Carbamoyl-Phosphate Synthase largechain, chloroplastic-like	$Spec^R$	*DNA fragment of Carbamoyl-Phosphate Synthase largechain, chloroplastic-like in pENTRY for Virus Induced Gene Silencing*
pENTRY_Dynamin-Related protein 1E-like	$Spec^R$	*DNA fragment of Dynamin-Related protein 1E-like in pENTRY for Virus Induced Gene Silencing*

pENTRY_Dynamin-2A-like	$Spec^R$	*DNA fragment of Dynamin-2A-like in pENTRY for Virus Induced Gene Silencing*
pENTRY_Coatomer subunit beta	$Spec^R$	*DNA fragment of Coatomer subunit beta in pENTRY for Virus Induced Gene Silencing*
pENTRY_Coatomer subunit alpha	$Spec^R$	*DNA fragment of Coatomer subunit alpha in pENTRY for Virus Induced Gene Silencing*
pENTRY_Myosin-17-like	$Spec^R$	*DNA fragment of Myosin-17-like in pENTRY for Virus Induced Gene Silencing*
pENTRY_Peroxisomal Fatty Acid Beta-Oxidation Multifunctional Protein AIM1-like	$Spec^R$	*DNA fragment of Peroxisomal Fatty Acid Beta-Oxidation Multifunctional Protein AIM1-like in pENTRY for Virus Induced Gene Silencing*
pENTRY_3-Ketoacyl-CoA thiolase 2, peroxisomal	$Spec^R$	*DNA fragment of 3-Ketoacyl-CoA thiolase 2, peroxisomal in pENTRY for Virus Induced Gene Silencing*
pENTRY_5´Nucleotidase domain-containing protein 4-like isoform X1	$Spec^R$	*DNA fragment of 5´Nucleotidase domain-containing protein 4-like isoform X1 in pENTRY for Virus Induced Gene Silencing*
pENTRY_Uncharacterized Protein LOC107820356	$Spec^R$	*DNA fragment of Uncharacterized Protein LOC107820356 in pENTRY for Virus Induced Gene Silencing*
pENTRY_Eukaryotic translation initiation factor 3 subunit J	$Spec^R$	*DNA fragment of Eukaryotic translation initiation factor 3 subunit J in pENTRY for Virus Induced Gene Silencing*
pENTRY_Uncharacterized Protein LOC107777101 isoform X2	$Spec^R$	*DNA fragment of Uncharacterized Protein LOC107777101 isoform X2 in pENTRY for Virus Induced Gene Silencing*
pENTRY_Nf-X1-type Zink Finger Protein nfxl1	$Spec^R$	*DNA fragment of Nf-X1-type Zink Finger Protein nfxl1 in pENTRY for Virus Induced Gene Silencing*
pENTRY_Dynamin-Related Protein 5a	$Spec^R$	*DNA fragment of Dynamin-Related Protein 5a in pENTRY*

		for Virus Induced Gene Silencing
pENTRY_Dynamin-like Protein ARC5 isoform X1	$Spec^R$	*DNA fragment of Dynamin-like Protein ARC5 isoform X1 in pENTRY for Virus Induced Gene Silencing*
pENTRY_ Dead´-Box ATP-dependent RNA helicase 3, chloroplastic	$Spec^R$	*DNA fragment of Dead´-Box ATP-dependent RNA helicase 3, chloroplastic in pENTRY for Virus Induced Gene Silencing*
EXP VECTOR_PDS	Kan^R	*DNA fragment of PDS in Expression vector for Virus Induced Gene Silencing*
EXP VECTOR _Lipoxygenase	Kan^R	*DNA fragment of Lipoxygenase in Expression vector for Virus Induced Gene Silencing*
EXP VECTOR _Putative Carboxylesterase 120	Kan^R	*DNA fragment of Putative Carboxylesterase 120 in Expression vector for Virus Induced Gene Silencing*
EXP VECTOR _4-Coumarate –CoA ligase 1	Kan^R	*DNA fragment of 4-Coumarate –CoA ligase 1 in Expression vector for Virus Induced Gene Silencing*
EXP VECTOR _Serine/Threonine Protein Phosphatase PP2A catalytic subunit	Kan^R	*DNA fragment of Serine/Threonine Protein Phosphatase PP2A catalytic subunit in Expression vector for Virus Induced Gene Silencing*
EXP VECTOR _Trans-Cinnamate 4-Monooxygenase	Kan^R	*DNA fragment of Trans-Cinnamate 4-Monooxygenase in Expression vector for Virus Induced Gene Silencing*
EXP VECTOR _Carbamoyl-Phosphate Synthase largechain, chloroplastic-like	Kan^R	*DNA fragment of Carbamoyl-Phosphate Synthase largechain, chloroplastic-like in Expression vector for Virus Induced Gene Silencing*
EXP VECTOR _Dynamin-Related protein 1E-like	Kan^R	*DNA fragment of Dynamin-Related protein 1E-like in Expression vector for Virus Induced Gene Silencing*

EXP VECTOR _Dynamin-2A-like	Kan^R	*DNA fragment of Dynamin-2A-like in Expression vector for Virus Induced Gene Silencing*
EXP VECTOR _Coatomer subunit beta	Kan^R	*DNA fragment of Coatomer subunit beta in Expression vector for Virus Induced Gene Silencing*
EXP VECTOR _Coatomer subunit alpha	Kan^R	*DNA fragment of Coatomer subunit alpha in Expression vector for Virus Induced Gene Silencing*
EXP VECTOR _Myosin-17-like	Kan^R	*DNA fragment of Myosin-17-like in Expression vector for Virus Induced Gene Silencing*
EXP VECTOR _Peroxisomal Fatty Acid Beta-Oxidation Multifunctional Protein AIM1-like	Kan^R	*DNA fragment of Peroxisomal Fatty Acid Beta-Oxidation Multifunctional Protein AIM1-like in Expression vector for Virus Induced Gene Silencing*
EXP VECTOR _3-Ketoacyl-CoA thiolase 2, peroxisomal	Kan^R	*DNA fragment of 3-Ketoacyl-CoA thiolase 2, peroxisomal in Expression vector for Virus Induced Gene Silencing*
EXP VECTOR _5´Nucleotidase domain-containing protein 4-like isoform X1	Kan^R	*DNA fragment of 5´Nucleotidase domain-containing protein 4-like isoform X1 in Expression vector for Virus Induced Gene Silencing*
EXP VECTOR _Uncharacterized Protein LOC107820356	Kan^R	*DNA fragment of Uncharacterized Protein LOC107820356 in Expression vector for Virus Induced Gene Silencing*
EXP VECTOR _Eukaryotic translation initiation factor 3 subunit J	Kan^R	*DNA fragment of Eukaryotic translation initiation factor 3 subunit J in Expression vector for Virus Induced Gene Silencing*
EXP VECTOR _Uncharacterized Protein LOC107777101 isoform X2	Kan^R	*DNA fragment of Uncharacterized Protein LOC107777101 isoform X2 in Expression vector for Virus Induced Gene Silencing*

EXP VECTOR _Nf-X1-type Zink Finger Protein nfxl1	Kan^R	*DNA fragment of Nf-X1-type Zink Finger Protein nfxl1 in Expression vector for Virus Induced Gene Silencing*
EXP VECTOR _Dynamin-Related Protein 5a	Kan^R	*DNA fragment of Dynamin-Related Protein 5a in Expression vector for Virus Induced Gene Silencing*
EXP VECTOR _Dynamin-like Protein ARC5 isoform X1	Kan^R	*DNA fragment of Dynamin-like Protein ARC5 isoform X1 in Expression vector for Virus Induced Gene Silencing*
EXP VECTOR _ Dead´-Box ATP-dependent RNA helicase 3, chloroplastic	Kan^R	*DNA fragment of Dead´-Box ATP-dependent RNA helicase 3, chloroplastic in Expression vector for Virus Induced Gene Silencing*
pGG-35S-myr-mCherry-myc UMAG_04039-dummy-Ubq10-BastaR	$Spec^R$	*Effector tagged to the m*yristoylation *tag for Mislocalization assay*
pGG-35S-dummy-UMAG_04039-NLS-mCherry-myc-Ubq10-BastaR	$Spec^R$	*Effector tagged to the nuclear localization signaling tag for Mislocalization assay*
pGG-35S-dummy-UMAG_04039-NES-mCherry-myc-Ubq10-BastaR	$Spec^R$	*Effector tagged to the nuclear export signaling tag for Mislocalization assay*
pGG-35S-myr-mCherry-myc UMAG_05927-dummy-Ubq10-BastaR	$Spec^R$	*Effector tagged to the m*yristoylation *tag for Mislocalization assay*
pGG-35S-dummy-UMAG_05927-NLS-mCherry-myc-Ubq10-BastaR	$Spec^R$	*Effector tagged to the nuclear localization signaling tag for Mislocalization assay*
pGG-35S-dummy-UMAG_05927-NES-mCherry-myc-Ubq10-BastaR	$Spec^R$	*Effector tagged to the nuclear export signaling tag for Mislocalization assay*
pGG-35S-myr-mCherry-myc UMAG_02826-dummy-Ubq10-BastaR	$Spec^R$	*Effector tagged to the m*yristoylation *tag for Mislocalization assay*
pGG-35S-dummy-UMAG_02826-NLS-mCherry-myc-Ubq10-BastaR	$Spec^R$	*Effector tagged to the nuclear localization signaling tag for Mislocalization assay*

pGG-35S-dummy-UMAG_02826-NES-mCherry-myc-Ubq10-BastaR	Spec^R	*Effector tagged to the nuclear export signaling tag for Mislocalization assay*
pGG-35S-myr-mCherry-myc UMAG_06119-dummy-Ubq10-BastaR	Spec^R	*Effector tagged to the m*yristoylation *tag for Mislocalization assay*
pGG-35S-dummy-UMAG_06119-NLS-mCherry-myc-Ubq10-BastaR	Spec^R	*Effector tagged to the nuclear localization signaling tag for Mislocalization assay*
pGG-35S-dummy-UMAG_06119-NES-mCherry-myc-Ubq10-BastaR	Spec^R	*Effector tagged to the nuclear export signaling tag for Mislocalization assay*

The following strain of A. tumefaciens was used:

Strain	Genotype	Application	Reference
GV3101/pMP90 **pSOUP**	C58C1: pGv3101 RifR; pTiC58 ΔTDNA GentR; pSoup TetR	Used for plant infection	Koncz & Schell, 1986; Hellens et al., 2000

And following A. Tumefaciens strains were generated in this study:

Notation	Genotype	Application	Resistance
GV3101 pGG p35S:: Lipoxygenase-NOS terminator-KanR	C58C1: pGv3101 RifR; pTiC58 ΔTDNA GentR; pSoup TetR; pGG p35S:: Lipoxygenase-NOS terminator-KanR	Transient expression in *Nicotiana benthamiana*	Rif^R Gent^R Tet^R Kan^R
GV3101 pGG p35S:: Putative Carboxylesterase 120-NOS terminator-KanR	C58C1: pGv3101 RifR; pTiC58 ΔTDNA GentR; pSoup TetR; p35S:: Putative Carboxylesterase 120-NOS terminator-KanR	Transient expression in *Nicotiana benthamiana*	Rif^R Gent^R Tet^R Kan^R
GV3101 pGG p35S:: 4-Coumarate –CoA ligase 1-NOS terminator-KanR	C58C1: pGv3101 RifR; pTiC58 ΔTDNA GentR; pSoup TetR; pGG p35S:: 4-Coumarate –CoA ligase 1-NOS terminator-KanR	Transient expression in *Nicotiana benthamiana*	Rif^R Gent^R Tet^R Kan^R

GV3101 pGG p35S:: Serine/Threonine Protein Phosphatase PP2A catalytic subunit -NOS terminator-KanR	C58C1: pGv3101 RifR; pTiC58 ΔTDNA GentR; pSoup TetR; pGG p35S:: Serine/Threonine Protein Phosphatase PP2A catalytic subunit -NOS terminator-KanR	Transient expression in *Nicotiana benthamiana*	Rif^R $Gent^R$ Tet^R Kan^R
GV3101 pGG p35S:: Trans-Cinnamate 4-Monooxygenase -NOS terminator-KanR	C58C1: pGv3101 RifR; pTiC58 ΔTDNA GentR; pSoup TetR; pGG p35S:: Trans-Cinnamate 4-Monooxygenase -NOS terminator-KanR	Transient expression in *Nicotiana benthamiana*	Rif^R $Gent^R$ Tet^R Kan^R
GV3101 pGG p35S:: Carbamoyl-Phosphate Synthase largechain, chloroplastic-like -NOS terminator-KanR	C58C1: pGv3101 RifR; pTiC58 ΔTDNA GentR; pSoup TetR; pGG p35S:: Carbamoyl-Phosphate Synthase largechain, chloroplastic-like -NOS terminator-KanR	Transient expression in *Nicotiana benthamiana*	Rif^R $Gent^R$ Tet^R Kan^R
GV3101 pGG p35S:: Dynamin-Related protein 1E-like -NOS terminator-KanR	C58C1: pGv3101 RifR; pTiC58 ΔTDNA GentR; pSoup TetR; pGG p35S:: Dynamin-Related protein 1E-like -NOS terminator-KanR	Transient expression in *Nicotiana benthamiana*	Rif^R $Gent^R$ Tet^R Kan^R
GV3101 pGG p35S:: Dynamin-2A-like -NOS terminator-KanR	C58C1: pGv3101 RifR; pTiC58 ΔTDNA GentR; pSoup TetR; pGG p35S:: Dynamin-2A-like -NOS terminator-KanR	Transient expression in *Nicotiana benthamiana*	Rif^R $Gent^R$ Tet^R Kan^R
GV3101 pGG p35S:: Coatomer subunit beta e-NOS terminator-KanR	C58C1: pGv3101 RifR; pTiC58 ΔTDNA GentR; pSoup TetR; pGG p35S:: Coatomer subunit beta e-NOS terminator-KanR	Transient expression in *Nicotiana benthamiana*	Rif^R $Gent^R$ Tet^R Kan^R
GV3101 pGG p35S:: Coatomer subunit alpha -NOS terminator-KanR	C58C1: pGv3101 RifR; pTiC58 ΔTDNA GentR; pSoup TetR; pGG p35S::	Transient expression in *Nicotiana benthamiana*	Rif^R $Gent^R$ Tet^R Kan^R

	Coatomer subunit alpha -NOS terminator-KanR		
GV3101 pGG p35S:: Myosin-17-like e-NOS terminator-KanR	C58C1: pGv3101 RifR; pTiC58 ΔTDNA GentR; pSoup TetR; pGG p35S:: Myosin-17-like e-NOS terminator-KanR	Transient expression in *Nicotiana benthamiana*	Rif^R $Gent^R$ Tet^R Kan^R
GV3101 pGG p35S:: Peroxisomal Fatty Acid Beta-Oxidation Multifunctional Protein AIM1-like -NOS terminator-KanR	C58C1: pGv3101 RifR; pTiC58 ΔTDNA GentR; pSoup TetR; pGG p35S:: Peroxisomal Fatty Acid Beta-Oxidation Multifunctional Protein AIM1-like -NOS terminator-KanR	Transient expression in *Nicotiana benthamiana*	Rif^R $Gent^R$ Tet^R Kan^R
GV3101 pGG p35S:: 3-Ketoacyl-CoA thiolase 2, peroxisomal -NOS terminator-KanR	C58C1: pGv3101 RifR; pTiC58 ΔTDNA GentR; pSoup TetR; pGG p35S:: 3-Ketoacyl-CoA thiolase 2, peroxisomal -NOS terminator-KanR	Transient expression in *Nicotiana benthamiana*	Rif^R $Gent^R$ Tet^R Kan^R
GV3101 pGG p35S:: 5´Nucleotidase domain-containing protein 4-like isoform X1-NOS terminator-KanR	C58C1: pGv3101 RifR; pTiC58 ΔTDNA GentR; pSoup TetR; pGG p35S:: 5´Nucleotidase domain-containing protein 4-like isoform X1-NOS terminator-KanR	Transient expression in *Nicotiana benthamiana*	Rif^R $Gent^R$ Tet^R Kan^R
GV3101 pGG p35S:: Uncharacterized Protein LOC107820356-NOS terminator-KanR	C58C1: pGv3101 RifR; pTiC58 ΔTDNA GentR; pSoup TetR; pGG p35S:: Uncharacterized Protein LOC107820356-NOS terminator-KanR	Transient expression in *Nicotiana benthamiana*	Rif^R $Gent^R$ Tet^R Kan^R
GV3101 pGG p35S:: Eukaryotic translation initiation factor 3 subunit J -NOS terminator-KanR	C58C1: pGv3101 RifR; pTiC58 ΔTDNA GentR; pSoup TetR; pGG p35S:: Eukaryotic translation initiation factor 3 subunit J -NOS terminator-KanR	Transient expression in *Nicotiana benthamiana*	Rif^R $Gent^R$ Tet^R Kan^R

GV3101 pGG p35S:: Uncharacterized Protein LOC107777101 isoform X2-NOS terminator-KanR	C58C1: pGv3101 RifR; pTiC58 ΔTDNA GentR; pSoup TetR; pGG p35S:: Uncharacterized Protein LOC107777101 isoform X2-NOS terminator-KanR	Transient expression in *Nicotiana benthamiana*	Rif^R $Gent^R$ Tet^R Kan^R
GV3101 pGG p35S:: Nf-X1-type Zink Finger Protein nfxl1-NOS terminator-KanR	C58C1: pGv3101 RifR; pTiC58 ΔTDNA GentR; pSoup TetR; pGG p35S:: Nf-X1-type Zink Finger Protein nfxl1-NOS terminator-KanR	Transient expression in *Nicotiana benthamiana*	Rif^R $Gent^R$ Tet^R Kan^R
GV3101 pGG p35S:: Dynamin-Related Protein 5a -NOS terminator-KanR	C58C1: pGv3101 RifR; pTiC58 ΔTDNA GentR; pSoup TetR; pGG p35S:: Dynamin-Related Protein 5a -NOS terminator-KanR	Transient expression in *Nicotiana benthamiana*	Rif^R $Gent^R$ Tet^R Kan^R
GV3101 pGG p35S:: Dynamin-like Protein ARC5 isoform X1-NOS terminator-KanR	C58C1: pGv3101 RifR; pTiC58 ΔTDNA GentR; pSoup TetR; pGG p35S:: Dynamin-like Protein ARC5 isoform X1-NOS terminator-KanR	Transient expression in *Nicotiana benthamiana*	Rif^R $Gent^R$ Tet^R Kan^R
GV3101 pGG p35S:: Dead´-Box ATP-dependent RNA helicase 3, chloroplastic -NOS terminator-KanR	C58C1: pGv3101 RifR; pTiC58 ΔTDNA GentR; pSoup TetR; pGG p35S:: Dead´-Box ATP-dependent RNA helicase 3, chloroplastic -NOS terminator-KanR	Transient expression in *Nicotiana benthamiana*	Rif^R $Gent^R$ Tet^R Kan^R
GV3101 pGG-p35S::mCherry-mCherry-myc-UBQ10-BastaR	C58C1: pGv3101 RifR; pTiC58 ΔTDNA GentR; pSoup TetR; pGG-p35S::mCherry-mCherry-myc-UBQ10-BastaR	Transient expression in *Nicotiana benthamiana*	Rif^R $Gent^R$ Tet^R $Spec^R$
GV3101 pGG-p35S::myr-mCherry-myc-UMAG_05927-UBQ10-BastaR	C58C1: pGv3101 RifR; pTiC58 ΔTDNA GentR; pSoup TetR; pGG-p35S::myr-mCherry-myc-UMAG_05927-UBQ10-BastaR	Transient expression in *Nicotiana benthamiana*	Rif^R $Gent^R$ Tet^R $Spec^R$

GV3101 pGG-p35S:: UMAG_05927- NLS-mCherry-myc--UBQ10-BastaR	C58C1: pGv3101 RifR; pTiC58 ΔTDNA GentR; pSoup TetR; pGG-p35S:: UMAG_05927- NLS-mCherry-myc--UBQ10-BastaR	Transient expression in *Nicotiana benthamiana*	Rif^R $Gent^R$ Tet^R $Spec^R$
GV3101 pGG-p35S:: UMAG_05927- NES-mCherry-myc--UBQ10-BastaR	C58C1: pGv3101 RifR; pTiC58 ΔTDNA GentR; pSoup TetR; pGG-p35S:: UMAG_05927- NES-mCherry-myc--UBQ10-BastaR	Transient expression in *Nicotiana benthamiana*	Rif^R $Gent^R$ Tet^R $Spec^R$
GV3101 pGG-p35S:: UMAG_05927-mCherry-myc--UBQ10-BastaR	C58C1: pGv3101 RifR; pTiC58 ΔTDNA GentR; pSoup TetR; pGG-p35S:: UMAG_05927-mCherry-myc--UBQ10-BastaR	Transient expression in *Nicotiana benthamiana*	Rif^R $Gent^R$ Tet^R $Spec^R$
GV3101 pGG-p35S::myr-mCherry-myc-UMAG_04039-UBQ10-BastaR	C58C1: pGv3101 RifR; pTiC58 ΔTDNA GentR; pSoup TetR; pGG-p35S::myr-mCherry-myc-UMAG_04039-UBQ10-BastaR	Transient expression in *Nicotiana benthamiana*	Rif^R $Gent^R$ Tet^R $Spec^R$
GV3101 pGG-p35S:: UMAG_04039- NLS-mCherry-myc--UBQ10-BastaR	C58C1: pGv3101 RifR; pTiC58 ΔTDNA GentR; pSoup TetR; pGG-p35S:: UMAG_04039- NLS-mCherry-myc--UBQ10-BastaR	Transient expression in *Nicotiana benthamiana*	Rif^R $Gent^R$ Tet^R $Spec^R$
GV3101 pGG-p35S:: UMAG_04039- NES-mCherry-myc--UBQ10-BastaR	C58C1: pGv3101 RifR; pTiC58 ΔTDNA GentR; pSoup TetR; pGG-p35S:: UMAG_04039- NES-mCherry-myc--UBQ10-BastaR	Transient expression in *Nicotiana benthamiana*	Rif^R $Gent^R$ Tet^R $Spec^R$
GV3101 pGG-p35S:: UMAG_04039-mCherry-myc--UBQ10-BastaR	C58C1: pGv3101 RifR; pTiC58 ΔTDNA GentR; pSoup TetR; pGG-p35S:: UMAG_04039-mCherry-myc--UBQ10-BastaR	Transient expression in *Nicotiana benthamiana*	Rif^R $Gent^R$ Tet^R $Spec^R$

GV3101 pGG-p35S::myr-mCherry-myc-UMAG_02826-UBQ10-BastaR	C58C1: pGv3101 RifR; pTiC58 ΔTDNA GentR; pSoup TetR; pGG-p35S::myr-mCherry-myc-UMAG_02826-UBQ10-BastaR	Transient expression in *Nicotiana benthamiana*	Rif^R $Gent^R$ Tet^R $Spec^R$
GV3101 pGG-p35S:: UMAG_02826- NLS-mCherry-myc--UBQ10-BastaR	C58C1: pGv3101 RifR; pTiC58 ΔTDNA GentR; pSoup TetR; pGG-p35S:: UMAG_02826- NLS-mCherry-myc--UBQ10-BastaR	Transient expression in *Nicotiana benthamiana*	Rif^R $Gent^R$ Tet^R $Spec^R$
GV3101 pGG-p35S:: UMAG_02826- NES-mCherry-myc--UBQ10-BastaR	C58C1: pGv3101 RifR; pTiC58 ΔTDNA GentR; pSoup TetR; pGG-p35S:: UMAG_02826- NES-mCherry-myc--UBQ10-BastaR	Transient expression in *Nicotiana benthamiana*	Rif^R $Gent^R$ Tet^R $Spec^R$
GV3101 pGG-p35S:: UMAG_02826-mCherry-myc--UBQ10-BastaR	C58C1: pGv3101 RifR; pTiC58 ΔTDNA GentR; pSoup TetR; pGG-p35S:: UMAG_02826-mCherry-myc--UBQ10-BastaR	Transient expression in *Nicotiana benthamiana*	Rif^R $Gent^R$ Tet^R $Spec^R$
GV3101 pGG-p35S::myr-mCherry-myc-UMAG_06119-UBQ10-BastaR	C58C1: pGv3101 RifR; pTiC58 ΔTDNA GentR; pSoup TetR; pGG-p35S::myr-mCherry-myc-UMAG_06119-UBQ10-BastaR	Transient expression in *Nicotiana benthamiana*	Rif^R $Gent^R$ Tet^R $Spec^R$
GV3101 pGG-p35S:: UMAG_06119- NLS-mCherry-myc-UBQ10-BastaR	C58C1: pGv3101 RifR; pTiC58 ΔTDNA GentR; pSoup TetR; pGG-p35S:: UMAG_06119- NLS-mCherry-myc-UBQ10-BastaR	Transient expression in *Nicotiana benthamiana*	Rif^R $Gent^R$ Tet^R $Spec^R$
GV3101 pGG-p35S:: UMAG_06119- NES-mCherry-myc-UBQ10-BastaR	C58C1: pGv3101 RifR; pTiC58 ΔTDNA GentR; pSoup TetR; pGG-p35S:: UMAG_06119- NES-mCherry-myc-UBQ10-BastaR	Transient expression in *Nicotiana benthamiana*	Rif^R $Gent^R$ Tet^R $Spec^R$

GV3101 pGG-p35S:: UMAG_06119-mCherry-myc-UBQ10-BastaR	C58C1: pGv3101 RifR; pTiC58 ΔTDNA GentR; pSoup TetR; pGG-p35S:: UMAG_06119-mCherry-myc-UBQ10-BastaR	Transient expression in *Nicotiana benthamiana*	Rif^R $Gent^R$ Tet^R $Spec^R$
GV3101 pGG-pUbq10::myr-mCherry-myc-UMAG_04039-UBQ10-BastaR	C58C1: pGv3101 RifR; pTiC58 ΔTDNA GentR; pSoup TetR; pGG-pUbq10::myr-mCherry-myc-UMAG_04039-UBQ10-BastaR	Transient expression in Nicotiana benthamiana	RifR GentR TetR SpecR
GV3101 pGG-pUbq10:: UMAG_04039- NLS-mCherry-myc--UBQ10-BastaR	C58C1: pGv3101 RifR; pTiC58 ΔTDNA GentR; pSoup TetR; pGG-pUbq10:: UMAG_04039- NLS-mCherry-myc--UBQ10-BastaR	Transient expression in Nicotiana benthamiana	RifR GentR TetR SpecR
GV3101 pGG-pUbq10:: UMAG_04039- NES-mCherry-myc--UBQ10-BastaR	C58C1: pGv3101 RifR; pTiC58 ΔTDNA GentR; pSoup TetR; pGG-pUbq10:: UMAG_04039- NES-mCherry-myc--UBQ10-BastaR	Transient expression in Nicotiana benthamiana	RifR GentR TetR SpecR
GV3101 pGG-pUbq10:: UMAG_04039-mCherry-myc--UBQ10-BastaR	C58C1: pGv3101 RifR; pTiC58 ΔTDNA GentR; pSoup TetR; pGG-pUbq10:: UMAG_04039-mCherry-myc--UBQ10-BastaR	Transient expression in Nicotiana benthamiana	RifR GentR TetR SpecR
GV3101 pGG-pUbq10::myr-mCherry-myc-UMAG_02826-UBQ10-BastaR	C58C1: pGv3101 RifR; pTiC58 ΔTDNA GentR; pSoup TetR; pGG-pUbq10::myr-mCherry-myc-UMAG_02826-UBQ10-BastaR	Transient expression in Nicotiana benthamiana	RifR GentR TetR SpecR
GV3101 pGG-pUbq10:: UMAG_02826- NLS-mCherry-myc--UBQ10-BastaR	C58C1: pGv3101 RifR; pTiC58 ΔTDNA GentR; pSoup TetR; pGG-pUbq10:: UMAG_02826- NLS-mCherry-myc--UBQ10-BastaR	Transient expression in Nicotiana benthamiana	RifR GentR TetR SpecR

GV3101 pGG-pUbq10:: UMAG_02826- NES-mCherry-myc--UBQ10-BastaR	C58C1: pGv3101 RifR; pTiC58 ΔTDNA GentR; pSoup TetR; pGG-pUbq10:: UMAG_02826- NES-mCherry-myc--UBQ10-BastaR	Transient expression in Nicotiana benthamiana	RifR GentR TetR SpecR
GV3101 pGG-pubq10:: UMAG_02826-mCherry-myc--UBQ10-BastaR	C58C1: pGv3101 RifR; pTiC58 ΔTDNA GentR; pSoup TetR; pGG-pUbq10:: UMAG_02826-mCherry-myc--UBQ10-BastaR	Transient expression in Nicotiana benthamiana	RifR GentR TetR SpecR

In this thesis following *Ustilago maydis* strains were used:

Strain	Genotype	Application	Reference
Sg200	a1 mfa2 bE1 bW2	Infection assay in *Zea mays*	Kämper et al., 2006
Sg200 *ΔUMAG_04039*	a1 mfa2 bE1 bW2 *ΔUMAG_04039*	Infection assay in *Zea mays*	S.Uhse & A.Stirnberg
Sg200 *ΔUMAG_05927*	a1 mfa2 bE1 bW2 *ΔUMAG_05927*	Infection assay in *Zea mays*	S.Uhse & A.Stirnberg
Sg200 *ΔUMAG_02826*	a1 mfa2 bE1 bW2 *ΔUMAG_02826*	Infection assay in *Zea mays*	S.Uhse & A.Stirnberg

6.1.6. Oligonucleotides

Oligonucleotides used in this thesis were generated using Primer3 software (v.0.4.0) and ordered from Eurofins Genomics.

For silencing purposes, the following primer pairs were designed to isolate DNA fragments of identified potential interacting proteins:

Name	**Sequence (5‘-3‘)**	**Application**
aaVIGSfw1	*atatCCATGGtttagTGCTTGGAGGGCAATCTTAT*	*TRV silencing of NbPDS(DQ469932)*
aaVIGSrv1	*atatGCGGCCGCGACTTGGCCACCTTTTGACT*	

aaVIGSfw2	*atatCCATGGtttagTGGATGCAATCAGTGGAAAA*	*TRV silencing of Lipoxygenase(R4S2V6)*
aaVIGSrv2	*atatGCGGCCGCCCTCATCATCCCAATCAAATG*	
aaVIGSfw3	*atatCCATGGtttagAAGCCAAAGATTTGCTCGTC*	*TRV silencing of GID1B(A0A1J6IEQ0)*
aaVIGSrv3	*atatGCGGCCGCTGTTGGCATGGAAATAAACAA*	
aaVIGSfw4	*atatCCATGGtttagCGCTAGTGAAAATGATGTGAAGG*	*TRV silencing of 4-coumarate--CoA ligase 1(O24145)*
aaVIGSrv4	*atatGCGGCCGCTGGAACAAAGGCAAAACACA*	
aaVIGSfw5	*atatCCATGGtttagTTCGCAATTTTGACCGTGTA*	*TRV silencing of Serine/threonine-protein phosphatase PP2A catalytic subunit(Q9XGH7)*
aaVIGSrv5	*atatGCGGCCGCCCCTGGAATCATCAACTTCC*	
aaVIGSfw6	*atatCCATGGtttagCCTCACTGAATATGCCAAGAAA*	*TRV silencing of Trans-cinnamate 4-monooxygenase(A0A1J6I9C1)*
aaVIGSrv6	*atatGCGGCCGCTTCCCACCCACCCCTATACT*	
aaVIGSfw7	*atatCCATGGtttagTGTGTGGCCTCATGAATTGT*	*TRV silencing of carbamoyl-phosphate synthase large chain(A0A1S4CW91)*
aaVIGSrv7	*atatGCGGCCGCCCCATTACCTCACCAGTGCT*	
aaVIGSfw8	*atatCCATGGtttagAAACTCCCGTTTGACCGATA*	*TRV silencing of dynamin-related protein 1E-like(A0A1S4BTR8)*
aaVIGSrv8	*atatGCGGCCGCCCGAAATTTTTCTAAGGCTTCA*	
aaVIGSfw9	*atatCCATGGtttagGGTTACAAGTTTCGAGGGGAAC*	*TRV silencing of dynamin-2A-like(A0A1S3Y6L1)*
aaVIGSrv9	*atatGCGGCCGCGCAATTGCTACAACCTCTCTCTT*	
aaVIGSfw10	*atatCCATGGtttagTTGGTGATCACAGGGCTAGG*	*TRV silencing of flotillin-like protein 4(A0A1S4AA23)*
aaVIGSrv10	*atatGCGGCCGCTCCTTCAATGATACCTTGCACA*	
aaVIGSfw11	*atatCCATGGtttagTGCTCCTGAGTCAAGCAAAC*	*TRV silencing of Coatomer subunit beta(A0A1U7XFG7)*
aaVIGSrv11	*atatGCGGCCGCGCATTTCATGTTGGTTGATTTG*	
aaVIGSfw12	*atatCCATGGtttagTGCTTTAAGGCAGGCAATCT*	*TRV silencing of Coatomer subunit alpha(A0A1S3YFI6)*
aaVIGSrv12	*atatGCGGCCGCAACTGCAAGATCGCAAACAG*	
aaVIGSfw13	*atatCCATGGtttagTCAGCCATAGAGGTCCCAGA*	*TRV silencing of myosin-17-like(A0A1S3XJA5)*
aaVIGSrv13	*atatGCGGCCGCCAGTGAGCTGCTGCTTGAAC*	
aaVIGSfw14	*atatCCATGGtttagGGAGGCTCTATTGCGTCATC*	*TRV silencing of acetyl-CoA carboxylase 1-like(A0A1S4A3W1)*
aaVIGSrv14	*atatGCGGCCGCTGCCGATACTAAGGACCTCAA*	
aaVIGSfw15	*atatCCATGGtttagGGTTCTCTAAAGCTGTTGAAATGA*	*TRV silencing of peroxisomal fatty acid beta-oxidation multifunctional protein AIM1-like (A0A1S4A6H4)*
aaVIGSrv15	*atatGCGGCCGCTACGTCAATGCATGCCAACT*	
aaVIGSfw16	*atatCCATGGtttagTGGTTTTCCTGAAACTGTGC*	*TRV silencing of 3-ketoacyl-coa thiolase 2(A0A1J6K4R7)*
aaVIGSrv16	*atatGCGGCCGCAACTGCAGCCTGGTCTTGTT*	
aaVIGSfw17	*atatCCATGGtttagAGAAAGGAGAAATCCCTGAGC*	

aaVIGSrv17	*atatGCGGCCGCAGTCCGTACAGCCAAAGCAC*	*TRV silencing of Beta-adaptin-like protein(A0A1S4DPH0)*
aaVIGSfw18	*atatCCATGGtttagCGATCAATAAGTGTAATTGGTTACG*	*TRV silencing of 5'-nucleotidase domain-containing protein 4-like isoform X1 (A0A1S4BHF0)*
aaVIGSrv18	*atatGCGGCCGCCTCCTTACGCAGATCAACCAG*	
aaVIGSfw19	*atatCCATGGtttagGCGTCGATCTACAGTTG*	*TRV silencing of uncharacterized protein LOC107820356 (A0A1S4CLK2)*
aaVIGSrv19	*atatGCGGCCGCAAAGTGAAACTGACCCGGACT*	
aaVIGSfw20	*atatCCATGGtttagCATCCCCAAAAGTGAGAATGA*	*TRV silencing of Eukaryotic translation initiation factor 3 subunit J (A0A1S3Y190)*
aaVIGSrv20	*atatGCGGCCGCAACCATCATATGCATTTACCACA*	
aaVIGSfw21	*atatCCATGGtttagTTCCACATCATCCCACTGAA*	*TRV silencing of uncharacterized protein LOC107777101 isoform (A0A1S3YK08)*
aaVIGSrv21	*atatGCGGCCGCTTCCCAAGCTCCTTTAAACTG*	
aaVIGSfw22	*atatCCATGGtttagCTGCATCAGCAGTGACATCC*	*TRV silencing of Nf-x1-type zinc finger protein nfxl1 (A0A1J6IJ82)*
aaVIGSrv22	*atatGCGGCCGCCCTGGCTCACTAACAGGTTCC*	
aaVIGSfw23	*atatCCATGGtttagAGCAGTTGAGGGACAATCTGA*	*TRV silencing of Dynamin-related protein 5a (A0A1J6JKH5)*
aaVIGSrv23	*atatGCGGCCGCATCTTGTTGAGAACGATTGACG*	
aaVIGSfw24	*atatCCATGGtttagGGATCGTCCTTCAAGTGGTC*	*TRV silencing of dynamin-like protein ARC5 isoform X1 (A0A1S3YU74)*
aaVIGSrv24	*atatGCGGCCGCGGGTAATGGGAGGGCATT*	
aaVIGSfw25	*atatCCATGGtttagAACTGCCCAATGATCCAGAG*	*TRV silencing of Dead-box atp-dependent rna helicase 3 (A0A1J6J3H5)*
aaVIGSrv25	*atatGCGGCCGCAGCAGCAAGGGCATTTACTC*	
aaVIGSfw26	*atatCCATGGtttagACTCGAGTCGATTGGAAGGA*	*TRV silencing of 17.6 kDa class I heat shock protein-like (A0A1S3Z7Q2)*
aaVIGSrv26	*atatGCGGCCGCTGACATCAGGCTTCTTCACCT*	
aaVIGSfw27	*atatCCATGGtttagCTACCGACGCACGATTTTC*	*TRV silencing of large proline-rich protein BAG6 isoform X4 (A0A1U7V2V6)*
aaVIGSrv27	*atatGCGGCCGCGCAAAACTTGTTGCCCATCT*	

For qPCR analysis the below listed primer pairs were used:

Name	**Sequence (5‘-3‘)**	**Application**
Elena3qPCRf1	*GCCTTCCTGCAGCTTACG*	*Efficiency of Silencing for Putative carboxylesterase 120 checked by qPCR*
Elena3qPCRr1	*GATAGACCCGACTCAAATCAGC*	
Elena3qPCRf2	*CAGCTTTTGCCACTTCATGC*	
Elena3qPCRr2	*GCTTTGACCCTCCATTTGC*	
Elena4qPCRf1	*TTCTGATGCTGCTGTTGTCC*	*Efficiency of Silencing for 4-coumarate--CoA ligase 1 checked by qPCR*
Elena4qPCRr1	*CCTCAGTGATGGCAGATCC*	
Elena4qPCRf2	*GTGAAAATCCAGCCAGACG*	

Elena4qPCRr2	*CGTCAACATCACACCTTTCG*	
Elena5qPCRf1	*GGGCCCATGATCAAAAGG*	*Efficiency of Silencing for Serine/threonine-protein phosphatase PP2A catalytic subunit checked by qPCR*
Elena5qPCRr1	*CCCTGGAATCATCAACTTCC*	
Elena5qPCRf2	*GTTGTGGCAATATGGCATCC*	
Elena5qPCRr2	*TACATCTGGCTCCCCTCTCC*	
Elena6qPCRf1	*TAGGCCAGAGAGGTTCTTCG*	*Efficiency of Silencing for Trans-cinnamate 4-monooxygenase checked by qPCR*
Elena6qPCRr1	*CAGCTCCTCCTACCAACACC*	
Elena6qPCRf2	*TAGGCCAGAGAGGTTCTTCG*	
Elena6qPCRr2	*CAGCTCCTCCTACCAACACC*	
Elena7qPCRf1	*CCACTATTTCCCCACTCTGC*	*Efficiency of Silencing for carbamoyl-phosphate synthase largechain,chloroplastic-like checked by qPCR*
Elena7qPCRr1	*TGTGACCCAAAACGGATAGC*	
Elena7qPCRf2	*GTCGCACATTCCAAGAATCC*	
Elena7qPCRr2	*ATTTGTCCCAATCCCAGTCC*	
Elena2qPCRf1	*CTGGAAAGCTTGAGGAATGG*	*Efficiency of Silencing for lipoxygenase checked by qPCR*
Elena2qPCRr1	*AGCTCTTTGCCTTTGTCTGG*	
Elena2qPCRf2	*CTGGAAAGCTTGAGGAATGG*	
Elena2qPCRr2	*AGCTCTTTGCCTTTGTCTGG*	
Elena13qPCRf1	*AGAACTTACATGGCGGTTGC*	*Efficiency of Silencing for myosin-17-like checked by qPCR*
Elena13qPCRr1	*AGTGCCTCCTGTAGCTTTGC*	
Elena13qPCRf2	*GCAGAGGCTTGAAGAGAAGC*	
Elena13qPCRr2	*GTTGGTGACATGGTCAAAGC*	
Elena15qPCRf1	*CGGAGTTAAGGTGACGATGG*	*Efficiency of Silencing for peroxisomal fatty acid beta-oxidation multifunctional protein AIM1-like checked by qPCR*
Elena15qPCRr1	*CCAGCGATAATGGGAATAGC*	
Elena15qPCRf2	*GGCTTTGGAGGTACACAACG*	
Elena15qPCRr2	*CGGCATCAATAAGACCAAGC*	
Elena16qPCRf1	*TTGGGAAGGATCAGTCAACC*	*Efficiency of Silencing for 3-ketoacyl-coa thiolase 2, peroxisomal checked by qPCR*
Elena16qPCRr1	*GTCACACCAAAACGATGTGC*	
Elena16qPCRf2	*TTGGGAAGGATCAGTCAACC*	
Elena16qPCRr2	*GCCTTGTCACACCAAAACG*	
Elena18qPCRf1	*CTTGGTCAAAGCACCAAAGG*	*Efficiency of Silencing for 5'-nucleotidase domain-containing protein 4-like isoform X1 checked by qPCR*
Elena18qPCRr1	*TTTGCCACCTCCTCAATAGG*	
Elena18qPCRf2	*CCAGGTGGGTTGTACTCTGG*	
Elena18qPCRr2	*GGAGATGGACCTTGGATACG*	
Elena19qPCRf1	*GGGGTATCCAAAGGAAAAGG*	*Efficiency of Silencing for uncharacterized protein LOC107820356 checked by qPCR*
Elena19qPCRr1	*GGGCCAAAGTGAAACTGACC*	
Elena19qPCRf2	*GAACTGTGGGAAGCTTGTCG*	
Elena19qPCRr2	*GGGCCAAAGTGAAACTGACC*	
Elena20qPCRf1	*AGGCACCCAAGAAGTCTGC*	*Efficiency of Silencing for Eukaryotic translation initiation factor 3 subunit J checked by qPCR*
Elena20qPCRr1	*CTTCTTCCACAAGCCTTTGC*	
Elena20qPCRf2	*AGCAACCAGGGAGTAAATGG*	
Elena20qPCRr2	*ACAGGCTCCTCTTCATCTTCC*	
Elena21qPCRf1	*GAGAACCGATGGGAAGAACC*	*Efficiency of Silencing for uncharacterized protein LOC107777101 isoform X2 checked by qPCR*
Elena21qPCRr1	*CATAACAGGCGACCTTCTCC*	
Elena21qPCRf2	*GGGTTTTTATTGCGGTGAGG*	
Elena21qPCRr2	*ATTCCATCTTCTGGCACACC*	

Elena22qPCRf1	*TCCACTACCTTGTGGAACACC*	*Efficiency of Silencing for Nf-x1-type zinc finger protein nfxl1 checked by qPCR*
Elena22qPCRr1	*TGGCAGCTGTGAGTAGATGG*	
Elena22qPCRf2	*GAACAGACTTGCCATGTTGG*	
Elena22qPCRr2	*CCTTTCACACCCATGTCTCC*	
Elena23qPCRf1	*GCAGAATTTGGACACCTTCC*	*Efficiency of Silencing for Dynamin-related protein 5a checked by qPCR*
Elena23qPCRr1	*TTAGAACGGCCTGTCTCTCG*	
Elena23qPCRf2	*GGACATTTGGTGTTCTGACG*	
Elena23qPCRr2	*TGAGAACGATTGACGACACC*	
Elena24qPCRf1	*GCCCAGGACAGATGTAAAGC*	*Efficiency of Silencing for dynamin-like protein ARC5 isoform X1 checked by qPCR*
Elena24qPCRr1	*CCTCCTGTTCCAAAGTGTGC*	
Elena24qPCRf2	*GGCGTACAATGAGCTACACG*	
Elena24qPCRr2	*ATTAGTGCCTCCACCAGTGC*	
Elena25qPCRf1	*CACAGCAAAATGCACTGACC*	*Efficiency of Silencing for Dead-box atp-dependent rna helicase 3, chloroplastic checked by qPCR*
Elena25qPCRr1	*CGTCGAGGACCAAATATTCC*	
Elena25qPCRf2	*GTCATCAGCTGAGCATGTGG*	
Elena25qPCRr2	*GGGCATTTACTCCTTGTTGC*	
Actin(partial)qPCRf1	*TGTTGCTATTCAGGCTGTCC*	*Actin (fragment) used as control for qPCR*
Actin(partial)qPCRr1	*TGACACCATCACCAGAGTCC*	
Nb actin qPCRf1	*GGATTTGCTGGAGATGATGC*	*Actin used as control for qPCR*
Nb actin qPCRr1	*GCATCTTTCTGTCCCATTCC*	

Other primers used during this study:

Name	**Sequence (5‘-3‘)**	**Application**
pJET-SEQ-F	*TGGAGCAGGTTCCATTCATTG*	*Sequencing of pJET vector constructs*
pJET-SEQ-R	*GTTCCTGATGAGGTGGTTAGCATAG*	
pENTRY-SEQ-F	*CAGAGCTGCAGCTGGATGG*	*Sequencing of pENTRY vector constructs*
pENTRY-SEQ-R	*AGTTAGTTACTTAAGCTCG*	
TRV2seq_F	*TTCACTGGGAGATGATACGC*	*Sequencing of Expression vector constructs*
TRV2seq_R	*TACCGATCAATCAAGATCAG*	
GGUbi10Pro_seqF	*TAGGGTTTCATAGATATC*	*Green Gate sequencing from Ubiquitin10 promoter region forward sequencing primer*
GG35SPro_seqF	*TCAAAGCAAGTGGATTGATG*	*Green Gate sequencing from 35S promoter region forward sequencing primer*
GGct-mCherry_seqR	*CTGGGTGCCCTCGTAGGG*	*Green Gate c-terminal mCherry reverse sequencing primer*
Ubi_Term_SeqR	*GAAAGAGATAACAGGAACGG*	*Green Gate Ubiquitin termination reverse sequencing primer*

6.2. Methods

6.2.1. Media and culture conditions

6.2.1.1. Growth Conditions of bacterial cultures

All *E. coli and A. tumefaciens* cells were grown either in dYT or LB liquid medium or on LB agar plates at 37 °C or 28°C, respectively. Liquid cultures were grown shaking at 180 rpm. To reduce the issue of contamination in transformed cells, antibiotics such as Ampicillin, Spectinomycin, Kanamycin, Gentamycin and Rifampicin were added in concentration of 100 mg/L to the liquid or solid media.

Agro LB liquid medium:

1 %	Tryptone (w/v)
0.5 %	Yeast extract
1%	NaCl
10mM	MES-NaOH pH 5.6
0.15mM	Acetosyringone

dYT liquid medium:

1.6 %	Tryptone (w/v)
0.5 %	Yeast extract (w/v)
0.5%	NaCl (w/v)

dYT agar:

1.6%	Tryptone (w/v)
0.5%	Yeast extract (w/v)
0.5%	NaCl (w/v)
2.0%	Bacto-Agar (w/v)

SOC medium:

2%	Bacto-Trypton (w/v)
0.5%	Bacto-Yeast extract (w/v)
10M	NaCl
2.5mM	KCl
10M	$MgCl_2$
20mM	Glucose

6.2.1.2. Growth Conditions of Ustilago maydis

Ustilago maydis was grown in $YEPS_{light}$ (yeast extract peptone sucrose) liquid media or on solid PD (potato dextrose) agar plates at 28°C for 2 days with shaking at 180 rpm.

$YEPS_{light}$ liquid media:

0.4 %	Bacto-peptone
0.4 %	Bacto yeast extract
2 %	Sucrose

PD agar:

2.4 %	Potato Dextrose Broth (w/v)
2 %	Bacto-agar (w/v)

6.2.2. Molecular biological methods

6.2.2.1. Isolation of plasmid DNA from Escherichia coli

To isolate plasmid DNA from *E. coli* cells, the strain containing the desired plasmid was grown in 2 ml dYT medium containing the respective antibiotics shaking on 180 rpm at 37°C. To isolate the plasmid DNA, 2 ml of the culture media was transferred into a 2 ml Eppendorf tube and then centrifuged for 10 min at 13000 rpm. The pellet was resuspended in 250 µl of P1-buffer including 100mg/mL RNaseA. For lysing the cells 250 µl of P2-buffer (Qiagen) was added and the tube was inverted several times. After 5 min of incubation 350 µl of N3-buffer (Qiagen) were added. Afterwards, the tubes were inverted several times and then centrifuged at 13000 rpm for at least 10 min. The supernatant was subsequently transferred to columns with silica gel filters (CenticBiotec) and centrifuged for 1 min at 13000 rpm. Afterwards, the bound DNA was washed once with 500 µl of PB buffer and with 750 µl of PE buffer. The filters were centrifuged again at 13000 rpm for 2 min to remove residual ethanol. To elute the bound DNA the columns were placed into a fresh 1.5 ml Eppendorf tube and 50 µl of water was added onto the filter. To ensure complete hydration of the bridges the

samples were incubated for 1 min at room temperature before centrifuging 1 minute at 13000 rpm. DNA concentrations were measured with ND-1000 spectrophotometer (Peqlab, Germany).

Buffer P1:

50mM	Tris-HCl, pH 8.0
10mM	EDTA
100µg/ml	RNase A

PB solution:

5M	Guanidine hydrochloride
30%	Isopropanol

PE Solution:

10mM	Tris-HCl, pH 7.5
80%	Ethanol

6.2.2.2. Isolation of genomic DNA from Nicotiana benthamiana

For genomic DNA isolation 1 cm^2 leaf material of *Nicotiana benthamiana* was sampled and immediately frozen in liquid nitrogen. Grinding was performed using the Retsch MM400 before adding GEX buffer. Afterwards, samples were centrifuged on maximal speed for 5 min on RT. Supernatant was transferred into columns with silica gel filters (CenticBiotec) and centrifuged for 1 min on maximal speed. Washing step was done using 500 µl of PE buffer (*see PE buffer solution, section 2.2.2.1*). Liquid was removed from the column and centrifugation was repeated for 2 min on maximal speed to dry the column. To elute the bound DNA, the columns were placed into a fresh 1.5 ml Eppendorf tube and 50 µl of water was added onto the filter. Samples were incubated for 2 min at room temperature before centrifuging 1 min at 13000 rpm. DNA concentrations were measured with ND-1000 spectrophotometer (Peqlab, Germany).

GEX buffer:

5.5 M	GuSCN
20 mM	Tris-HCl, pH 6.6

6.2.2.3. DNA restriction

To cleave the double-stranded DNA at the specific site that contains our desired sequence, type II restriction enzymes (New England Biolabs) were used. Reaction conditions were chosen according to manufacturer's recommendations and all samples were incubated around 1 hour. After digestion the fragment lengths were checked on an agarose gel.

For each reaction the following mix was prepared:

3 µL	vector DNA
2 µL	10x NEBuffer
15 µL	Mono Q H_2O
0.3 µL	restriction enzyme(s)

6.2.2.4. DNA elution

After amplification via PCR and separation over an agarose gel, distinct DNA fragments were excised with a scalpel and transferred into a 1.5 ml Eppendorf tube. The DNA was purified using the Wizard and Sv Gen and PCR Clean-Up System (Promega) according to the manufacturer´s protocol.

6.2.2.5. DNA ligation

To ligate a certain DNA fragment, T4 DNA ligase (New England Biolabs) was used. The fragment was ligated into the expression vector pJET with an approximate ratio of 1:5. Ligation reactions were incubated for 1 hour at room temperature before continuing with transformation into chemocompetent *E.coli* cells (*see section 2.2.3.1. Transformation of chemo-competent E. coli)*. For further use the plasmid was later isolated from the cells *(see 2.2.2.1 Isolation of plasmid DNA from Escherichia coli).*

For each ligation the following mix was prepared:

1µl	Vector
3µl	Insert
1µl	T4 ligase buffer
0.5µl	T4 DNA ligase
4.5µl	Mono Q H2O

6.2.2.6. Agarose gel electrophoresis

Different percentages (0.8%, 1% or 2 %) of TAE-agarose gels were used to separate PCR amplified DNA fragments according to their size. For gel preparation, agarose was dissolved in 1xTAE buffer by boiling. The solution was then cooled down to 55°C before adding 4 µl peqGreen dye per 100 ml agarose solution. The gel was run for 30-40 min and the voltage was limited to 100-120 V. The stained DNA-bands were excited by UV light and the fluorescence was detected. If purification of the DNA fragments was necessary, the desired region of the gel was cut out under UV-light and the DNA from the gel section was eluted (*see section 2.2.2.4 DNA elution).*

TAE Buffer:

40 mM	Tris
1 mM	EDTA, pH 8.0
20mM	acetic acid

6x DNA loading dye:

50 %	Saccharose (v/v)
0.1 %	Bromphenol blue (v/v)
	dissolved in TE buffer

6.2.2.7. Polimerase Chain Reactions (PCRs)

Polymerase chain reactions were performed to amplify DNA fragments for cloning or analytical purpose. Depending on the application different polymerases were used

and described in the following sub-sections. The PCR programmes used for respective polymerases included the following thermocycling steps:

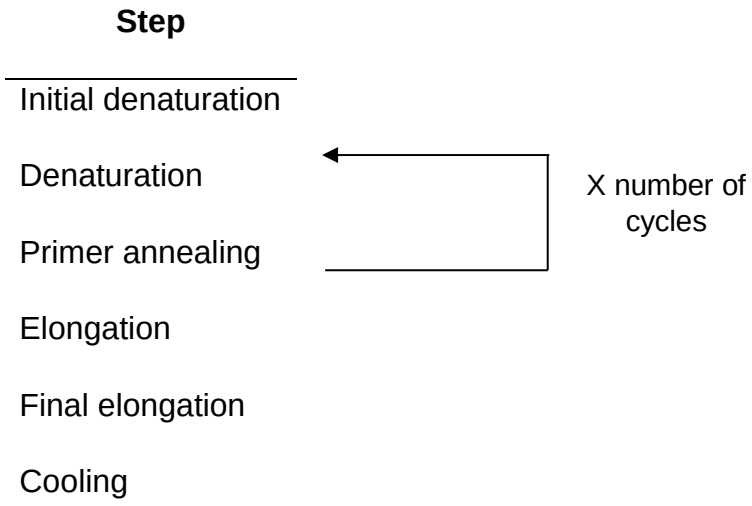

The elongation time was chosen based on the expected fragment size and synthesis rate of the polymerase.

1) Q5 PCR

To amplify DNA fragments for VIGS purposes a polymerase chain reaction with Q5 polymerase was carried out in a total volume of 25 µl. All primers used were diluted 1:20.

For each reaction the following mix was prepared:

5 µl	5x Q5 reaction buffer
17.25 µl	Mono Q H2O
0.5 µl	dNTP (10mM)
0.5 µl	forward primer (100µM)
0.5 µl	reverse primer (100µM)
0.25 µl	Q5 polymerase
1 µl	DNA template

Thermocycling conditions for Q5:

Step	Temperature	Time	
Initial denaturation	98 °C	30 sec	
Denaturation	98 °C	10 sec	40x
Primer annealing	primer specific	20 sec	
Elongation	72 °C	30 sec/kb	
Final elongation	72°C	5 min	
Cooling	12 °C	∞	

2) Phusion PCR

For DNA fragments that were not successfully isolated by Q5 polimerase, phusion polimerase was used for DNA amplification for VIGS purposes. Reaction volume of one reaction was 25 µl. All primers used were diluted 1:20.

For each reaction the following mix was prepared:

5 µl	5x Phusion HF buffer
2 µl	DMSO
15.25 µl	Mono Q H2O
0.5 µl	dNTP (10mM)
0.5 µl	forward primer (100µM)
0.5 µl	reverse primer (100µM)
0.25 µl	Phusion polymerase
1 µl	DNA template

Thermocycling conditions for Phusion:

Step	Temperature	Time
Initial denaturation	98 °C	30 sec
Denaturation	98 °C	10 sec
Primer annealing	primer specific	20 sec
Elongation	72 °C	20 sec/kb
Final elongation	72°C	5 min
Cooling	12 °C	∞

35x

3) Direct PCR

Screening for positive bacterial colonies were done using direct PCR. OneTaq 2x Mastermix (New England Biolabs) which contain all components for a PCR reaction except primers and template, was diluted with dd$H_2$0. Liquid cultures from *E. coli* were directly added as template.

One direct PCR reaction contained the following components:

5 µl	OneTaq 2x Mastermix
5 µl	ddH2O
0.1 µl	forward primer
0.1 µl	reverse primer
1 µl	liquid *E.coli* culture

Step	Temperature	Time
Initial denaturation	94 °C	30 sec
Denaturation	94 °C	20 sec
Primer annealing	primer specific	20 sec
Elongation	68 °C	60 sec/kb
Final elongation	68°C	5 min
Cooling	12 °C	∞

40x

6.2.2.8. Gateway Cloning

The gateway cloning technique is an *in vitro* cloning strategy based on the site-specific recombination system to integrate and excise DNA fragments. To get the silencing experiment correctly done and get the gene of interest into the expression vector from the pENTRY, LR Clonase reaction was performed. This reaction takes place between the attL site of the generated pENTRY and the attR site of the destination vector, catalyzed by the LR-clonase®II-enzyme mix. As a result, the expression vector is generated containing the gene of interest with the attB sites and a toxic byproduct with attP sites as shown in figure 6. Once the reaction was completed, transformation into competent *E.coli* cells was performed and positive colonies were selected. Kanamycin was used here as selection marker.

Gateway-reaction:

5 µl	destination vector (150 ng/µl)
1 µl	entry vector (50 – 100 ng)
0.5 µl	TE buffer, pH 7.5
0.5 µl	LR-Clonase ® II enzyme mix

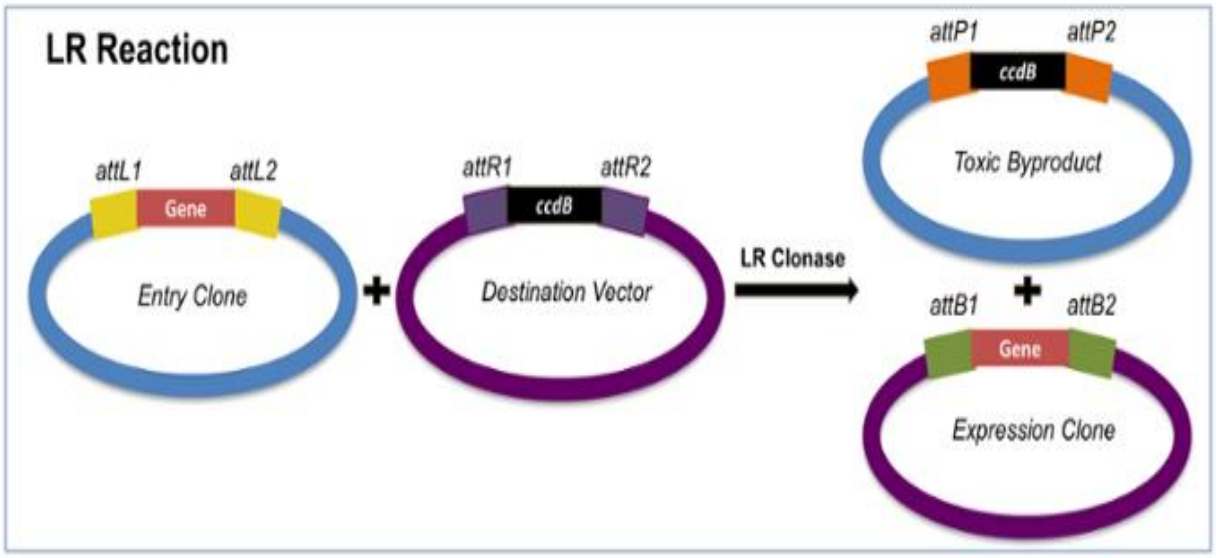

Figure 6: Principle of the Gateway Cloning method. With the LR-clonase®II-enzyme mix, the gene of interest in the pENTRY gets transferred into the expression vector though a site-specific recombination system. Image adapted from: Soriano 2017.

6.2.2.9. Isolation and quantification of RNA

1) RNA extraction (Semi-automated KingFisher)

Nicotiana benthamiana leaves were homogenized using Retsch MM400 and 20 mg of powder was weighted into a 2 ml Eppendorf tube. A total volume of 450 µl GEX buffer was added and put for 30 mins on RT with shaking. Further processing of total RNA isolation was performed as given in the manufacturer's protocol (High performance RNA bead isolation, Molecular Biology Service).

2) DNase treatment of RNA and cDNA synthesis

Pure RNA was carried out for reverse transcription to generate cDNA from mRNA. mRNA was transcribed into cDNA employing the Super III First Strand Synthesis Super Mix Kit or RevertAid First Strand cDNA Synthesis Kit (Thermo Fisher Scientific). Reverse transcription was performed according to the manufacturers' protocols. Each reaction contained 1 µg DNase-treated total RNA. Reverse transcription was performed using oligo-d(T)-primers.

One reaction tube for cDNA synthesis contained:

1 µl	Oligo d(T) primers
1 µl	dNTPs
1 µl	of RNA
12 µl	Free RNase H_2O
	Incubation on 65°C, 5 min

Additionally, to the reaction was added:

4 µl	RT buffer 5x
1 µl	Maxima H Minus Enzyme mix
	Incubation on 50°C, 30 min a
	85°C, 5 min

3) Quantitative real time PCR

To determine gene expression quantitative real time PCR (qPCR) was conducted. Realtime PCR was performed with the Light-Cycler® 96 system (Roche) according to manufacturer's instructions. For measurements with the Light-Cycler instrument the qPCR reagent 'FastStart Essential DNA Green Master' (Roche) was used.

Following program set up was used:

Step	**Temperature**	**Time**	
Initial denaturation	95 °C	10 min	
Denaturation	95 °C	15 sec	45x
Primer annealing	60 °C	15 sec	
Elongation	72 °C	15 sec/kb	

Specificity of the reaction was ensured by melting curve calculations after the qPCR run. The determination of threshold cycles was performed using the Roche Lightcycler software v1.1.01320. Relative expression values were calculated with the 2-ΔΔCt method (Livak and Schmittgen, 2001).

6.2.2.10. Golden Gate

Golden Gate cloning is a cloning technique allowing standardized, quasi-scarless, multi-part DNA assembly (Engler et al., 2008). The reaction relies on the use of Type II endonucleases. The restriction enzyme BsaI was used to cleave the DNA from an entry vector containing six different types of modules. The six module types are: plant promoter, N-terminal tag, coding sequence (i.e. the gene of interest), C-terminal tag, plant terminator and plant resistance cassette as shown in figure 7. The six modules are then ligated between the left border (LB) and the right border (RB) sequences of the destination vector. Afterwards 3 µL of the reaction are used to transform *E. coli* cells (*see section 2.2.3.1 Transformation of chemo-competent E. coli)*.

Golden Gate reaction:

x µl	Vector (~10ng)
y µl	Insert (100g)
2 µl	T4 Ligase buffer
0.5 µl	ATP
0.5 µl	T4 Ligase
0.5 µl	Type II restriction enzyme
	add to 20 µL ddH2O

Golden Gate program set up:

Step	**Temperature**	**Time**	
1	37°C	10 min	10x
2	37°C	5 min	
3	16°C	10 min	
4	37°C	10 min	
5	50°C	5 min	
6	80°C	5 min	
7	12°C	∞	

After the Golden Gate reaction cycles, Plasmid Safe was performed. In a Plasmid Safe reaction, the used type IIs restriction enzyme as well as an exonuclease were added to eliminate all unligated linear DNA fragments.

Plasmid safe:

1 µl	PlasmidSafe enzyme
1 µl	ATP

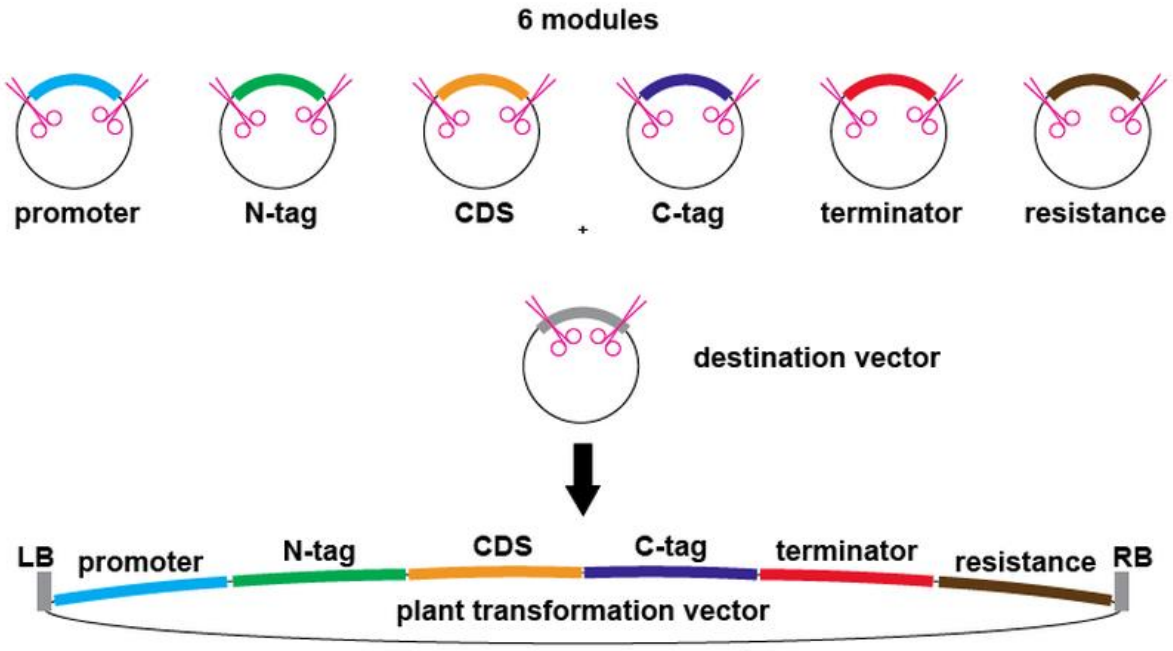

Figure 7: Principle of the Golden Gate Cloning system. Six different modules are cutted out with the BsaI restriction enzyme and then ligated with the T4 DNA ligase between the left border (LB) and the right border (RB) sequences encompassing a a plant promoter, an N-terminal tag, a coding sequence (i.e. the gene of interest), a C-terminal tag, a plant terminator and a plant resistance cassette for selection of transgenic plants. Image adapted from: Lampropoulos et al. 2013.

6.2.2.11. Sequencing

Sequencing was performed at the Vienna BioCenter Core Facilities (VBCF). At least 150 ng plasmid DNA with 5 pg primer were prepared with ddH_2O in a total volume of 7 µl. For direct sequencing of PCR products, 2 µl of a reaction were send directly with 5 pg primer in a total volume of 7 µl.

6.2.3. Microbiological Methods

6.2.3.1. Transformation of chemo-competent E. coli

To facilitate efficient transformation, 50 µl of chemo-competent Mach1 *E. coli* cells were thawed on ice and mixed with ~100 ng plasmid DNA. After incubation on ice for 30 min, the cells were heat-shocked at 42°C for 45 sec. Afterwards the cells were placed back on ice and resuspended in 200 µl SOC medium. After regeneration of the cells at 37°C (shaking at 800 rpm) for 1 hour, the cells were plated onto selection

plates and incubated at 37°C, ON. If Ampicillin was used for selection, regeneration was not necessary, and the cells were plated out directly.

6.2.3.2. Transformation of A.tumefaciens

Electrocompetent bacterial cells were transformed by electroporation. Cells were thawed on ice and mixed with ~1 µg of DNA. The cells were then transferred into a pre-cooled electroporation cuvette and placed into the electroporation device (Gene Pulser Xcell from BioRad). A pulse of 1700 V was applied, and the cells immediately resuspended in 1ml SOC medium. The cells were recovered in SOC for 2h at 28°C, shaking. 50-100 µl of the recovered cells were plated onto LB plates containing suitable antibiotics and were incubated at 28°C for 2-3 days until colonies appeared.

6.2.4. Biochemical Methods

6.2.4.1. Protein extraction and Western Blot

Nicotiana benthamiana leaves were harvested and frozen in liquid nitrogen. After homogenizing with Retsch MM40 in 2ml Eppendorf tubes at 30 Hz for 1 min 30 sec, plant material was thawed in 5x protein extraction buffer (1/3 vol.4xLDS, 25 mM DTT; stock at 1M; 1:40 dilution and H_2O) and incubated on ice for 15 min. Samples were afterwards denatured at 75°C for 10 mins before centrifugation at maximal speed for 5 mins (RT). Supernatant was transferred into new 1.5 ml Eppendorf tubes.

To separate the proteins, samples were loaded and fractionated on a 10% SDS-polyacrylamide gel consisting of a resolving gel and stacking gel. The higher, stacking gel is slightly acidic (pH6.8) and has large sized pores to concentrate all proteins into one band. The lower gel, the resolving gel, is basic (pH8.8) and allowed proteins then to separate according to their molecular weight.

To identify the size of the proteins, the pre-stained protein PageRuler (ThermoFisher Scientific, USA) was used as reference. Separation of the proteins was performed at different voltages. To concentrate the proteins on the same level gel was run on 20mA, where the actual separation was at 25mA.

Resolving gel (1.5mm. 10%):

3.01 ml	MQ H_2O
1.88 ml	1.5M Tris-HCl pH 8.8
2.50 ml	30% Acrylamide
75 µl	10% SDS
3.75 µl	TEMED
37.5 µl	10% APS

Stacking gel (1.5mm. 4%):

2.25 ml	MQ H_2O
0.9 ml	1.5M Tris-HCl pH 6.8
0.5 ml	30% Acrylamide
37.5 µl	10% SDS
3.75 µl	TEMED
18.75 µl	10% APS

4x LDS Sample buffer:

40%	Glycerol
1M	Tris-HCl pH 8.5
2mM	EDTA
8%	LDS
0.2%	Bromophenol blue

SDS Running buffer

1M	MES
1M	Tris
2%	SDS
20mM	EDTA

After gel electrophoresis, blotting was done onto a nitrocellulose membrane using Trans-Blot® TurboTM Transfer System (BioRad). The blotting components were assembled in that way that the gel was placed on the nitrocellulose membrane

covered from both sides with several layers of soaking paper. Turbo blotting buffer was used to soak the membrane and papers before the transfer. Settings were applied according to the manufacturer's protocol.

Turbo blotting buffer:

200 ml	EtOH
200 ml	5x Trans-Blot® TurboTM Buffer
600 ml	MQ H_2O

1x TBS-T (for 1L MQ H_2O, set to pH 7.6)

6.05g	Tris
8.76g	NaCl
0.05%	Tween20

Blocking of the membrane was done using 8% milk powder previously dissolved in blocking buffer. To avoid black spots caused by milk aggregates, the dissolved milk was filtered through a 40 µl nylon mesh. After the blocking, the membrane was washed 3x in washing buffer for 5 mins before adding the first antibodies (1:2000 diluted in washing buffer for α-MYC; mouse). Incubation of the membrane in the primary antibody solution was done for 1 hour with shaking on room temperature. To remove unbound primary antibodies, the membrane was the washed 3x in washing buffer. The secondary antibody solution (1:20000 diluted in washing buffer, HRP-coupled anti-mouse antibody; sheep) was added and incubated for 1 hour with shaking on room temperature. Washing step was afterwards repeated as mentioned before 3x. Imaging was performed using the ChemiDoc™ imaging system (BioRad, USA) according to the manufacturers protocol.

Washing Buffer: 50mM Tris, 200mM NaCl, 0.05% Tween, pH 7.2

1M	Tris
5M	NaCl
25%	Tween

Blocking Buffer: 100mM Tris, 200mM NaCl, 0.05% Tween, pH 7.2

1M	Tris
5M	NaCl
25%	Tween

6.2.4.2. Mass Spectrometry

Nicotiana benthamiana plants were infiltrated 3 days before harvesting with ROSIE 1-mCherry, ROSIE 2-mCherry, ROSIE 3-mCherry, ROSIE 4-mCherry and mCherry-mCherry as control. Infiltrated leaves were sampled and immediately frozen into liquid nitrogen. With pestle and mortar, samples were grinded, and 0.5 g of fresh weight was put in 5 ml Eppendorf tubes and send out for Mass Spectrometry analysis.

6.2.4.3. Tobacco Rattle Virus - based Virus Induced Gene Silencing (TRV-VIGS) Assay in Nicotiana benthamiana

The TRV-based VIGS system was used for gene silencing. To generate the silencing constructs, a 300 bp fragment of the targeted gene was PCR amplified from *Nicotiana benthamiana* and the product was cloned into pJET. After successful sequencing and obtaining the wanted plasmid, through the process of DNA digestion with restriction enzymes NotI and NcoI the DNA fragment was cut out and then ligated into the pENTRY vector with spectinomycin resistance as a selection marker. After obtaining the pENTRY clone with the VIGS target region, the Gateway LR-reaction between the pENTRY and the pTRV2 empty vector was carried out. Here kanamycin resistance was used as the selective marker, respectively. To obtain the final wanted vector, transformation into *E.coli* cells was done before transformation in Agrobacterium tumefaciens for the purpose of plant agroinfiltration.

6.2.4.4. ROS Burst Assay

Reactive oxygen species (ROS) measurement was performed on a luminol/peroxidase-based assay. Leaf discs of four weeks old *Nicotiana benthamiana* plants were collected using a Miltex biopsy punch with plunger (diameter=4mm) and

floated in a black 96-well plate in sterile water overnight. Measurements were carried out using Syngery plate reader after treatment with luminol solution or sterile water as control. The luminescence was recorded over a 40 mins period and displayed as the sum of photon counts.

Flagellin working solution:

10 ml	MQ H_2O
10 µl	Flg22 (100 µM)
10 µl	HRP stock (10mg/ml)
20 µl	Luminol stock (17mg/ml)

6.2.4.5. Cell Death Staining/Trypan Blue Staining

In order to visualize cell death, at least two plant leaves were sampled and stained with trypan blue dye. Inoculated leaves were cut with scissors, put into a tip box and then covered with 20ml of fresh trypan blue solution. Tip boxes were placed on an orbital shaker at 25 rpm to ensure that the leaves are completely covered in the liquid. After a total time of 40 mins, the trypan solution was replaced with 20ml of 100% ethanol. This step was repeated 3 times after 45-60 mins. Leaves were then left in ethanol overnight to become completely colorless. Afterwards, ethanol was removed, and leaves were placed into a petri dish containing 60% glycerol and sealed with parafilm till visualization.

Imaging was performed using the ChemiDoc™ imaging system (BioRad, USA) set for Coomassie blue with exposure time 1 sec.

6.2.5. Methods involving plants

6.2.5.1. Plant Material

Nicotiana benthamiana was used throughout this study. Plants were grown in controlled short-day conditions (16h light/8h dark photoperiod) at 22°C. Seeds were

germinated in soil ‘Einheitserde SP ED63 T’ (Einheitserdewerke Werkverband e.V.) with perlite. Watering occurred every two days for 15 mins.

Zea mays variety Early Golden Bantam (EGB) was used. Plants were grown in a greenhouse at controlled temperature conditions (28°C at day/20°C at night) and seedlings were grown on ‘Einheitserde SP ED63 T’ (Einheitserdewerke Werkverband e.V.) with perlite. Watering occurred every three days.

6.2.5.2. Infiltration Assay in Nicothana benthamiana

Protein expression *in planta* was achieved by *Agrobacterium tumefaciens* mediated transformation of *Nicotiana benthamiana*. Agrobacterium strains harboring an expression plasmid for subcellular localization assay or VIGS constructs were grown in liquid Agro LB medium with appropriate antibiotics by shaking at 28°C on 180 rpm overnight.

1) Subcellular mislocalization assay

For the subcellular localization assays, *Nicotiana benthamiana* plants were 4-5 weeks old before used for infiltration. Cells were harvested by centrifugation at 3000 g for 10 min and resuspended in ARM medium to a final OD600 of 0.1 or 0.2 After 3 hours incubation, cultures were syringe infiltrated into 4-5 weeks old *Nicotiana benthamina* plants. Leaves were harvested 1 or 2 days post infection and ROS Burst Assay was performed *(see section 2.2.4.4. ROS burst assay)*

2) VIGS

Nicotiana benthamiana plants used for silencing were around 2-3 weeks old where they showed the first 2 true leaves emerge beside the cotyledons. For each independent experiment, 5 plants for each tested construct were used. Before being able to infiltrate them into plant leaves, cells were harvested and centrifuged at 3000 g for 10 min before resuspending them in ARM medium to a final OD600 of 0.4. Cells were afterwards incubated at room temperature for 3 hours. Bacterial cultures were then mixed containing the pTRV1(encodes the replication and movement of viral

functions) and pTRV2 (harbors the coat protein and the sequence used for VIGS) in a ratio 1:1. First mixing these 2 strains together results in gene silencing. To avoid cross-contamination, gloves were changed between infiltration of different constructs. Leaves were harvested 3-4 weeks after infiltrating them and used for ROS Burst assay *(described section 2.2.4.4. ROS burst assay)*. Further, parts of the leaves were immediately frozen in liquid nitrogen and stored in -80°C until further use. As a control for VIGS efficiency, silencing of phytoene desaturase (PDS) was used which causes photobleaching.

LB (MES AS):

10 mM	MES NaOH, pH5.6
0.2 mM	Acetosyringone
	In LB

ARM:

10 mM	MES NaOH, pH5.6
10 mM	MgCl2
0.15 mM	Acetosyringone
	In LB

6.2.5.3. Virulence assay of Zea mays with Ustilago maydis

To assess the viral impact of our *Ustilago maydis* effectors on mays, virulence assay was performed as described by Kämper et al. 2006. Therefore, we conducted infections on 7 days old maize seedlings by using a needle and a syringe. Infection preculture was prepared by inoculating fungal material in 4 ml YEPlight at 28°C on 180 rpm overnight. The main culture was then prepared by diluting the preculture 1:3000 and put for shaking at 28°C overnight. When the OD600 of 0.6-0.8 was reached, cells were harvested and transferred into a falcon tube before spinning them for 10 min at 3500 rpm. Afterwards, the OD600 of the cell suspension was set to 1 by resuspending them in an adequate volume of water. The cultures were injected around 1 cm above the soil into the center of the leaf whorl. The virulent progenitor

strain SG200 was used as reference. Seven days after infection, disease symptoms were scored. Each plant was observed as an individuum and the most severe symptoms were scored according to following categories:

Plant symptoms	Description
No symptoms	The plant shows no signs of infection
Chlorosis	The plant shows chlorotic discoloration of the infected leaves (third leaf and younger)
Small galls	The largest galls of the plant are <1.5 mm
Normal galls	Galls of the plant are 2-4 mm in diameter
Heavy galls	Very strong galls leading to a stunted growth of stem
Stunted growth	The plant indicates dead symptoms after infection with *Ustilago maydis*

6.2.6. Microscopy

Tissue of infected *Nicotiana benthamiana* plants were harvested by punching a leaf disc right around the infected area. Confocal laser scanning microscopy was performed using the LSM780 Axio Observer (inverted) microscope from Zeiss. Images were processed using the software ZEN Black (2.3 SP1).

6.2.7. Bioinformatics Tools

Database	Description	Reference/URL
UniProt	Protein sequences and general information of interacting proteins were acquired through this page	*https://www.uniprot.org*
Sol Genomics Network	Checking for coding region and best target for Virus Induced Gene Silencing.	*https://solgenomics.net* *http://vigs.solgenomics.net/*
NCBI	Homology searches and sequence analysis's	*https://www.ncbi.nlm.nih.gov/*
CLC	Analysis of all DNA and protein sequences	*CLC main work bench 7 (Quiagen Bioinformatics)*
Primer3	Generating of oligonucleotide sequences	*http://primer3.ut.ee*

6.2.8. Statistical Analysis

In this study statistical analysis was performed using several statistical packages. Graphical outputs were done in Microsoft Office Excel 10. Data set analysis were performed using the statistical environment RStudio (Version 1.0.143-© 2009-2016 RStudio, Inc.) and IBM SPSS Statistics (Version 24.0. Armonk, NY: IBM Corp, 2016). Statistics were performed using analysis of variance (ANOVA) test with Tuckey's comparison at a 95% confidence level ($p < 0.05$) or t-test, 2-tailed with 95% confidence level analyzed in GraphPad Prism v6.0 (GraphPad Software). Significance level are indicated by stars (*, P<0.05; **, P <0.01; ***, P <0.001; ****, P <0.0001). Details are shown in figure legends.

For disease scoring in *Zea mays* an R-script was used to process data. The collected data was evaluated by using Fisher exact test to specify if the distribution into scoring classes is significant and if there is a difference between two observed samples. Additionally, Wilcoxon Rank Sum and Signed Rank Tests (Wilcoxon or Mann-Whitney test) was performed, to convert scoring data into ranked values according to symptoms, followed by a t-test, to clarify if there is a general shift in symptom severity between condition.

7. REFERENCES

Ahn, Hee-Kyung; Kang, Yong Won; Lim, Hye Min; Hwang, Inhwan; Pai, Hyun-Sook (2015): Physiological Functions of the COPI Complex in Higher Plants. In *Molecules and cells* 38 (10), pp. 866–875. DOI: 10.14348/molcells.2015.0115.

Ali, Muhammad; Cheng, Zhihui; Ahmad, Husain; Hayat, Sikandar (2018): Reactive oxygen species (ROS) as defenses against a broad range of plant fungal infections and case study on ROS employed by crops against Verticillium dahliae wilts. In *Journal of Plant Interactions* 13 (1), pp. 353–363. DOI: 10.1080/17429145.2018.1484188.

Arent, Susan; Christensen, Caspar E.; Pye, Valerie E.; Nørgaard, Allan; Henriksen, Anette (2010): The multifunctional protein in peroxisomal beta-oxidation. Structure and substrate specificity of the Arabidopsis thaliana protein MFP2. In *The Journal of biological chemistry* 285 (31), pp. 24066–24077. DOI: 10.1074/jbc.M110.106005.

Arimura, Shin-ichi; Aida, Gen Paul; Fujimoto, Masaru; Nakazono, Mikio;Tsutsumi, Nobuhiro (2004): Arabidopsis Dynamin-Like Protein 2a (ADL2a), Like ADL2b, is Involved in Plant Mitochondrial Division. In *Plant and Cell Physiology* 45 (2), pp. 236–242. DOI: 10.1093/pcp/pch024.

Asano, Tomoya; Masuda, Daisuke; Yasuda, Michiko; Nakashita, Hideo; Kudo, Toshiaki; Kimura, Makoto et al. (2008): AtNFXL1, an Arabidopsis homologue of the human transcription factor NF-X1, functions as a negative regulator of the trichothecene phytotoxin-induced defense response. In *The Plant journal : for cell and molecular biology* 53 (3), pp. 450–464. DOI: 10.1111/j.1365-313X.2007.03353.x.

Avisar, Dror; Abu-Abied, Mohamad; Belausov, Eduard; Sadot, Einat; Hawes, Chris; Sparkes, Imogen A. (2009): A comparative study of the involvement of 17 Arabidopsis myosin family members on the motility of Golgi and other organelles. In *Plant physiology* 150 (2), pp. 700–709. DOI: 10.1104/pp.109.136853.

Ballesteros, Isabel; Domínguez, Teresa; Sauer, Michael; Paredes, Pilar; Duprat, Anne; Rojo, Enrique et al. (2013): Specialized functions of the PP2A subfamily II catalytic subunits PP2A-C3 and PP2A-C4 in the distribution of auxin fluxes and development in Arabidopsis. In *The Plant journal : for cell and molecular biology* 73 (5), pp. 862–872. DOI: 10.1111/tpj.12078.

Banuett, F.; Herskowitz, I. (1996): Discrete developmental stages during teliospore formation in the corn smut fungus, Ustilago maydis. In *Development* 122 (10), pp. 2965–2976.

Bari, Rajendra; Jones, Jonathan D. G. (2009): Role of plant hormones in plant defence responses. In *Plant molecular biology* 69 (4), pp. 473–488. DOI: 10.1007/s11103-008-9435-0.

Basse, Christoph W.; Steinberg, Gero (2004): Ustilago maydis, model system for analysis of the molecular basis of fungal pathogenicity. In *Molecular plant pathology* 5 (2), pp. 83–92. DOI: 10.1111/j.1364-3703.2004.00210.x.

Bigeard et al. (2015): Signaling Mechanisms in Pattern-Triggered Immunity (PTI). In *Molecular Plant* 8 (4), pp. 521–539. DOI: 10.1016/j.molp.2014.12.022.

Bölker, M. (2001): Ustilago maydis--a valuable model system for the study of fungal dimorphism and virulence. In *Microbiology (Reading, England)* 147 (Pt 6), pp. 1395–1401. DOI: 10.1099/00221287-147-6-1395.

Boyd, Lesley A.; Ridout, Christopher; O'Sullivan, Donal M.; Leach, Jan E.; Leung, Hei (2013): Plant-pathogen interactions. Disease resistance in modern agriculture. In *Trends in genetics : TIG* 29 (4), pp. 233–240. DOI: 10.1016/j.tig.2012.10.011.

Brefort, Thomas; Doehlemann, Gunther; Mendoza-Mendoza, Artemio; Reissmann, Stefanie; Djamei, Armin; Kahmann, Regine (2009): Ustilago maydis as a Pathogen. In *Annual review of phytopathology* 47, pp. 423–445. DOI: 10.1146/annurev-phyto-080508-081923.

Camagna, Maurizio; Takemoto, Daigo (2018): Hypersensitive Response in Plants: American Cancer Society, 1/22/2018. Available online at https://onlinelibrary.wiley.com/doi/full/10.1002/9780470015902.a0020103.pub2.

Castanheira, Sónia; Pérez-Martín, José (2015): Appressorium formation in the corn smut fungus Ustilago maydis requires a G2 cell cycle arrest. In *Plant signaling & behavior* 10 (4), e1001227. DOI: 10.1080/15592324.2014.1001227.

Creelman, Robert A.; Mullet, John E. (1997): BIOSYNTHESIS AND ACTION OF JASMONATES IN PLANTS. In *Annual review of plant physiology and plant molecular biology* 48, pp. 355–381. DOI: 10.1146/annurev.arplant.48.1.355.

Djamei, Armin; Schipper, Kerstin; Rabe, Franziska; Ghosh, Anupama; Vincon, Volker; Kahnt, Jörg et al. (2011): Metabolic priming by a secreted fungal effector. In *Nature* 478 (7369), pp. 395–398. DOI: 10.1038/nature10454.

Doehlemann, Gunther; Ökmen, Bilal; Zhu, Wenjun; Sharon, Amir (2017): Plant Pathogenic Fungi. In *Microbiology spectrum* 5 (1). DOI: 10.1128/microbiolspec.FUNK-0023-2016.

Doehlemann, Gunther; Reissmann, Stefanie; Assmann, Daniela; Fleckenstein, Martin; Kahmann, Regine (2011): Two linked genes encoding a secreted effector and a membrane protein are essential for Ustilago maydis-induced tumour formation. In *Molecular microbiology* 81 (3), pp. 751–766. DOI: 10.1111/j.1365-2958.2011.07728.x.

Doehlemann, Gunther; van der Linde, Karina; Assmann, Daniela; Schwammbach, Daniela; Hof, Alexander; Mohanty, Amitabh et al. (2009): Pep1, a secreted effector protein of Ustilago maydis, is required for successful invasion of plant cells. In *PLoS pathogens* 5 (2), e1000290. DOI: 10.1371/journal.ppat.1000290.

Fürstenberg-Hägg, Joel; Zagrobelny, Mika; Bak, Søren (2013): Plant defens against insect herbivores. In *International journal of molecular sciences* 14 (5), pp. 10242–10297. DOI: 10.3390/ijms140510242.

Gao, Hongbo; Kadirjan-Kalbach, Deena; Froehlich, John E.; Osteryoung, Katherine W. (2003): ARC5, a cytosolic dynamin-like protein from plants, is part of the chloroplast division machinery. In *Proceedings of the National Academy of Sciences of the United States of America* 100 (7), pp. 4328–4333. DOI: 10.1073/pnas.0530206100.

Gladieux et al. (2010): Epidemiology and Evolution of Fungal Pathogens in Plants and Animals: Elsevier, 12/24/2010.

Glazebrook, Jane (2005): Contrasting mechanisms of defense against biotrophic and necrotrophic pathogens. In *Annual review of phytopathology* 43, pp. 205–227. DOI: 10.1146/annurev.phyto.43.040204.135923.

Gu, Lili; Xu, Tao; Lee, Kwanuk; Lee, Kwang Ho; Kang, Hunseung (2014): A chloroplast-localized DEAD-box RNA helicaseAtRH3 is essential for intron splicing and plays an important role in the growth and stress response in Arabidopsis thaliana. In *Plant physiology and biochemistry : PPB* 82, pp. 309–318. DOI: 10.1016/j.plaphy.2014.07.006.

Gupta, Ravi; Lee, So Eui; Agrawal, Ganesh K.; Rakwal, Randeep; Park, Sangryeol; Wang, Yiming; Kim, Sun T. (2015): Understanding the plant-pathogen

interactions in the context of proteomics-generated apoplastic proteins inventory. In *Frontiers in plant science* 6, p. 352. DOI: 10.3389/fpls.2015.00352.

Hardham, Adrienne R. (2013): Microtubules and biotic interactions. In *The Plant journal: for cell and molecular biology* 75 (2), pp. 278–289. DOI: 10.1111/tpj.12171.

Hemetsberger, Christoph; Herrberger, Christian; Zechmann, Bernd; Hillmer, Morten; Doehlemann, Gunther (2012): The Ustilago maydis effector Pep1 suppresses plant immunity by inhibition of host peroxidase activity. In *PLoS pathogens* 8 (5), e1002684. DOI: 10.1371/journal.ppat.1002684.

J., B.; E., M.; E., C. (2012): Investigating Host Induced Meiosis in a Fungal Plant Pathogen. In Abrahan Hernández-Hernández, Gerardo H. Vázquez-Nin, Rosario Ortiz Hernádez (Eds.): Epigenetics of the Synaptonemal Complex: INTECH Open Access Publisher.

Jwa, Nam-Soo; Hwang, Byung Kook (2017): Convergent Evolution of Pathogen Effectors toward Reactive Oxygen Species Signaling Networks in Plants. In *Frontiers in plant science* 8, p. 1687. DOI: 10.3389/fpls.2017.01687.

Kadota, Yasuhiro; Shirasu, Ken; Zipfel, Cyril (2015): Regulation of the NADPH Oxidase RBOHD During Plant Immunity. In *Plant & cell physiology* 56 (8), pp. 1472–1480. DOI: 10.1093/pcp/pcv063.

Kadota et al. (2014): Direct Regulation of the NADPH Oxidase RBOHD by the PRR Associated Kinase BIK1 during Plant Immunity. In *Molecular Cell* 54 (1), pp. 43–55. DOI: 10.1016/j.molcel.2014.02.021.

Kämper, Jörg; Kahmann, Regine; Bölker, Michael; Ma, Li-Jun; Brefort, Thomas; Saville, Barry J. et al. (2006): Insights from the genome of the biotrophic fungal plant pathogen *Ustilago maydis*. In *Nature* 444 (7115), p. 97. DOI: 10.1038/nature05248.

Kang, B.-H. (2003): Members of the Arabidopsis Dynamin-Like Gene Family, ADL1, Are Essential for Plant Cytokinesis and Polarized Cell Growth. In *THE PLANT CELL ONLINE* 15 (4), pp. 899–913. DOI: 10.1105/tpc.009670.

Kao, Yun-Ting; Gonzalez, Kim L.; Bartel, Bonnie (2018): Peroxisome Function, Biogenesis, and Dynamics in Plants. In *Plant physiology* 176 (1), pp. 162–177. DOI: 10.1104/pp.17.01050.

Kazan, Kemal; Lyons, Rebecca (2014): Intervention of Phytohormone Pathways by Pathogen Effectors. In *The Plant cell* 26 (6), pp. 2285–2309. DOI: 10.1105/tpc.114.125419.

Koeck, Markus; Hardham, Adrienne R.; Dodds, Peter N. (2011): The role of effectors of biotrophic and hemibiotrophic fungi in infection. In *Cellular microbiology* 13 (12), pp. 1849–1857. DOI: 10.1111/j.1462-5822.2011.01665.x.

Koh, Serry; Andre, Aurelie; Edwards, Herb; Ehrhardt, David; Somerville, Shaun (2005): Arabidopsis thaliana subcellular responses to compatible Erysiphe cichoracearum infections. In *The Plant journal : for cell and molecular biology* 44 (3), pp. 516–529. DOI: 10.1111/j.1365-313X.2005.02545.x.

König, Stefanie; Feussner, Kirstin; Kaever, Alexander; Landesfeind, Manuel; Thurow, Corinna; Karlovsky, Petr et al. (2014): Soluble phenylpropanoids are involved in the defense response of Arabidopsis against Verticillium longisporum. In *The New phytologist* 202 (3), pp. 823–837. DOI: 10.1111/nph.12709.

Koo, Abraham J. K.; Chung, Hoo Sun; Kobayashi, Yuichi; Howe, Gregg A. (2006): Identification of a peroxisomal acyl-activating enzyme involved in the biosynthesis of jasmonic acid in Arabidopsis. In *The Journal of biological chemistry* 281 (44), pp. 33511–33520. DOI: 10.1074/jbc.M607854200.

Koornneef, Annemart; Pieterse, Corné M. J. (2008): Cross talk in defense signaling. In *Plant physiology* 146 (3), pp. 839–844. DOI: 10.1104/pp.107.112029.

Lampropoulos, Athanasios; Sutikovic, Zoran; Wenzl, Christian; Maegele, Ira; Lohmann, Jan U.; Forner, Joachim (2013): GreenGate---a novel, versatile, and efficient cloning system for plant transgenesis. In *PloS one* 8 (12), e83043. DOI: 10.1371/journal.pone.0083043.

Lanver, Daniel; Berndt, Patrick; Tollot, Marie; Naik, Vikram; Vranes, Miroslav; Warmann, Tobias et al. (2014): Plant Surface Cues Prime Ustilago maydis for Biotrophic Development. In *PLOS Pathogens* 10 (7), e1004272. DOI: 10.1371/journal.ppat.1004272.

Lanver, Daniel; Tollot, Marie; Schweizer, Gabriel; Lo Presti, Libera; Reissmann, Stefanie; Ma, Lay-Sun et al. (2017): Ustilago maydis effectors and their impact on virulence. In *Nature reviews. Microbiology* 15 (7), pp. 409–421. DOI: 10.1038/nrmicro.2017.33.

LI, Hong; ZHANG, Ziding (2016): Systems understanding of plant–pathogen interactions through genome-wide protein–protein interaction networks. In *Front. Agr. Sci. Eng.* 3 (2), p. 102. DOI: 10.15302/J-FASE-2016100.

Li, Lei; Li, Meng; Yu, Liping; Zhou, Zhaoyang; Liang, Xiangxiu; Liu, Zixu et al. (2014): The FLS2-associated kinase BIK1 directly phosphorylates the NADPH oxidase RbohD to control plant immunity. In *Cell host & microbe* 15 (3), pp. 329–338. DOI: 10.1016/j.chom.2014.02.009.

Livanos, Pantelis; Galatis, Basil; Apostolakos, Panagiotis (2014): The interpla between ROS and tubulin cytoskeleton in plants. In *Plant signaling & behavior* 9 (3), e28069. DOI: 10.4161/psb.28069.

Lo Presti, Libera; Lanver, Daniel; Schweizer, Gabriel; Tanaka, Shigeyuki; Liang, Liang; Tollot, Marie et al. (2015): Fungal effectors and plant susceptibility. In *Annual review of plant biology* 66, pp. 513–545. DOI: 10.1146/annurev-arplant-043014-114623.

Lu, Dongping; Wu, Shujing; Gao, Xiquan; Zhang, Yulan; Shan, Libo; He, Pin (2010): A receptor-like cytoplasmic kinase, BIK1, associates with a flagellin receptor complex to initiate plant innate immunity. In *Proceedings of the National Academy of Sciences of the United States of America* 107 (1), pp. 496–501. DOI: 10.1073/pnas.0909705107.

Machado, João Paulo B.; Calil, Iara P.; Santos, Anésia A.; Fontes, Elizabeth P. B. (2017): Translational control in plant antiviral immunity. In *Genetics and molecular biology* 40 (1 suppl 1), pp. 292–304. DOI: 10.1590/1678-4685-GMB-2016-0092.

Macho, Alberto P.; Zipfel, Cyril (2014): Plant PRRs and the activation of innate immune signaling. In *Molecular Cell* 54 (2), pp. 263–272. DOI: 10.1016/j.molcel.2014.03.028.

Miyagishima, Shin-ya; Kuwayama, Hidekazu; Urushihara, Hideko; Nakanishi, Hiromitsu (2008): Evolutionary linkage between eukaryotic cytokinesis and chloroplast division by dynamin proteins. In *Proceedings of the National Academy of Sciences of the United States of America* 105 (39), pp. 15202–15207. DOI: 10.1073/pnas.0802412105.

Mollá-Morales, Almudena; Sarmiento-Mañús, Raquel; Robles, Pedro; Quesada, Víctor; Pérez-Pérez, José M.; González-Bayón, Rebeca et al. (2011): Analysis of ven3 and ven6 reticulate mutants reveals the importance of arginine biosynthesis in Arabidopsis leaf development. In *The Plant journal : for cell and molecular biology* 65 (3), pp. 335–345. DOI: 10.1111/j.1365-313X.2010.04425.x.

Mou, Zhonglin; Fan, Weihua; Dong, Xinnian (2003): Inducers of plant systemi acquired resistance regulate NPR1 function through redox changes. In *Cell* 113 (7), pp. 935–944.

Mueller, André N.; Ziemann, Sebastian; Treitschke, Steffi; Aßmann, Daniela; Doehlemann, Gunther (2013): Compatibility in the Ustilago maydis-maize interaction requires inhibition of host cysteine proteases by the fungal effector Pit2. In *PLoS pathogens* 9 (2), e1003177. DOI: 10.1371/journal.ppat.1003177.

Muñoz, Alfonso; Castellano, M. Mar (2012): Regulation of Translation Initiation unde Abiotic Stress Conditions in Plants. Is It a Conserved or Not so Conserved Process among Eukaryotes? In *Comparative and functional genomics* 2012, p. 406357. DOI: 10.1155/2012/406357.

O'Brien, Jose A.; Daudi, Arsalan; Butt, Vernon S.; Paul Bolwell, G. (2012): Reactive oxygen species and their role in plant defence and cell wall metabolism. In *Planta* 236 (3), pp. 765–779. DOI: 10.1007/s00425-012-1696-9.

Ogasawara, Yoko; Kaya, Hidetaka; Hiraoka, Goro; Yumoto, Fumiaki; Kimura, Sachie; Kadota, Yasuhiro et al. (2008): Synergistic activation of the Arabidopsis NADPH oxidase AtrbohD by Ca2+ and phosphorylation. In *The Journal of biological chemistry* 283 (14), pp. 8885–8892. DOI: 10.1074/jbc.M708106200.

País, Silvia Marina; Téllez-Iñón, María Teresa; Capiati, Daniela Andrea (2009): Serine/threonine protein phosphatases type 2A and their roles in stress signaling. In *Plant signaling & behavior* 4 (11), pp. 1013–1015.

Pye, Valerie E.; Christensen, Caspar E.; Dyer, James H.; Arent, Susan; Henriksen, Anette (2010): Peroxisomal plant 3-ketoacyl-CoA thiolase structure and activity are regulated by a sensitive redox switch. In *The Journal of biological chemistry* 285 (31), pp. 24078–24088. DOI: 10.1074/jbc.M110.106013.

Redkar, Amey; Hoser, Rafal; Schilling, Lena; Zechmann, Bernd; Krzymowska, Magdalena; Walbot, Virginia; Doehlemann, Gunther (2015): A Secreted Effector Protein of Ustilago maydis Guides Maize Leaf Cells to Form Tumors. In *The Plant cell* 27 (4), pp. 1332–1351. DOI: 10.1105/tpc.114.131086.

Richmond, T. A. (1999): A Defect in beta-Oxidation Causes Abnormal Inflorescence Development in Arabidopsis. In *THE PLANT CELL ONLINE* 11 (10), pp. 1911–1924. DOI: 10.1105/tpc.11.10.1911.

Sadeghi, Mahnaz; Dehghan, Sara; Fischer, Rainer; Wenzel, Uwe; Vilcinskas, Andreas; Kavousi, Hamid Reza; Rahnamaeian, Mohammad (2013): Isolation and characterization of isochorismate synthase and cinnamate 4-hydroxylase during salinity stress, wounding, and salicylic acid treatment in Carthamus tinctorius. In *Plant signaling & behavior* 8 (11), e27335. DOI: 10.4161/psb.27335.

Schilmiller, Anthony L.; Gilgallon, Karin; Ghosh, Banibrata; Jones, A. Daniel; Last, Robert L. (2016): Acylsugar Acylhydrolases. Carboxylesterase-Catalyzed Hydrolysis of Acylsugars in Tomato Trichomes. In *Plant physiology* 170 (3), pp. 1331–1344. DOI: 10.1104/pp.15.01348.

Shapiguzov, Alexey; Vainonen, Julia P.; Wrzaczek, Michael; Kangasjärvi, Jaakko (2012): ROS-talk - how the apoplast, the chloroplast, and the nucleus get the message through. In *Frontiers in plant science* 3, p. 292. DOI: 10.3389/fpls.2012.00292.

Soltani, Bahram M.; Ehlting, Jürgen; Douglas, Carl J. (2006): Genetic analysis and epigenetic silencing of At4CL1 and At4CL2 expression in transgenic Arabidopsis. In *Biotechnology journal* 1 (10), pp. 1124–1136. DOI: 10.1002/biot.200600140.

Staswick, Paul E.; Tiryaki, Iskender (2004): The oxylipin signal jasmonic acid is activated by an enzyme that conjugates it to isoleucine in Arabidopsis. In *The Plant cell* 16 (8), pp. 2117–2127. DOI: 10.1105/tpc.104.023549.

Steinberg, Gero; Perez-Martin, Jose (2008): Ustilago maydis, a new fungal model system for cell biology. In *Trends in cell biology* 18 (2), pp. 61–67. DOI: 10.1016/j.tcb.2007.11.008.

Stirnberg, Alexandra; Djamei, Armin (2016): Characterization of ApB73, a virulence factor important for colonization of Zea mays by the smut Ustilago maydis. In *Molecular plant pathology* 17 (9), pp. 1467–1479. DOI: 10.1111/mpp.12442.

Sun, Yadong; Li, Lei; Macho, Alberto P.; Han, Zhifu; Hu, Zehan; Zipfel, Cyril et al. (2013): Structural basis for flg22-induced activation of the Arabidopsis FLS2-BAK1 immune complex. In *Science (New York, N.Y.)* 342 (6158), pp. 624–628. DOI: 10.1126/science.1243825.

Tanaka, Shigeyuki; Brefort, Thomas; Neidig, Nina; Djamei, Armin; Kahnt, Jörg; Vermerris, Wilfred et al. (2014): A secreted Ustilago maydis effector promotes virulence by targeting anthocyanin biosynthesis in maize. In *eLife* 3, e01355. DOI: 10.7554/eLife.01355.

Thatcher, Louise F.; Anderson, Jonathan P.; Singh, Karam B. (2005): Plant defence responses. What have we learnt from Arabidopsis ? In *Functional Plant Biol.* 32 (1), p. 1. DOI: 10.1071/FP04135.

Thomma, B. P.; Eggermont, K.; Tierens, K. F.; Broekaert, W. F. (1999): Requirement of functional ethylene-insensitive 2 gene for efficient resistance of Arabidopsis to infection by Botrytis cinerea. In *Plant physiology* 121 (4), pp. 1093–1102.

Torres, Miguel Angel; Dangl, Jeffery L. (2005): Functions of the respiratory burst oxidase in biotic interactions, abiotic stress and development. In *Current opinion in plant biology* 8 (4), pp. 397–403. DOI: 10.1016/j.pbi.2005.05.014.

Torres, Miguel Angel; Jones, Jonathan D. G.; Dangl, Jeffery L. (2006): Reactive oxygen species signaling in response to pathogens. In *Plant physiology* 141 (2), pp. 373–378. DOI: 10.1104/pp.106.079467.

Uhse, Simon; Djamei, Armin (2018): Effectors of plant-colonizing fungi and beyond. In *PLoS pathogens* 14 (6), e1006992. DOI: 10.1371/journal.ppat.1006992.

Underwood, William; Melotto, Maeli; He, Sheng Yang (2007): Role of plant stomata in bacterial invasion. In *Cellular microbiology* 9 (7), pp. 1621–1629. DOI: 10.1111/j.1462-5822.2007.00938.x.

Wang, Keri; Senthil-Kumar, Muthappa; Ryu, Choong-Min; Kang, Li; Mysore, Kirankumar S. (2012): Phytosterols play a key role in plant innate immunity *physiology* 158 (4), pp. 1789–1802. DOI: 10.1104/pp.111.189217.

Woldemariam, Melkamu G.; Ahern, Kevin; Jander, Georg; Tzin, Vered (2018): A role for 9-lipoxygenases in maize defense against insect herbivory. In *Plant signaling & behavior* 13 (1), e1422462. DOI: 10.1080/15592324.2017.1422462.

Yang, Long; Qin, Li; Liu, Guosheng; Peremyslov, Valera V.; Dolja, Valerian V.; Wei, Yangdou (2014): Myosins XI modulate host cellular responses and penetration resistance to fungal pathogens. In *Proceedings of the National Academy of Sciences of the United States of America* 111 (38), pp. 13996–14001. DOI: 10.1073/pnas.1405292111.

Zhang, Xinchun; Hu, Jianping (2010): The Arabidopsis chloroplast division protein DYNAMIN-RELATED PROTEIN5B also mediates peroxisome division. In *The Plant cell* 22 (2), pp. 431–442. DOI: 10.1105/tpc.109.071324.

8. SUPPLEMENTAL MATERIAL

Supplement Figure 1: ROS burst screen for ROSIEs. ROS accumulation measured upon flagellin induction for ROSIE 1-4, show a complete suppression in ROSIE 1 and ROSIE 3, where ROSIE 2 and ROSIE 4 show a partial suppression of ROS generation. mCherry was used as control.

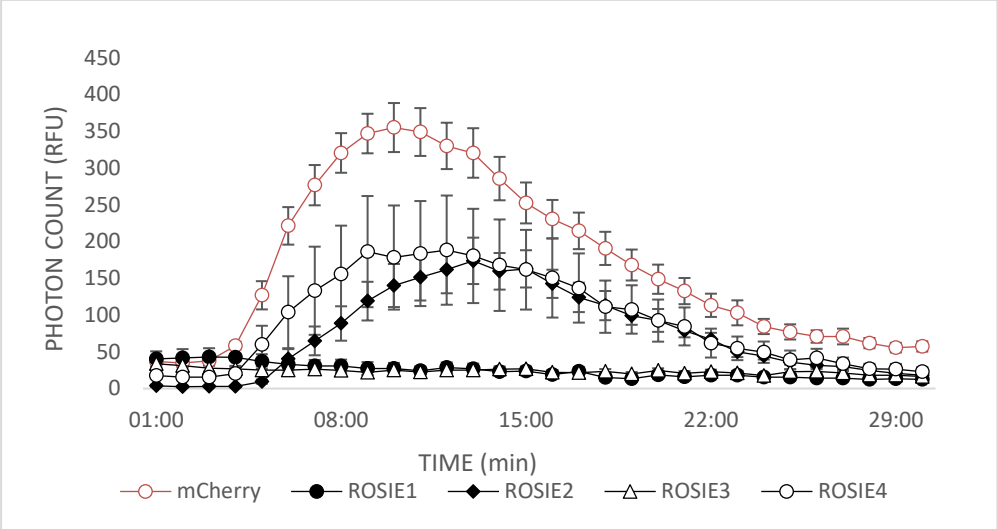

Supplement Figure 2: Fluorescence images of the subcellular localization of ROSIE 1-4. *N*- or *C*- terminal mCherry fusion of ROSIEs with the MYR (*Myrstoylation*), NLS (*Nuclear Localization Signal*) or NES (*Nuclear Export Signal*) tags were constructed and tested in *Nicotiana benthamiana*. Expression was observed using confocal laser scanning microscopy.Scale bar, 20 µm.

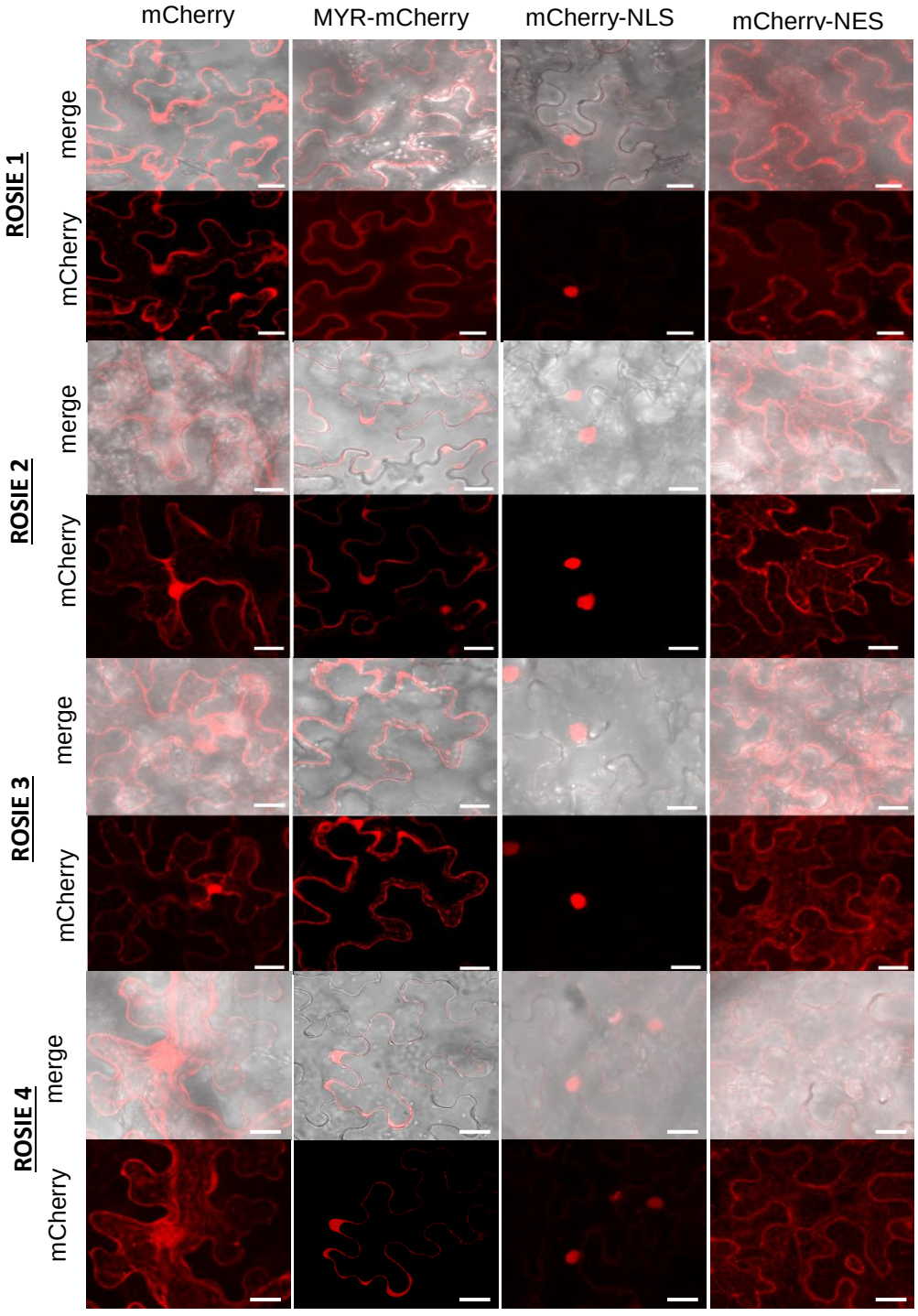

Supplement Figure 3: ROS burst assay performed for ROSIE 1 in different subcellular compartment. (A) ROSIE 1 expressed under the constitutive strong 35S promoter and **(B)** expressed under the Ubiquitin 10 promoter.

A

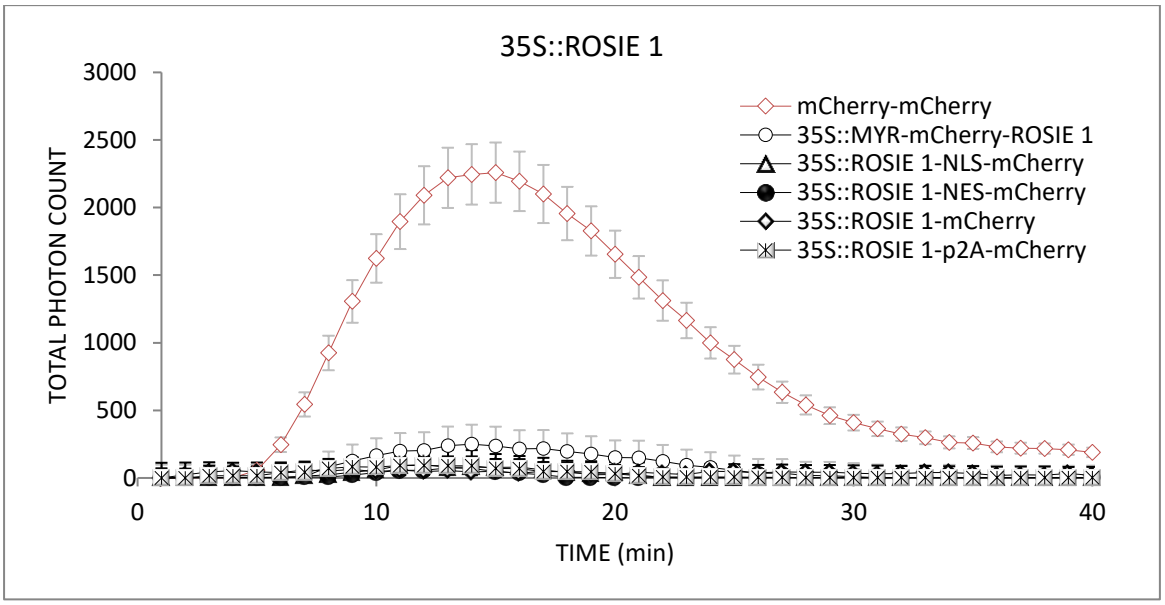

B

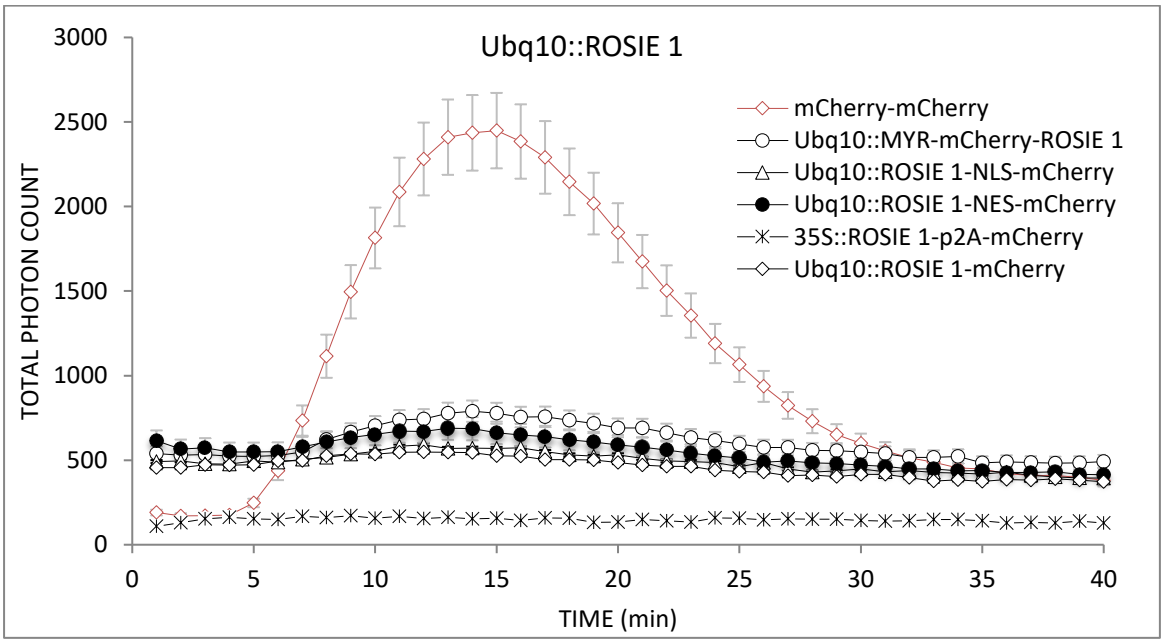

Supplement Figure 4: ROS burst assay performed for ROSIE 3 in different subcellular compartment. (A) ROSIE 3 expressed under the constitutive strong 35S promoter and **(B)** expressed under the Ubiquitin 10 promoter.

A

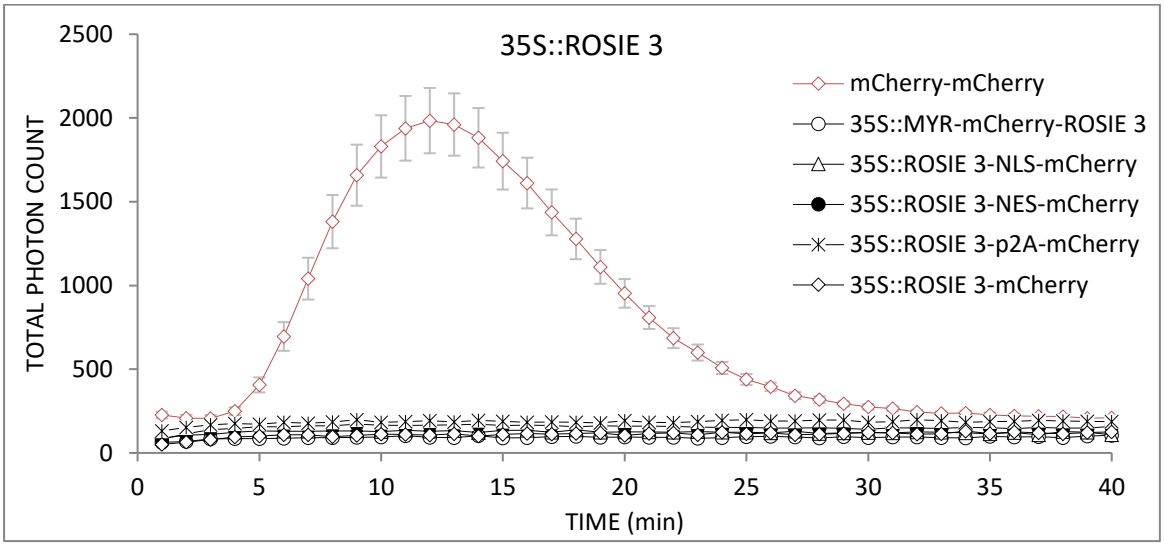

B